

## Imaging in Cardiovascular Procedures

### The role of Imaging Modalities in the Evaluation and Percutaneous Treatment of Patent Foramen Ovale

Dr. Mustafa Ozan Gürsoy, Dr. Sadık Volkan Emren

Foramen ovale which is supposed to close during physiological changes soon after birth, closes in 75% of the adult population and remains open in the rest 25%; defined as patent foramen ovale (PFO).<sup>1</sup> It has been associated with several disorders (migraine with aura, decompression sickness, etc.) including cerebrovascular disease. Despite detailed evaluation, the cause of ischemic stroke remains unclear in 25% of the patients which is defined as cryptogenic stroke. The relationship between PFO and cryptogenic stroke may be associated with paradoxical embolism, thrombus formation in the tunnel, left atrial dysfunction and atrial arrhythmias. Epidemiological data and clinical observational studies are supported by recent randomized studies which demonstrated the reduction in recurrent cerebrovascular events after percutaneous closure of PFO.<sup>2</sup> The use of multimodality imaging tools is necessary in diagnosis and percutaneous treatment of PFO.

#### Imaging

The imaging tools play an essential role in diagnosis and guiding the treatment of PFO like the other structural heart diseases that were treated percutaneously. These tools include fluoroscopy, angiography, transthoracic echocardiography (TTE) and transeophageal echocardiography (TEE). Intracardiac echocardiography (ICE) may be less frequently preferred by interventionalists. Among these tools, TEE is the gold standart to diagnose and manage the treatment of PFO as well as fluorocopy which is definitely used during percutaneous closure of the defect.<sup>3</sup> The role of each imaging modality for the steps of PFO closure is demonstrated in the Table 1.

#### The Imaging Steps

##### Before the Intervention

TTE is the initial monitoring tool in diagnosis of PFO. It is widely available in the hospitals and can be performed noninvasively (except the use of agitated saline or other

Table 1. Imaging Modalities Used During PFO Closure

Process	Useful (I)	Potentially useful (II)	Not useful (111)
Pre-procedure imaging			
PFO scanning	I	II	TD: I
Detection of shunt volume	I	I	TD: I
Presence of atrial septal aneurysm	II	I	
PFO tunnel length			
Thickness of the septum secundum	III		
Evaluation of additional structures	III		
- ASD	II		
- Chiari network eustachian valve	III	I	
Procedural imaging			
Device positioning and stabilization	III	I	Fluoroscopy: I
Post-procedure imaging			
Embolism	I	I	BT: II
Follow-up (device thrombus complete closure)	II	I	BT: II

CT: Computed tomography; TD: Transcranial doppler; TEE: Transesophageal echocardiography; TTE: Transthoracic echocardiography; I: Useful; II: Potentially useful; III: Not useful.

Fahriye Vatansever Ağca<sup>1</sup>   
 Gamze Babur Güler<sup>2</sup>   
 Mustafa Ozan Gürsoy<sup>3</sup>   
 Özge Özden<sup>4</sup>   
 Ertan Andaç Al<sup>6</sup>  
 Mert Pehlivan Altın<sup>5</sup>   
 İrem Dilara Can<sup>6</sup>  
 Sadık Volkan Emren<sup>7</sup>   
 Ömer Furkan Demir<sup>7</sup>   
 Emir Derviş<sup>8</sup>   
 İrem Dinçer<sup>9</sup>   
 Gökhan Kahveci<sup>10</sup>   
 Elmas Kaplan<sup>6</sup>  
 Alev Kılıçgedik<sup>11</sup>   
 İrem Müge Akbulut Koyuncu<sup>9</sup>   
 Volkan Kozluca<sup>9</sup>   
 Türkan Seda Tan Kürklü<sup>9</sup>   
 Selçuk Opan<sup>12</sup>   
 Kadriye Memiç Sancar<sup>2</sup>   
 Halenur Sarıbaş<sup>9</sup>  
 Büşra Güvendi Şengör<sup>13</sup>   
 Omac Tüfekçioğlu<sup>6</sup>   
 Selcen Yakar Tütüce<sup>14</sup>   
 Dilek Çiçek Yılmaz<sup>15</sup> 

<sup>1</sup>Department of Cardiology, University of Health Sciences, Bursa Faculty of Medicine, Bursa, Türkiye

<sup>2</sup>Department of Cardiology, University of Health Sciences, Mehmet Akif Ersoy Thoracic and Cardiovascular Surgery Training and Research Hospital, İstanbul, Türkiye

<sup>3</sup>Department of Cardiology, İzmir Katip Çelebi University Atatürk Training and Research Hospital, İzmir, Türkiye

<sup>4</sup>Department of Cardiology, Memorial Bahçelievler Hospital, İstanbul, Türkiye

<sup>5</sup>Department of Cardiology, Ankara City Hospital, Ankara, Türkiye

<sup>6</sup>Department of Cardiology, Siirt Kurtalan State Hospital, Siirt, Türkiye

<sup>7</sup>Yüksek İhtisas Training and Research Hospital, Cardiology Clinic, Bursa, Türkiye

<sup>8</sup>Department of Cardiology, Medipol University Faculty of Medicine, Bahçelievler Medipol Hospital, İstanbul, Türkiye

<sup>9</sup>Department of Cardiology, Ankara University Faculty of Medicine, Ankara, Türkiye

<sup>10</sup>Department of Cardiology, İstinye University Faculty of Medicine, Liv Hospital, İstanbul, Türkiye

<sup>11</sup>Department of Cardiology, Başakşehir Çam and Sakura City Hospital, İstanbul, Türkiye

<sup>12</sup>Department of Cardiology, Şanlıurfa Training and Research Hospital, Şanlıurfa, Türkiye

<sup>13</sup>Department of Cardiology, Kartal Koşuyolu Training and Research Hospital, İstanbul, Türkiye

<sup>14</sup>Department of Cardiology, İzmir Atatürk Training and Research Hospital, İzmir, Türkiye

<sup>15</sup>Department of Cardiology, Mersin University Faculty of Medicine, Mersin, Türkiye



Content of this journal is licensed under a Creative Commons Attribution - NonCommercial-NoDerivatives 4.0 International License.

echocardiographic contrast medium for a bubble test). During TTE study, interatrial septum can be evaluated in multiple windows. Especially, in apical 4-chamber view, a drop out may be noted and mistakenly considered as a septal defect but it should be remembered that the ultrasound beam is parallel to the interatrial septum in this view. Therefore, better views can be obtained in subxiphoid frontal and subcostal views where the interatrial being imaged is perpendicular to the ultrasound beam.<sup>4</sup>

As the patient is not sedated during TTE, he/she can perform strong and sustained Valsalva maneuvers; this increases the sensitivity of the method where the intravenously performed agitated saline contrast needs to fill the right atrium near the interatrial septum at the end.

In almost all echocardiography laboratories in Turkey, contrast bubbles are produced by mixing 9 mL of saline with 1 mL of air (and 1 mL of blood sometimes) which are rapidly squeezed back and forth between 2 syringes connected by a 3-way stopcock and administered by antecubital vein.

In patients with large Eustachian valve, the agitated serum contrast may not effectively reach interatrial septum due to the non-contrast stained blood coming from the lower extremities which washes out the contrast at the site of the PFO. This induces a 'negative contrast' image. In this situation, a more sustained and powerful Valsalva maneuver should be tried or the contrast test should be performed via lower extremity vein to be directed toward the PFO by the Eustachian valve. A more detailed information about contrast study is presented in the following 'Evaluation and Characterization of PFO by TEE' section.

Transcranial Doppler study, which is cheap and easy to perform, is an alternative highly sensitive imaging modality for indirectly detecting a PFO by assessing for the presence of right-to-left shunting. It allows functional assessment of the shunt through insonation of the middle cerebral arteries after venous injection of agitated saline and release of the Valsalva maneuver.<sup>5</sup> Being a higher sensitive test compared to TEE, makes transcranial Doppler study an essential screening modality for the detection of PFO.<sup>6</sup>

On the other hand, a right-to-left shunt, carries the possibility of being a false-positive for the presence of a PFO either from an ASD or intrapulmonary shunt. It should be remembered that transcranial Doppler study is an indirect functional test that does not depict IAS and thus a confirmatory test either with TEE or ICE (if available during percutaneous intervention) should be performed following a positive transcranial Doppler study.

### Evaluation and Characterization of PFO by TEE

The differential diagnosis of a right-to-left-shunt includes interatrial shunts, as well as shunts in the pulmonary vasculature. These shunts can be differentiated from a PFO-induced shunt by the time needed for the microbubbles to reach the left atrium; this can be difficult in patients with central pulmonary arteriovenous shunts.

TEE is an essential tool used in the diagnosis of PFO and other defects including ASD. IAS imaging by TEE predominantly includes upper esophageal short axis views as well as multiple midesophageal views. In midesophageal window, starting from 0 degrees (4 chamber), IAS and PFO tunnel can be delineated between mul-

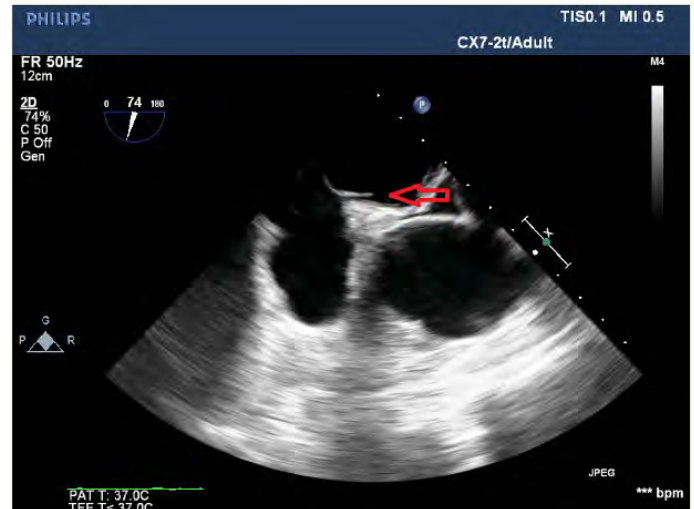


**Figure 1. Demonstration of the interatrial septum and PFO tunnel at the mid-esophageal level during TEE examination.**

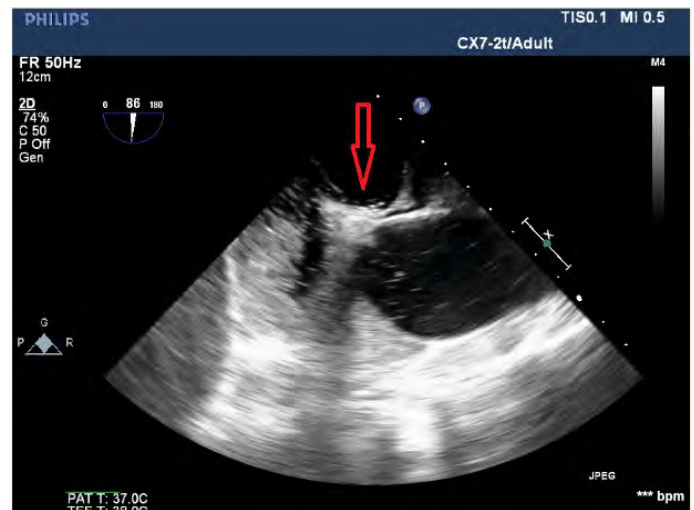


**Figure 2. The passage of microbubbles from right to left in contrast echocardiography is demonstrated.**

multiple degrees and views (especially 45°–60° short axis and 105°–120° bicaval) (Fig. 1). The color Doppler scale can be reduced slightly to approximately 35–40 cm/sec to capture low-velocity flow across a small fenestration, PFO, or smaller ASD.<sup>4</sup>

During contrast TEE study, inadequate technique may lead to a false negative result; therefore several points should be carefully taken into consideration. First of all, the steps should include: 1) The patient bears down for 5–10 seconds, 2) The saline is injected, 3) The contrast reaches right atrium, 4) The patient relaxes. The agitated saline should be correctly prepared and densely opacify the right heart. The interatrial septum should visibly shift from right to left ensuring the Valsalva was correctly performed. During TEE study, sedation and the presence of a probe inside the esophagus often decrease the Valsalva strain, which causes an inadequate Valsalva maneuver. Therefore, inferior vena cava (IVC) compression maneuver, which involves manual compression of the abdomen to produce partial IVC collapse and increased IVC flow upon release can be performed.<sup>7</sup>

Alternatively, the patient may be asked to cough that can be performed despite sedation. The Eustachian valve and Chiari network direct venous blood return from the lower extremities toward the PFO. Atrial septal aneurysm (ASA), when present, is frequently associated with PFO and large shunt. It may also lead to frequent openings of the PFO during forceful respiration. The presence of ASA and large shunt increases the risk of paradoxical embolism. The quantification of the shunt is based on the number of microbubbles crossing the PFO. The appearance of microbubbles in the left atrium within 3–6 cardiac beats after opacification of the right atrium is considered positive for the presence of an intracardiac shunt such as a PFO (Fig. 2).<sup>4</sup> Although cut-off values are not clear, >20 bubbles with intense opacification of the left atrium usually indicates a large shunt. It should be kept in mind that if the bubbles appear in the left atrium after 3–6 cycles (late bubbles), this represents a pulmonary arteriovenous malformation and usually rules out PFOs.

While IAS is being imaged with respect to diagnose any PFO, the characteristics of the septum and the tunnel should be evaluated and reported in detail: the relationship with surrounding structures (vena cava, coronary sinus, heart valves and pulmonary veins), the size of the shunt, length of the tunnel, the presence of any Eustachian valve, Chiari network and ASA, the thickness of septum secundum. Furthermore, other potential causes of stroke including left atrial appendage thrombus and aortic atheroma should also be excluded. The characteristics of complex PFO that may make the intervention more challenging are described in the Table 2.<sup>8</sup> In a recent study, Holda et al.<sup>9</sup> evaluated the PFO channel's morphological and functional features that could pose a risk for paradoxical embolism. The magnitude of the shunt is associated with multiplane opening of the PFO channel; there-

**Table 2. Complex PFO Features**

Accompanying atrial septal aneurysm\*

Tunnel length  $\geq 8$  mm

Septum secundum thickness  $\geq 10$  mm

Multiple fenestrations in atrial septum

Eustachian valve or Chiari network

Anatomy Changes Due to Aortic Root Enlargement

\*An atrial septal aneurysm is a deformity of the atrial septum, usually in the fossa ovalis region, bulging 10 mm towards either the right or left atrium, or a total of 15 mm towards both.

fore the larger the opening of the PFO channel is, the greater the probability of paradoxical embolism and greater the risk for ischemic stroke. They showed that PFO channel length reduction was identified as the strongest predictor of PFO-related stroke; when the PFO channel length decreases, it allows the thrombus to pass through its lumen much more easily than it does in longer channels. Furthermore, low PFO channel length/height ratio during the Valsalva maneuver was identified in this study as a cryptogenic stroke risk factor. Consequently, shorter and wider channels are found to be more prone to paradoxical embolism.

Imaging of the fossa ovalis is usually obtained using a 2D TEE bicaval plane view. In the last two decades, 3D TEE has emerged as an indispensable tool that compliments 2D imaging of cardiac structures and therefore may also permit a clearer understanding of PFO morphology. The surrounding structures within left and right atrium are that may have a relationship with PFO can

be easily delineated before and during the closure procedure.<sup>4</sup> <sup>10</sup> To depict the entire atrial septum 3D zoom mode is the most preferred method, especially in bicaval view, where the atrial septum lies perpendicular to the ultrasound beam. Superior and inferior vena cava are included in this view. With a 90° up-down angulation of the pyramidal data set, the entire left-sided aspect of the septum is shown in an "en face" view. Once the left side of the atrial septum is acquired, a 180° counterclockwise rotation shows the right side of the atrial septum and the fossa ovalis as a depression on the septum.<sup>4</sup> PFO is not a circular, but an elliptical structure. Furthermore, similar to atrial septal defect, dynamic changes in the area of PFO during cardiac cycle are observed (larger in ventricle systole compared to diastole). Maximum and minimum dimensions of the defect can be accurately calculated using multiplanar reconstruction and; therefore the optimal type and size of the closure device can be easily determined.

### Selection of the PFO Occluder

During percutaneous closure of PFO, mostly used devices include Amplatzer (Abbott; Chicago, Illinois) and Amplatzer-type occluders with a left atrial anchoring disc and an interconnected right atrial disc. Appropriate sizing is essential to prevent embolization of the device and ensure a stable position. At this time there is no consensus regarding the selection of device size for PFO closure; however, TEE provides precious clue regarding the selection of the optimal device including length and width (opening) of the tunnel, thickness of septum secundum, presence of ASA and/or coexisting atrial septal defect.

A thick septum secundum requires a larger right atrial disc as the right atrial disc may slide off the septum secundum and flip into the PFO tunnel.<sup>3</sup> Similar risk is also present for patients with a large ASA and very short PFO tunnel. Therefore, the presence of 1 or 2 of the risk factors (thick septum secundum, ASA, and short or no tunnel) should trigger selection of the larger PFO occluder (e.g., an Amplatzer 35 mm PFO Occluder), whereas the presence of all 3 risk factors mandates selection of the larger PFO Occluder.<sup>3</sup> Although long-tunnel PFO tracts pose particular challenges for device closure, long tunnel or a small PFO opening renders a thick septum secundum or an ASA less essential and may still allow a standard device to be used.<sup>3,11</sup> On the other hand, in patients with large ASA, multifenestrated 'cribriform' devices may be preferred by some operators following septostomy. During percutaneous closure of PFO, the use of "sizing balloons" is not generally required as it provides limited additional information (width and length of the PFO tunnel) and carries a small risk for complications such as tearing of a thin septum primum.

Briefly, TTE acts as an initial tool to describe some of the PFO characteristics, but subsequent two and three dimensional TEE, provides invaluable data about PFO to select the appropriate PFO occluder.<sup>12</sup>

### Periprocedural Imaging

Imaging during PFO closure procedure is mainly aimed to demonstrate the device deployment, device position and presence of the shunt. Fluoroscopy is sometimes the only preferred imaging method during periprocedural period by some operators; however, TEE or ICE gives more accurate information about the demonstration of device deployment and position. The main

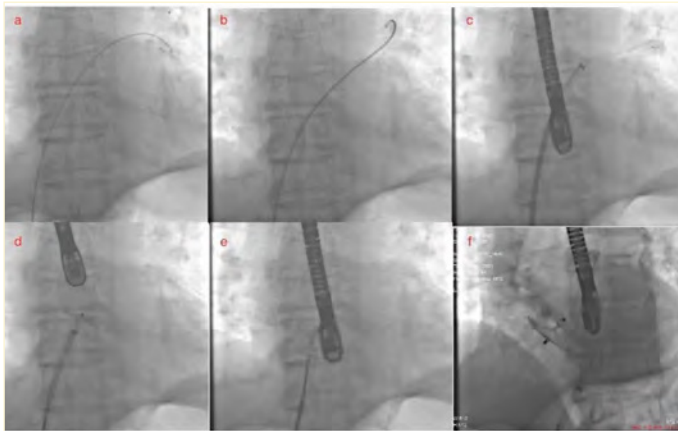


**Figure 3. A-F. Perioperative echocardiographic imaging. (A) Passage of the wire through the patent foramen ovale (PFO) tunnel. (B) Demonstration that the wire is in the pulmonary vein. (C) Positioning of the guide catheter in the left atrium. (D) Opening of the left atrial disc in the left atrium. (E) Positioning the left atrial disc against the septum and opening of the right atrial disc. (F) Release of the device covering the PFO and partially the septum.**

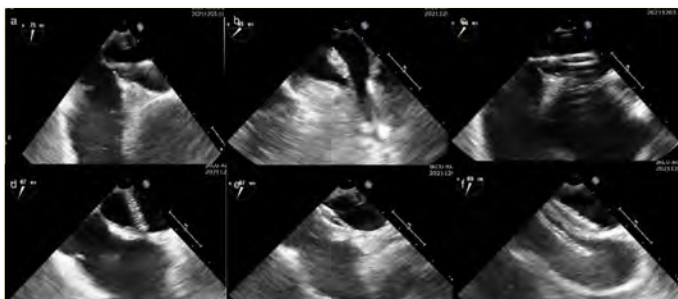


**Figure 4. A-F. Perioperative fluoroscopic imaging. (A) Passage of the wire through the patent foramen ovale (PFO) tunnel. (B) Advancement of the wire into the left upper pulmonary vein with a catheter. (C) Positioning of the guide catheter in the left atrium. (D) Opening of the left atrial disc in the left atrium. (E) Positioning the left atrial disc against the septum and opening of the right atrial disc. (F) Checking the position from a left oblique angle after the device is released.**

pitfalls of TEE may be the requirement of sedation and impairment of patient comfort. Furthermore, general anesthesia and intubation may be needed in case of TEE imaging to avoid aspiration while the patient is lying on supine position. Besides, being closed to the collimator may expose the echocardiographer to higher radiation (nearly 3 to 10 times) which is considered as another drawback of echocardiographic imaging during the procedure.<sup>13</sup> Fluoroscopic images are usually adequate to show the advancement of wire and catheter through the PFO tunnel. In this context, multipurpose catheter is positioned at 2 o'clock at the junction of right atrium and IVC, then advanced through the PFO tunnel over the 0.035- or 0.038-inch wire (Fig. 3A and 4A). The catheter and wire should be kept in a clockwise torque in order to stay positioned at pulmonary vein instead of left atrial appendix due to the concern of perforation (Fig. 3B and 4B). Before the advancement of delivery sheath, soft tip 0.035- or 0.038-inch wire should be exchanged with extra-stiff, floppy/-tipped 0.035-inch exchange-length guidewire. The position of

wire and catheter can be confirmed with echocardiography or fluoroscopy. Fluoroscopy is solely adequate during the advancement of delivery system. In this regard, delivery system should be advanced through PFO at 2 o'clock at anteroposterior view on fluoroscopy (Fig. 3C and 4C). In our practice, combination of fluoroscopic and echocardiographic imaging increases the success of procedure. We usually prefer TEE guidance to visualize the opening of the left atrial disc in left atrium without traumatizing the atrial wall (Fig. 3D and 4D) and the positioning of left atrial disc towards septum (Fig. 3E). Afterwards, the right atrial disc is opened and deployed and the occluder seats the septum (Fig. 4E). After unlocking the lock system, anatomical position of the device can be confirmed with the fluoroscopy or TEE (Fig. 3F and 4F). If 3D TEE is available, the relationship between guidewire and delivery system and surrounding structures may be better depicted, and this may reduce the total fluoroscopy time. Before discharge, the patient should be evaluated with TTE in terms of device position, and presence of any embolization, pericardial effusion and thrombus. The second echocardiographic (TTE or TEE) evaluation should be performed within 3 and 6 months after discharge.<sup>14</sup>

## Conclusion

PFO, which is a common finding in adult population, may be associated with several disorders including cryptogenic stroke. Percutaneous management of PFO has been shown to decrease recurrent cerebrovascular events. Multimodality imaging, including transthoracic and transesophageal echocardiography, is crucial in the evaluation of PFOs, and helps in selecting the optimal closure device and increases procedural success.

## Imaging Modalities in Evaluation and Percutaneous Treatment of Atrial Septal Defect

*Dr. Fahriye Vatanserver Ağca, Dr. Ömer Furkan Demir*

Atrial septal defects (ASD) constitute 10% of congenital heart diseases. Ostium secundum type defect is the fourth most common congenital heart disease and its incidence is 3.78/10 thousand live births.<sup>15</sup> Since the first case of percutaneous transcatheter closure (PTC) was reported in 1976, PTC has become the standard choice of therapy for secundum ASD with advances in transcatheter techniques, device technology, and imaging. Transthoracic echocardiography (TTE) is the first-line imaging modality for interatrial septal evaluation. However, transesophageal echocardiography (TEE) is required for further evaluation of atrial septal abnormalities before deciding on closure. With widely usage of three-dimensional (3D) TEE in recent years, the atrial septum is displayed as en-faced and more accurate measurements are obtained, especially in complex defects. Another technique, intracardiac echocardiography (ICE), can be used to guide ASD closure procedures and acquire imaging comparable to TEE.<sup>4, 16</sup> ASD can also be visualized and supplementary information can be obtained by cardiac magnetic resonance (MR) imaging and multislice computed tomographic angiography (CT).<sup>4</sup> However, this article will focus on echocardiographic imaging in ASD closure and review the use and guidance of echocardiography before, during, and after the procedure in percutaneous ASD closure.

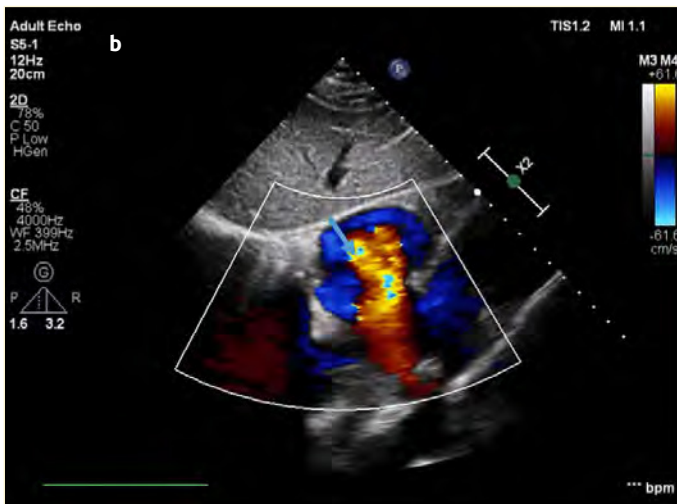


**Figure 5. A-B. (A) Subxiphoid four-chamber frontal window, visualization of a defect in the interatrial septum. (B) Subxiphoid four-chamber frontal window, visualization of left-to-right flow across the interatrial septum with color Doppler.**

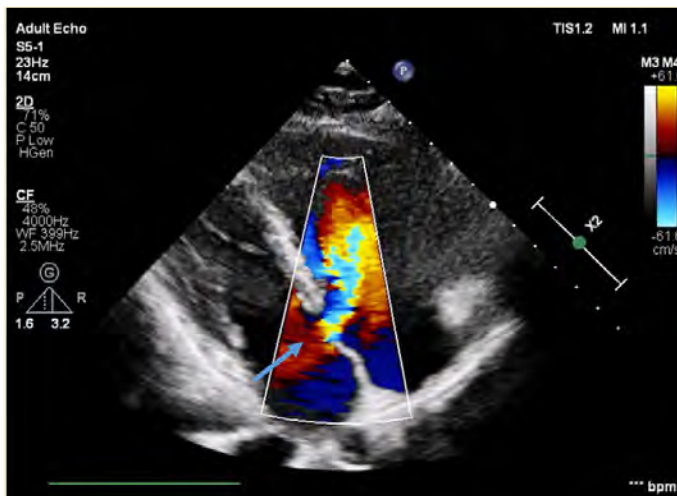


**Figure 6. Visualization of passage through the septum in a modified apical four-chamber view.**



**Figure 7. Visualization of the defect in the interatrial septum, along with the aortic and posterior rims, in the parasternal short-axis view.**

### Preprocedural Imaging

#### Transthoracic Echocardiographic Imaging

The interatrial septum (IAS) is a complex, dynamic and three-dimensional structure. The secundum type ASDs can be of different locations, diameters, shapes and numbers. TTE is the most important method to determine existence of ASD, evaluating its hemodynamic significance, and demonstrating other accompanying anomalies. Although TTE allows septum examination in multiple planes, the fact that the septum is far from the transducer in adults leads to suboptimal results, and it may cause drop-out defects or an overestimation of the existing defect diameter due to the parallel course of ultrasound waves to the IAS, especially in the apical windows. To circumvent this, subxiphoid windows provide the most important images of atrial septum and related structures, especially in pediatric population.

The subxiphoid four-chamber frontal window is best for viewing the atrial septum along the anteroposterior axis (Fig. 5A, B, Vid. 1A, B). This helps to avoid artifact which cause drop out image especially in the middle part of the septum and can helps to distinguish a true defect. The right pulmonary vein rim may be examined in this window. The subxiphoid sagittal TTE window is best for visualization of the atrial septum along its upper-lower axis. SVC and IVC rims can be measured in this window and is a convenient window to view a sinus venosus type defect. The modified apical four-chamber window, visualized by shifting probe from the apical four-chamber view to the medial border of sternum, is an alternative method for visualizing the atrial septum in patients where subcostal images are difficult to obtain (Fig. 6, Vid. 2). The parasternal short axis window is useful for measure the aortic and the posterior rims (or lack thereof) (Fig. 7, Vid. 3). Of the alternate windows, the left anterior oblique window is obtained by rotating the probe 45° counterclockwise from the four-chamber view. This window is used to view the length of the atrial septum and is useful for recognising the ostium primum defects and assessing coronary sinus dilatation. It is useful for evaluating SVC rim and the right-sided pulmonary venous return. The high right parasternal window is a parasagittal view obtained with the probe in the upper-lower orientation in the right lateral decubitus position. Ultrasound beam is perpen-

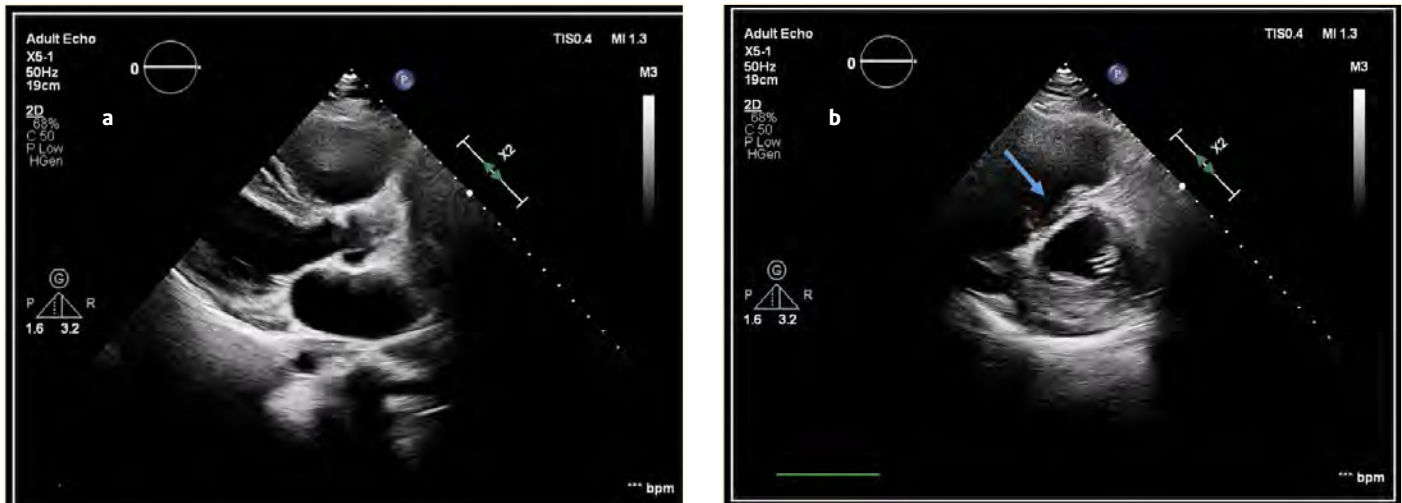


**Figure 8. A-B. (A) Visualization of a dilated right ventricle. (B) Diastolic flattening (D-shape) of the interventricular septum.**

dicular to septum and it is ideal for visualization of sinus venosus defects, especially while subxiphoid windows are suboptimal.<sup>3</sup>

Contrast echocardiography with agitated saline helps to detect the PFO/ASD when used in combination with physiologic maneuvers like valsalva and coughing. The test is accepted as positive if microbubbles are seen in the left atrium within 3-6 cardiac cycles after right atrial opacification.<sup>17</sup> Associated findings, like dilatation of right atrium, ventricle, and/or pulmonary artery, and diastolic flattening of the interventricular septum, are important signs of left-to-right shunts (Fig. 8, Vid. 4). However, despite all these standard and alternative imaging windows and techniques, TTE imaging in adults cannot provide sufficient information in evaluation for PTC, and TEE could be required.

**Table 3. TEE checklist of ASD evaluation for percutaneous closure**

Necessary steps	Assessment of ASD
Type of ASD	Primum, secundum, sinus venosus type, unroofed coronary sinus type
Doppler flow presence	Left to right, right to left or bidirectional flow
Need for surgery	Presence of anomalous pulmonary venous drainage Significant mitral valve or other pathology necessitating surgical intervention
Detailed assessment of defect	Defect size and shape Number of defects Measurement of all rims-aortic, RUPV superior, posterior, inferior, AV septal
Associated findings	Atrial septal aneurysm Eustachian valve Chiari network
Dynamic nature of ASD	Measurement of area and maximum/minimal diameters in end-systole and end-diastole

## Transesophageal Echocardiographic Imaging

### 2D TEE Imaging

To complete and systematically evaluation of the defect size, shape, location, and relationship with surrounding structures, the all interatrial septum should be scanned in 15-degree increments of transducer angle, starting with multiple and sequential standard

TEE windows. The examinations that should be done in standard TEE imaging for ASD are given in Table 3. While examining the IAS, after optimization of two-dimensional images, color Doppler imaging should be performed. Doppler scale should be reduced to 35-40 cm/sec in order to display low velocity currents. Next, the images should be examined using a pulsed and continuous Doppler to measure the speed, direction, and duration of the interatrial shunt. After detection of ASD, the relationship of the defect to both vena cava, pulmonary veins, mitral and tricuspid valves, aorta and coronary sinus must be evaluated. It is critical to measure the rims surrounding the defect for the patient's suitability for PTC. A missing rim is defined as lower than 5 mm of adequately thick rim length in multiple sequential views, which should be evaluated in at least three consecutively related multi-plane windows with 15° increments. Another window imaging is required to evaluate the hemodynamic consequences of ASD, like right heart chambers, pulmonary artery dilatation, and pulmonary artery pressure.<sup>4</sup> While the usage of TEE, five basic windows may be useful for evaluating IAS and surrounding structures.

### Upper Esophageal Short-Axis View

This window gained through the upper esophagus, the probe angle beginning at 0° and progressing slowly to at 15°, 30°, and 45°. This window allows to evaluate the upper part of the septum secundum, the roofs of the atria, and adjacent great vessels (superior vena cava and ascending aorta). By advancing probe into the middle esophagus and rotating the clockwise, we can visualize right pulmonary veins ostia. Abnormal pulmonary venous drainage and SVC type sinus venous defect is visualized from this window.

### Midesophageal Aortic Valve (AoV) Short-Axis View

It is the window in which the probe starts at an angle of approximately 30° in the middle esophagus and progresses step by step by recording additional images at 45°, 60°, and 75°. These view is used to obtain short axis views of the AoV and its surrounding septum and to measure the anterior (anterior superior, aortic) and posterior (posterior) rims of the defect. It is used to image the short-axis views of the AoV and its surrounding septum. It also allows to measure the anterior-posterior diameter of the defect (Fig. 9A). Total septal length can be measured from this window (Fig. 9A).

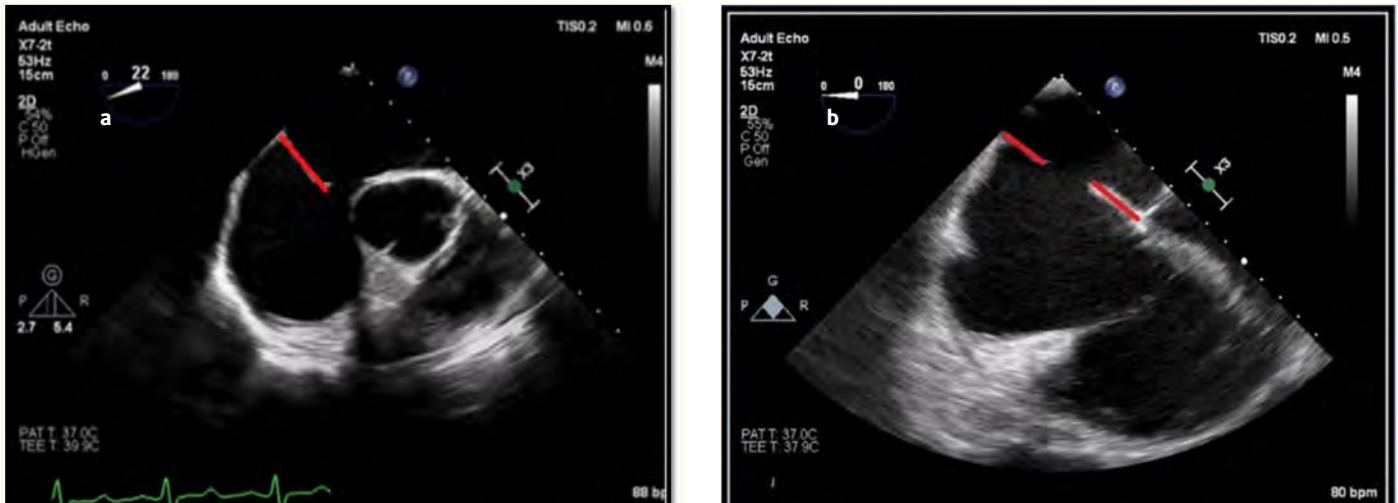


**Figure 9. A-B. (A) Mid-esophageal aortic valve short-axis view, measurement of the aortic (anterior superior) and posterior rims (deficient aortic rim). (B) Measurement of the AV valve and posterior rims in the mid-esophageal four-chamber view.**

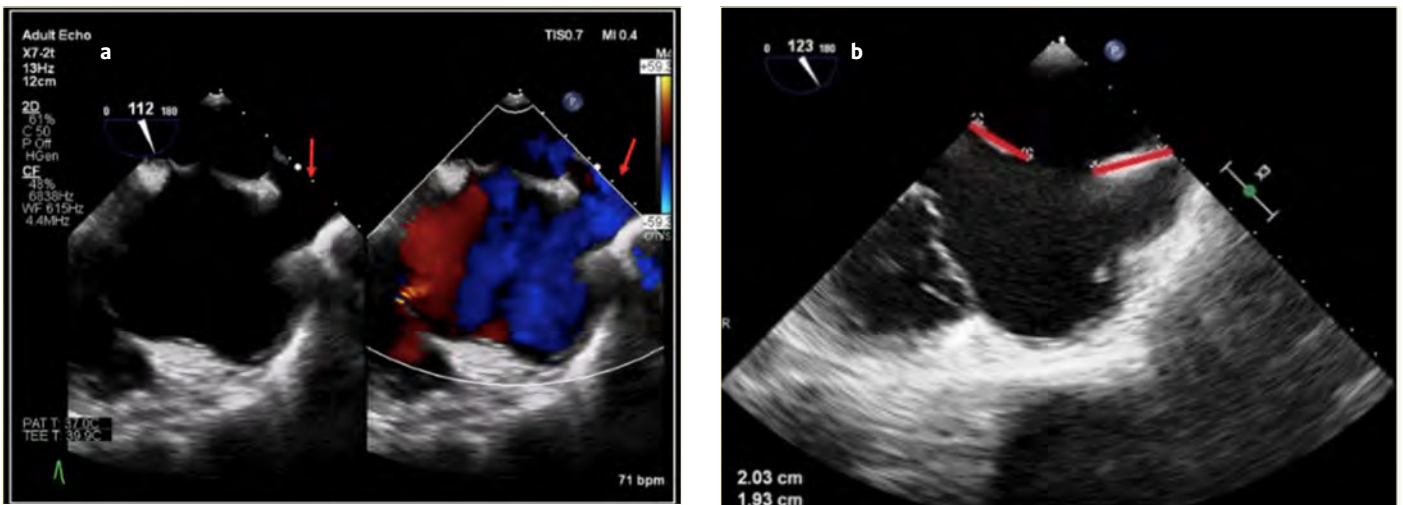


**Figure 10. A-B. (A) Visualization of SVC type sinus venus ASD in the mid-esophageal bicaval view. (B) Measurement of the SVC and IVC rims in the mid-esophageal bicaval view.**

### Midesophageal Four-Chamber View

These images are acquired from middle esophagus by beginning at angles of  $0^\circ$  and step by step increases to  $15^\circ$  and  $30^\circ$ . This image is used for evaluating relationship of the AV septum and any ASD to the AV valves. It is used to measure the anterior inferior (AV valve) rim. It should be noted that the aorta is closed in this window (Fig. 9B).

### Midesophageal Bicaval View

These view can be gained through the mid-esophagus multiplane by changing angles to  $90^\circ$ ,  $105^\circ$ , and  $120^\circ$ . By this window visualization of all of interatrial septum is possible. This window allows to evaluate sinus venus defects and abnormal pulmonary venous return (Fig. 10A). To examine IVC-type defects, the probe is advanced to the stomach, retroflexed, then slowly retracted into the lower esophagus, and the angle is evaluated at  $90^\circ \pm 20^\circ$ . Examining SVC type defects by pulling the probe back slightly towards the upper esophagus and increasing the angle towards  $120^\circ \pm 20^\circ$  enables these

defects to be viewed more easily. IVC (posterior inferior) rim and SVC (posterior superior) rims are measured from this window (Fig. 10B).

### Mid-Esophageal Long-Axis View

It is used to examine left atrium's roof while the percutaneous occlusion device is placed. These images are acquired from middle esophagus by changing multiplane angles to  $120^\circ$ ,  $135^\circ$  and  $150^\circ$ . Rotation past the LA appendage show the entry of left pulmonary veins into left atrium.

### 3D TEE Imaging

In ASD evaluation, 3D TEE is complementary to 2D TEE and is indispensable especially in complex anatomical defects. A wide and detailed 3D examination is usually achieved by starting with a real-time narrow-angle imaging after 2D image optimization from standard windows with electrocardiographically marked 3D wide-angle and zoom images to acquire high resolution images from temporal and spatial window. Three dimension images can be obtained from all standard 2D TEE windows, but the bicaval

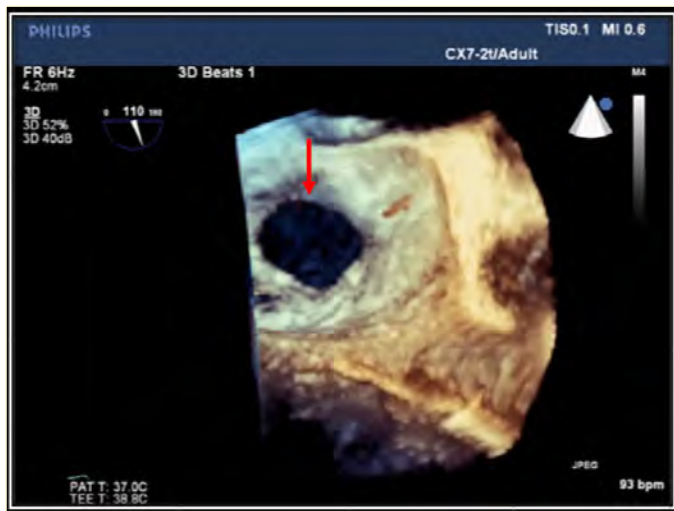


**Figure 11. 3D imaging of the ASD, examining the shape and number of defects, and the diameter of the defect during systole and diastole.**

window is most commonly used. With zoom mode viewing, the depth of pyramidal datasets should be adjusted to include only the left and right sides of the atrial septum in this window. Both the superior and inferior vena cava must be visualized. With the 90° up-down angulation of the pyramidal dataset, the left atrial side of the septum can be represented as "en-face perspective". After obtaining the left side of atrial septum, a 180° counterclockwise rotation is useful for visualizing right side of atrial septum and fossa ovalis as a depression on the septum. With appropriate gain setting, this window is used to examine the size and shape of the ASD in systole and diastole (Fig. 11).

### Indication for ASD Closure, Shunting and Hemodynamic Evaluation

ESC 2020 Adult Congenital Heart Disease Treatment Guidelines, with evidence of right ventricular volume overload (right ventricular enlargement with increased stroke volume) and without left ventricular disease and pulmonary arterial hypertension (no evidence of non-invasive PAP elevation, or invasive if such findings are present, PVR <3WU) closure of the ASD is recommended regardless of the symptom (class I, level of evidence B). Closure with a device is recommended for secundum ASD in technically eligible patients (class I, level of evidence C).<sup>18</sup> When performing shunt and hemodynamic evaluation in ASD patients, both structural examination and color and spectral Doppler examination should be performed. The shunt direction from the ASD is usually left to right, but in the presence of significant pulmonary hypertension, the shunt direction can be right-to-left or bidirectional.

Besides color Doppler, pulse wave spectral Doppler is useful to determine the shunt's direction. Besides color Doppler, pulse wave spectral Doppler's settings of the color scale must be optimized for low velocity of shunting (25-40 cm/sec). In cases with mitral stenosis, impaired LV compliance, or increased pressure from LV outflow obstruction, a higher-rate left-to-right shunt will occur. The amount of shunt may be calculated by the ratio of pulmonary blood flow (Qp) to systemic (Qs) blood flow. This is calculated from the formula by measuring the maximum systolic diameters of the RV and LV outflow tract and systolic velocity time integrals (VTI) obta-

ined with pulse wave Doppler.<sup>19</sup> This method has been compared with oxymetric methods and has been validated in the presence of accompanying pathologies such as pulmonary hypertension, mitral and tricuspid regurgitation, ventricular septal defect and Eisenmenger syndrome.<sup>20</sup> Dilatation in the right heart chambers should be evaluated. The grade of dilatation is related with relative compliance of these structures and the relative systemic and pulmonary vascular resistances, as well as the size of the ASD. In most patients, greater compliance of the RV compared to the LV and lower resistance of the pulmonary circulation compared to the systemic circulation result in a clear left-to-right shunt that leads to dilatation of the RV. A right ventricle diameter over 41 mm at baseline and over 35 mm in middle indicates RV dilatation. Additionally, a longitudinal diameter over 83 mm indicates RV dilatation.<sup>21</sup> RV end-diastolic volume measured by 3D echocardiography and indexed by body surface area is considered increased if it is  $\geq 87$  mL/m<sup>2</sup> in males and  $\geq 74$  mL/m<sup>2</sup> in females.<sup>22</sup> When volume overloads, in case of left-to-right shunt via the ASD, as the RV expands, the interventricular septum is displaced towards the LV in diastole, causing diastolic septal flattening. Systolic septal flattening may also be present in patients with ASD and pulmonary hypertension. Visual recognition of diastolic and systolic ventricular septal flattening is useful for diagnosis of RV volume and/or pressure overload. Examination of pulmonary hypertension is a mandatory stage of the echocardiographic evaluation of an ASD before intervention. Systolic PA pressure is calculated from tricuspid regurgitation jet velocity (V) and RV systolic pressure using the Bernoulli equation: RV systolic pressure =  $4(V)^2$  + estimated RA pressure. Normally, the peak RV systolic pressure must be lower than 30-35 mm Hg. PA diastolic pressure may be calculated for pulmonary regurgitation end-diastolic rate, and mean PA pressure may be calculated the peak pulmonary regurgitation diastolic rate.<sup>23</sup> With ongoing RV volume overload and increasing PA flow over time, some patients develop pulmonary hypertension (PH) and a smaller percentage may develop irreversible pulmonary vascular disease.<sup>24</sup> The type of ASD is also associated with the frequency and rate of pulmonary hypertension. Sinus venosus-type defects are associated with pulmonary hypertension earlier and more frequently than with secundum ASDs.<sup>25</sup> ESC guidelines require right heart catheterization to calculate PVR for all patients with pulmonary hypertension findings before deciding on closure. Percutaneous closure is not recommended for patients with PVR  $\geq 5$  WU, fenestrated ASD closure can be considered when PVR falls below 5 WU after targeted PAH therapy and in the presence of significant left-right shunt ( $Q_p/Q_s > 1.5$ ) (class IIb, level of evidence C). In the presence of significant shunt in patients with PVR between 3-5 WU, ASD closure is recommended as class IIa, level of evidence C.<sup>18</sup>

LV diastolic dysfunction that occurs with age can increase the left-to-right shunt, resulting in worsening of RV volume overload. Such patients are risky for acute heart failure after closing their ASD. Pre-procedural echocardiographic examination of LV diastolic function, together with evaluation of mitral inflow and annular velocities, can recognize such kind of patients. LV diastolic function abnormality may be masked by the ASD and pressure equalization between the left and the right heart. In these patients, it is recommended to determine the patients at risk of pulmonary edema with the balloon occlusion test and measurement of the LA pressure before the ASD closure procedure, and to make a decision by carefully weighing in terms of closing / closing by fenestrated device/not closing.<sup>18, 26</sup>

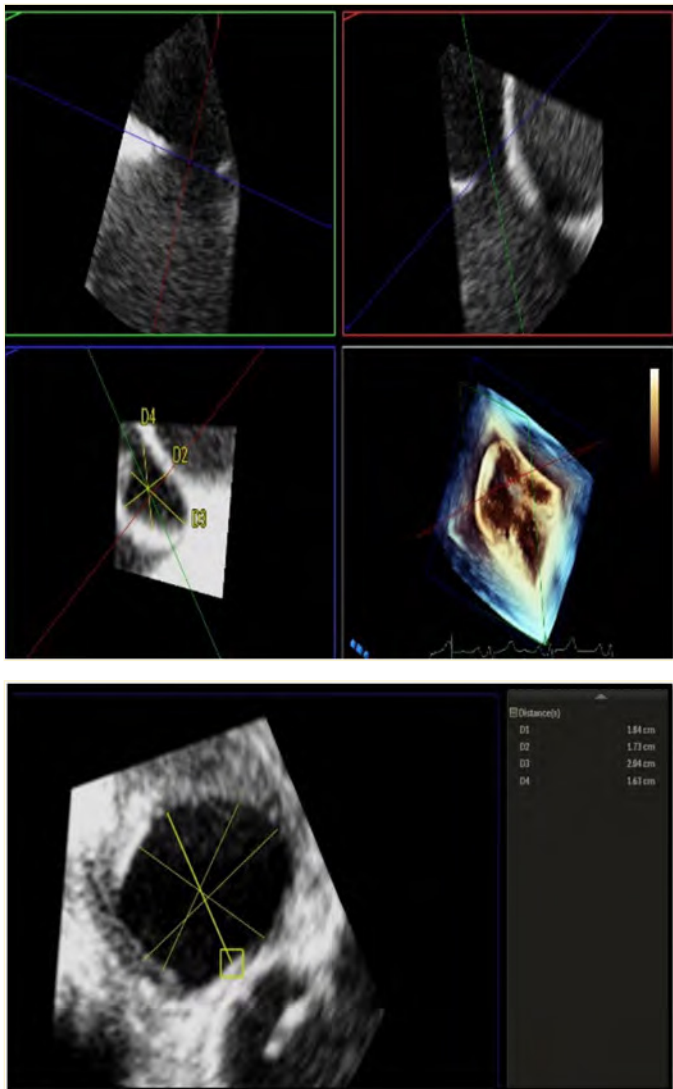


Figure 12. Measurement of the defect diameter with MPR in 3D-TEE.

### Measurement of ASD Size

The ideal defect for percutaneous transcatheter closure is a single ASD with intact and adequately sized rims with a maximum diameter of less than 20 mm, but defects lower than 40 mm in diameter may be repaired percutaneously.<sup>27</sup> As the ASD size change during the heart cycle; the maximal ASD diameter should be measured at the end of ventricular systole.<sup>28</sup> The change in ASD diameter of 50% or more according to the cardiac cycle is named "dynamic ASD". These is a situation that increases the risk of erosion.<sup>4</sup> If the maximal two-dimensional measurements, taken in all TEE planes [0, 45, 90, 135] are similar (1–2 mm) the largest measurement gives the ASD size. If the measurements differ significantly ( $\geq 3$  mm), it is recommended to reveal the shape of the defect with 3D TEE and take measurements. It is recommended to calculate the device size to be selected as the measured ASD size plus 20%.<sup>29</sup> However, it is recommended to add 25% in the presence of atrial septal aneurysm or in the absence of aortic rim.<sup>30</sup> The maximal jet width measured by color Doppler echocardiography is directly proportional to the surgically measured diameter of the defect in both TTE and TEE measurements, but it may cause an error when only this measurement

is used; therefore, it is recommended to rely on 2D or 3D measurements without color Doppler. Variability in color quality and color settings between devices can cause excessive coloration on the atrial septum, resulting in an overestimation of the true defect diameter.<sup>31</sup> 3D multi-plane reconstruction (MPR) provides a detailed evaluation of ASD and rims and is the gold standard method for measuring defect diameter. With 3D imaging, true long and short axis diameters of the defect are obtained quickly and more accurately (Fig. 12). 3D TEE ASD measurements appear to be more accurate compared to 2D. The latest 3D softwares allows measurements of the ASD diameter from the live 3D image instantly and directly from the live 3D image and make it available during the procedure.<sup>30, 32</sup>

Balloon sizing is an alternative method for determining the diameter of the defect and thus the size of the device. During the procedure, the balloon, which is inflated over the full defect by placing a mixture of opaque material and saline, is monitored echocardiographically and the measurement is taken with Color Doppler as soon as the flow is lost across the defect (stop flow technique). The central narrowest part of the inflated balloon gives us the diameter of the defect. The same measurement is also checked over the scope. This diameter is equal to the device diameter to be used. Even in patients with aortic rim deficiency, a device 2–4 mm

Table 4. Assessment of ASD, rims and periprocedural imaging by TEE

Anatomic rim	Atrial septal anatomy	Probe orientation	Suggested multiplane angles	Procedural assessment
Aortic rim	Superior/ anterior rim between the ASD and the AoV annulus and aortic root	Mid-esophageal/ short axis view	30, 45, 60, 75	Device relationship to AoV and posterior atrial wall
AV valve rim	Inferior/ anterior rim between the ASD and the AV valves	Mid-esophageal/ four-chamber view	0, 15, 30	Device relationship to AV valves
SVC rim	Superior/ posterior rim between the ASD and the SVC	Mid-esophageal/ bicaval view	90, 105, 120	Device relationship to RA roof/ dome
IVC rim	Inferior/ posterior rim between the ASD and the IVC	Mid-esophageal/ bicaval view	90, 105, 120	Device relationship to RA roof/ dome
Posterior rim	Posterior rim between ASD and posterior atrial walls	Mid-esophageal/ four-chamber view	0, 15, 30	Device relationship to posterior atrial wall
Right upper pulmonary vein (RUPV) rim	Posterior rim between the ASD and the RUPV	Mid to upper esophageal/ basal transverse view	0, 15, 30, 45	Device relationship in atrial roof

larger than the balloon diameter should not be used due to the risk of erosion. Many centers, like ours, have abandoned the routine application of balloon sizing due to the publications that stretched ASD diameter measurement in this way can lead to an increase in the diameter of the defect, and especially the highly successful

diameter measurements of 3D echocardiography. However, it may be useful in cases such as floppy rims or multiple defects.<sup>33</sup>

### Measurement of the ASD Rims

It is crucial to measure all of rims on TEE procedure to analyze if

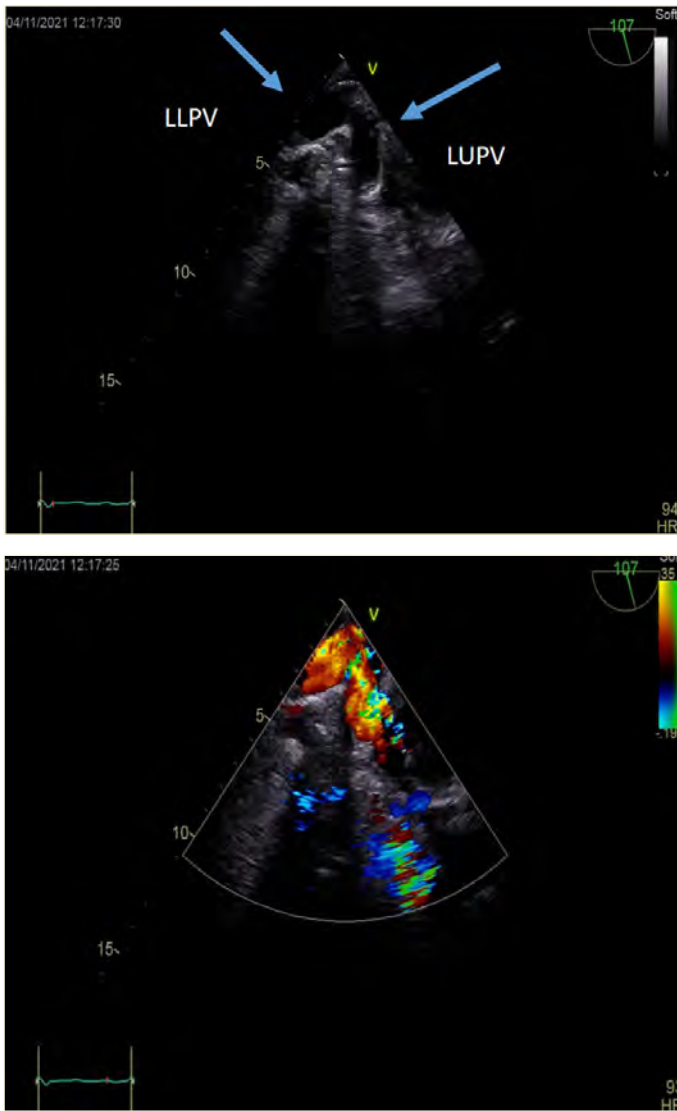


Figure 13. Imaging of the pulmonary vein.

the patient is suitable for PTC. The edges (rims) of the surrounding tissue are named according to the surrounding adjacent anatomical structures. The strength and integrity of the rim tissue is important, thin and loose rims are unlikely to have the strength to hold the device disc, despite appearing to be of sufficient length. Conventionally, surrounding tissue contains six anatomic rims (Table 4). The minimal two-dimensional measurement of rims are taken into account. Measurements should be made from the thick parts of the rims, thin and weak parts should not be included in the measurement (Fig. 9A,B; 10B). Rims should be more than 5 mm in length, the most important rim is the inferior vena cava (IVC) rim. The minimum two-dimensional dimension of the rims must be taken into account and must be at least 5 mm long. The most important and indispensable rim is the inferior vena cava (IVC) rim. Adequate SVC, RUPV, IVC, and AV valve rims are essential for transcatheter ASD closure. More than 40% of patients with ASD have aortic rim <5 mm (Fig. 10A). Although missing aortic rim is not an absolute contraindication for device closure, it is a potential risk factor for erosion.<sup>34</sup> However, as the increasing experience, defects with less rims can be successfully closed. PTC is not recommended if two or more rims are missing. The rims and features to be considered in the patient evaluated for ASD closure are given in Table 4.

### Associated Anatomical Findings

#### Partial Anomalous Pulmonary Venous Return (PAPVR)

PAPVR is relatively rare, only occurring in 0.1%–0.4% of the adult population.<sup>35</sup> Although it can also be seen in isolation, it more frequently accompanies sinus venosus type defects, but it can also rarely seen with secundum type defects. In the adult population, most abnormal pulmonary veins occur in the left upper lobe, less frequently in the right upper lobe.<sup>4, 36</sup> To view right pulmonary veins, the probe should be put at mid-oesophageal level at  $45^{\circ} \pm 10^{\circ}$ , rotated clockwise and gradually withdrawn until veins are visualised. Left pulmonary veins may be examined by placing the probe at mid-oesophageal level at  $120^{\circ} \pm 10^{\circ}$ , rotating counterclockwise with gradual withdrawal (Fig. 13A, B).<sup>37</sup> Pulmonary vein imaging is an indispensable part of ASD imaging, and the orifices of all four pulmonary veins should be visualized before the procedure, in case of doubt, cardiac MRI or multislice CT angiography should be examined, and cases with return anomaly should be referred to surgical closure (Fig. 14A–C).

#### Multiple Defects

To exclude the presence of multiple ASDs, the atrial septum should be scanned with color Doppler and 3D TEE (Fig. 15A, B). In 7.3% of

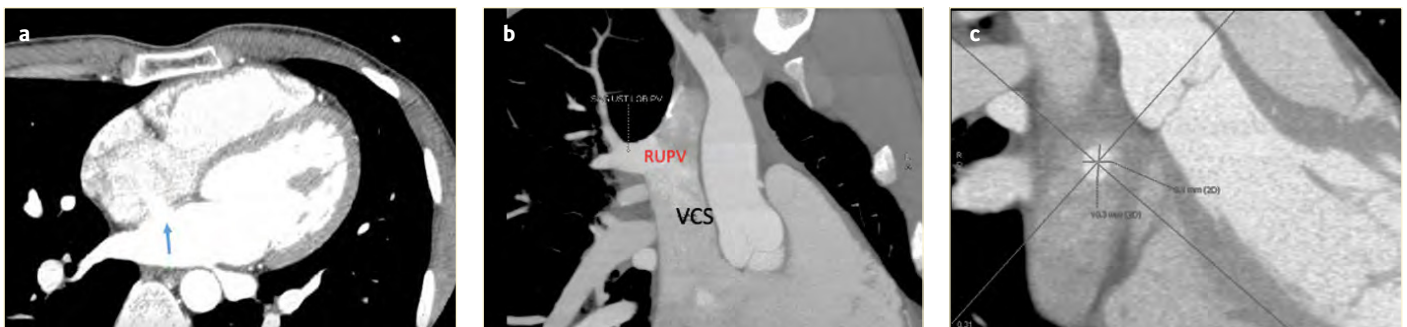
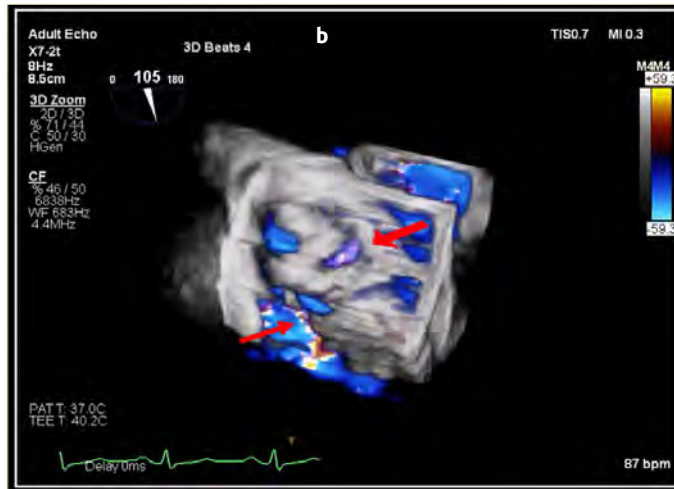
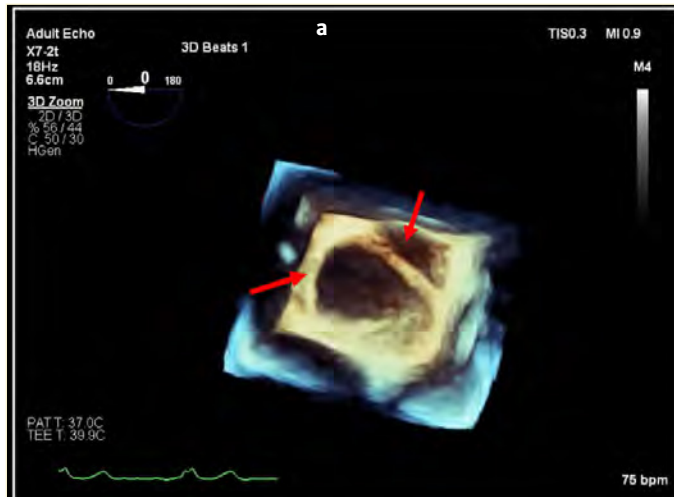


Figure 14. A–B–C. (A) Demonstration of left-to-right shunting in a patient with secundum type ASD using multislice CT angiography. (B) Demonstration of partial anomalous pulmonary venous return in a patient with secundum type ASD using multislice CT angiography, showing the right upper pulmonary vein draining into the superior vena cava (SVC). (C) Measurement of the defect diameter in a patient with secundum type ASD using the MPR method.



**Figure 15. A-B. Imaging of multiple defects with 3D TEE.**

patients with secundum type ASD, multiple defects are detected.<sup>38</sup> In patients with multiple defects, the distance between the defects is important to determine the number of devices to be used. If this distance is 7 mm or less, closure can be done with a single device. A major concern in the presence of two separate septal defects is the possibility of missing additional defects. Apart from scanning with 3D TEE and color Doppler, scanning can be performed along the entire septum with color Doppler, following the closure of the existing defect with a balloon during the procedure.

### Atrial Septal Aneurysm

ASA is an excess or saccular deformity of the atrial septum which leads to increased mobility. ASA is defined as a combined deviation of 10 mm or a total of 15 mm from the plane of the atrial septum to the RA or LA. ASA has been associated with multiple septal fenestrations (multi-fenestrated ASD) (Fig. 16A, B). It is crucial to measure the size of an ASD associated with a septal aneurysm, as ASD with a defect diameter (<20 mm) can be closed using a PFO closure device. An ASD closure device should be used when the associated defect diameter is >20 mm.<sup>39</sup>

### Eustachian Valve

As an embryologic remnant that lies at the junction of the inferior vena cava and right atrium, the valve size and proximity to

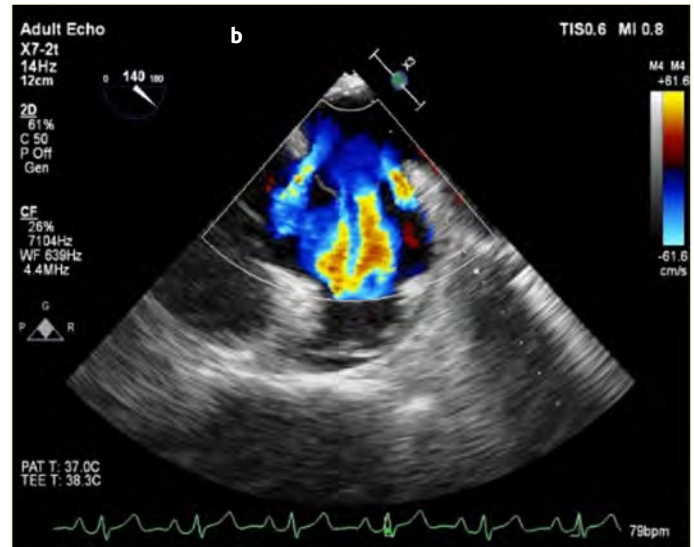
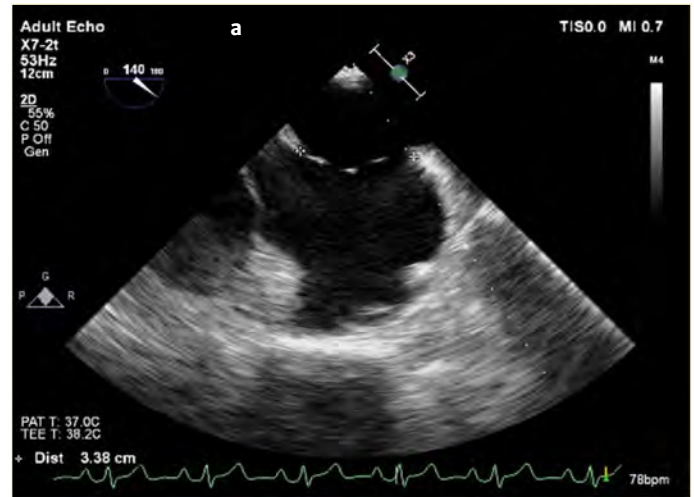


**Figure 16. A-B. Multifenestrated ASD: Visualization of four distinct defects on the septum in the same patient and the left-to-right shunting from each defect with color Doppler.**

the IAS must be calculated in the echocardiographic evaluation. A large valve close to the IAS, may interact with the device during opening of the RA disc of the closure device, may lead to inaccurate assessment of the defect and creating difficulty during the procedure. In such cases, it is recommended to perform the closure procedure with TEE guidance.<sup>4</sup>

### Chiari Network

The Chiari network can interact with wires, catheters, sheaths, cables, and devices as they pass through the RA. Therefore, investigation of the presence of Chiari network before device closure of the ASD should be part of the echocardiographic evaluation.<sup>4</sup>

### Cardiac Magnetic Resonance Imaging (CMR)

In recent years, CMR has emerged as an important imaging modality. CMR has dramatically evolved for congenital heart disease.<sup>40</sup> It offers superior temporal and spatial resolution, lesser operator dependence, large field of view, 3D multiplanar imaging, detailed cardiovascular anatomical imaging and highly accurate and reproducible measurements and calculations about cardiovascular physi-

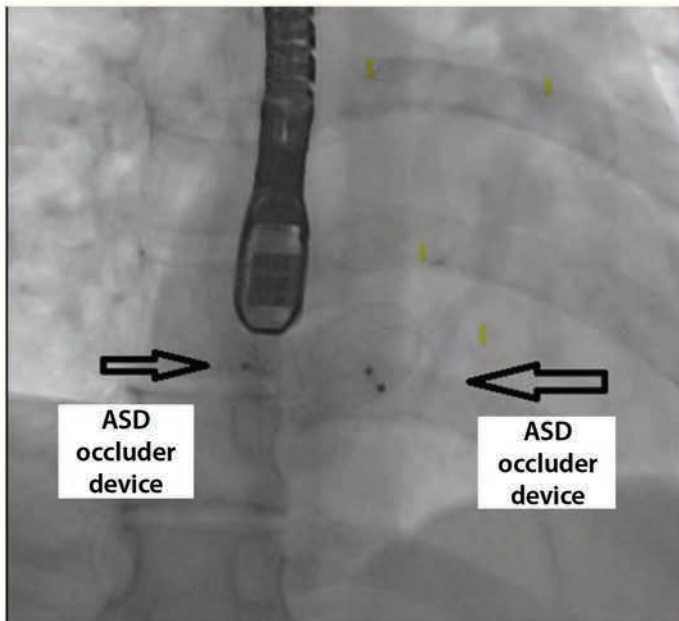


**Figure 17.** Imaging of two ASD closure devices implanted in the patient using cinefluoroscopy. In a patient with multifenestrated ASD, four defects located in the interatrial septum have been closed with two different devices.

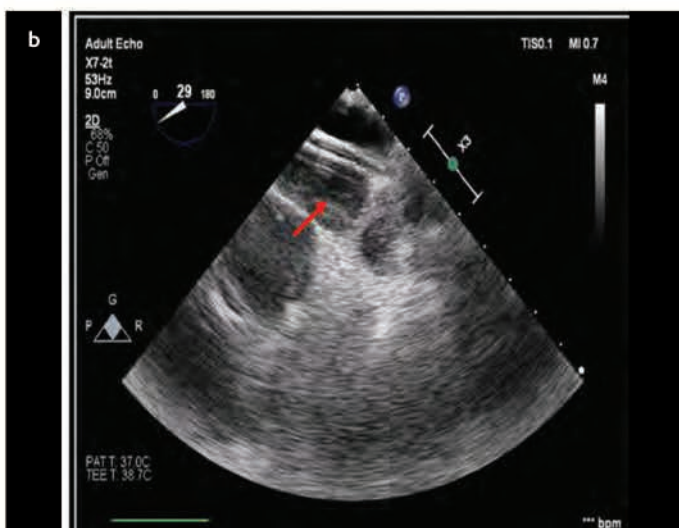
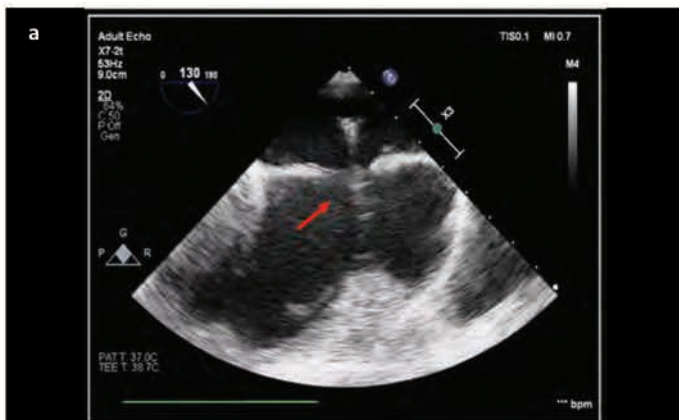


**Figure 18. A-B.** Visualization of the guide wire passing through the defect during the procedure and its positioning in the left upper pulmonary vein.

ology. It is the gold standard imaging method for right heart volume evaluation.<sup>41</sup> In patients with ASD, phase contrast CMR allows 3D en-face visualisation of the defect. Diameter can be measured, cardiac volumes can be calculated, and shunt ratio can be measured directly. CMR-derived defect dimensions are strongly correlated with balloon sizing results and are superior to 2D TEE measurements. CMR is very successful in detecting concomitant intracardiac and extracardiac anomalies like PAPVR. It is also very successful in imaging the posterior inferior rims, which are difficult to visualize with TEE. In a study, it was found that more than 70% of patients with deficient posterior inferior rim on TEE actually had sufficient rim on CMR and suitable for percutaneous closure.<sup>42</sup> Defects in floppy thin septums can be missed with cardiac MRI, and alternative imaging techniques should be used in these patients. Again, the use of MRI is limited in prosthetic valve patients, patients with claustrophobia, and patients who cannot hold their breath well.

### Cardiac Computed Tomographic Imaging

Cardiac computed tomography (CCT) has recently undergone major technological developments that currently allow quantification of cardiac morphology and function with low-dose radiation exposure in congenital heart disease. With CT, the Qp/Qs ratio can be measured non-invasively, the diameter and shape of the defect can be determined, and rim measurements can be made. The Qp/Qs ratio calculated with CT is correlated with right heart catheterization (Fig. 14A). The use of CT in the evaluation of ASD is presented as a reliable option and provides an opportunity to recognize additional malformations such as pulmonary venous return anomaly (Fig. 14B). Defect diameter and rims measured by the MPR (multiplanar reconstruction) method provide results in good correlation with TEE (Fig. 14C). Right and left heart volumes can also be measured. In addition, concomitant coronary artery anomalies and coronary artery stenosis can be observed simultaneously, especially in older patients. The use of contrast material and radiation exposure, are important hazards of CCT.<sup>43, 44</sup>

### Intraprocedural Imaging

#### Cinefluoroscopy

Cinefluoroscopy is an imaging method used in the catheter laboratory during the percutaneous closure procedure. Intraprocedural fluoroscopic imaging is complementary to echocardiography. Cinefluoroscopy specifically guides the interventional cardiologist during advancement, placement, and release of guidewire and closure device (Fig. 17).

#### Echocardiography

It is the primary imaging modality for procedural guidance during percutaneous transcatheter closure of ASDs. Real-time procedural echocardiography with TTE, TEE, 3D imaging or ICE acquires essential data before, during and after device insertion. While each imaging modality has its own advantages and disadvantages, all offer useful and detailed information for patient and device selection, procedural guidance, monitoring complications, and outcome evaluation. Transthoracic echocardiography is the least invasive imaging method and may be sufficient for procedural guidance, especially in children and smaller patients. Limitations include poor image quality and device-related artifacts in larger patients. Using TTE has the advantages of shorter procedure time, shorter hospital stay, and lower cost due to avoidance of general anaesthesia.<sup>45-47</sup>

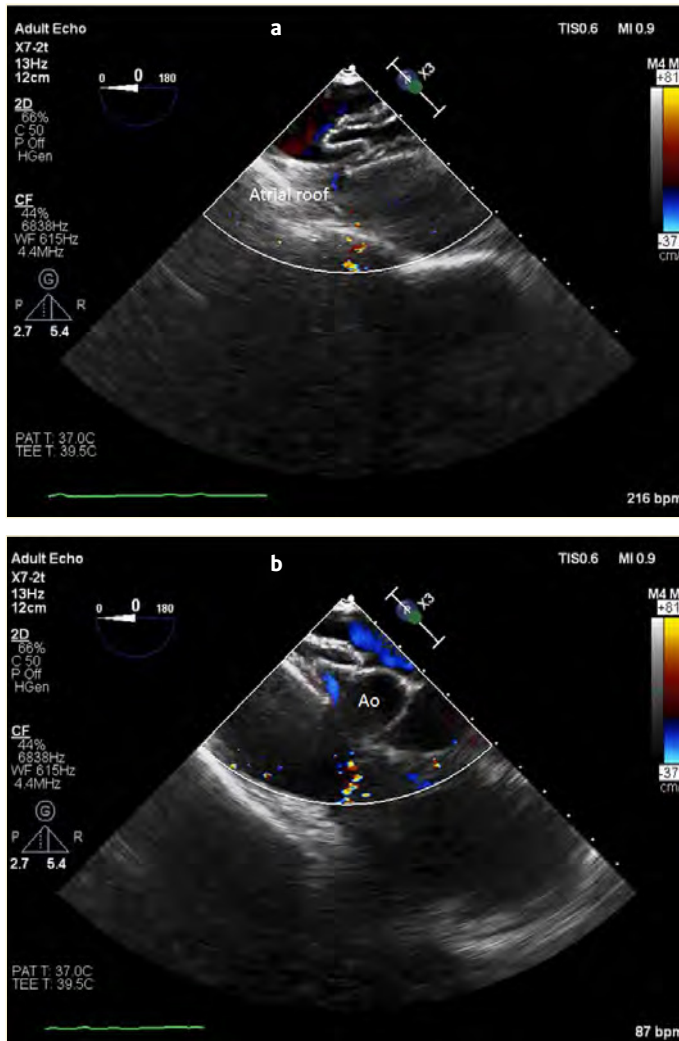


**Figure 19. A-B. Evaluation of the device's relationship with surrounding structures on all rims before releasing the device during the procedure, and residual shunt control.**

Transesophageal echocardiography provides more detailed information during the procedure. The disadvantage is that it requires conscious sedation or general anesthesia to reduce patient comfort and aspiration risk. During TEE-guided closure, a guide wire is advanced through the defect and left atrium, and is usually inserted into the left upper pulmonary vein (LUPV) (Fig. 18A, B). The echocardiographer should follow the guidewire on the mid-esophageal 40°-60° view and verify proper positioning from the RA through the defect and left atrium to the LUPV. With Live 3D imaging, guide catheters can be clearly observed and the operator can be guided simultaneously. Since the left atrial appendage is a thin-walled structure, it is important to prevent catheters and rigid guidewires from causing perforation and pericardial effusion. After the device is loaded into the delivery sheath, the insertion should be performed under the guidance of TEE. After making sure that the tip of the sheath is on the left atrium, the left disc can be inserted. The device is then pulled back towards the IAS under TEE guidance so that the bottom of the device captures the aortic rim or aortic root. The device is then retracted towards the RA until its upper portion captures

the upper portion of the ASD. With TEE, after ensuring that the LA disc is well positioned at the edges of the ASD, the right atrial disc of the device is opened within the RA and the device grasps the edges of the defect. The imager should confirm good apposition of both discs and evaluate the residual shunt (Fig. 19A, B). In addition, according to guideline recommendations, the device relationship with the AoV, posterior atrial wall, AV valves, and atrial roof should be evaluated (Table 4). In patients with inadequate IVC rim, it may cause obstruction of IVC or CS flows. In the presence of an insufficient AV rim, the device may interact with the mitral leaflets to produce mitral regurgitation. In the presence of insufficient SVC rim, SVC and RUPV currents may be compromised. Small residual shunts from the central or device edge are not uncommon. These are not clinically significant and disappears after endothelialization of the device. In the absence of the aortic rim, the device placed around the aorta should demonstrate a typical "Y" pattern. If this view is not present, the device must be repositioned due to the risk of erosion. The ASD occluder device is released after Minnesota maneuver.<sup>4, 35</sup>

### Postprocedural Imaging

In the early period, TTE should be performed the day after device insertion. TEE is usually performed when a clinical complication is suspected or cannot be decided with TTE. Immediately after the procedure, the presence of shunt should be evaluated with color Doppler and contrast echocardiography with agitated saline. In addition, the device and adjacent anatomical structures, improper placement of the device, aortic, mitral, or tricuspid valve functions, vena cavae, CS or pulmonary venous return obstruction, and pericardial effusion should be evaluated. Long-term follow-up with TTE should be performed at 3, 6, and 12 months after the procedure and thereafter, when clinically indicated. Residual shunts should be re-evaluated for long-term follow-up. In 7% of cases, there is a residual shunt in the early period immediately after the device is released. In the long term, complete shunt closure rates have been reported in 97% of cases.<sup>49</sup> Heart structure and functions usually normalize after ASD closure. RV volume overload is reversed in 3 weeks in children and in 1 to 9 months in adults after the procedure, and systolic pulmonary artery pressure almost normalizes in a few months.<sup>50, 51</sup>

### Conclusion

The most important parameter in successful percutaneous ASD closure is effective visualization of the defect and surrounding structures. Before the procedure, the location, size, shape of the defect and the adequacy of the rims should be determined echocardiographically. Although cardiac MRI, CT and intracardiac imaging methods can be used, but the main imaging method is TEE. In recent years, 3D TEE has provided very successful results in this regard and has become the gold standard imaging method in ASD evaluation. In cases with suboptimal TEE imaging or in case of additional congenital anomalies like venous return anomaly cardiac MRI or multislice CT angiography can be used. For intraprocedural imaging, intracardiac echocardiography eliminates the need for anesthesia and echocardiographer and provides satisfactory imaging. However, its access and use is very limited. Addition to optimal visualization of ASD, the experience and collaboration of the echocardiographer and interventional cardiologist are important factors that determine the success of the procedure.

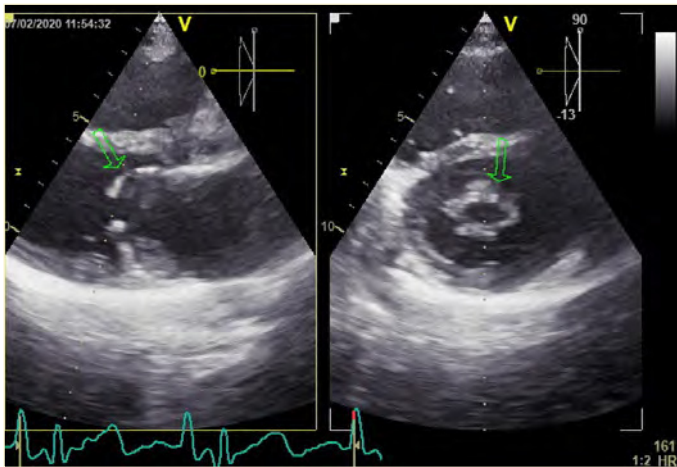


**Figure 20. Echocardiographic findings of rheumatic mitral stenosis. Thickening of the mitral valves and doming of the mitral anterior leaflet (left arrow), fish-mouth appearance of the mitral orifice opening due to commissural fusion (right arrow).**

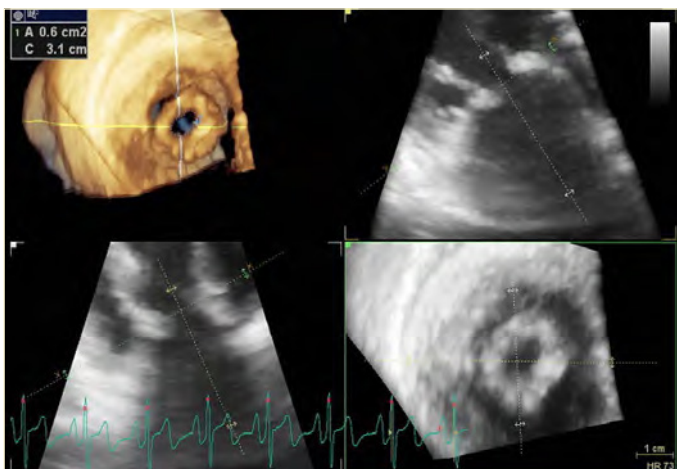


**Figure 21. Measurement of the mitral valve area with three-dimensional Transesophageal Echocardiography. The multiplane method allows for the measurement of the orifice area at the moment of maximum opening in diastole. The calculated mitral valve area is 0.6 cm<sup>2</sup>.**

## Imaging for Percutaneous Mitral Balloon Valvuloplasty

**Dr. Dilek Çiçek Yılmaz**

Percutaneous mitral balloon valvuloplasty (PMBV) is the procedure of choice in symptomatic patients with severe rheumatic mitral stenosis and suitable mitral valve anatomical features. Echocardiography plays a central role in all aspects of PMBV. The success of PMBV depends on the echocardiographic assessment of the pliability of the leaflets, the degree of degeneration and calcification of the commissures, subvalvular apparatus, annulus, and valve leaflets, and determination of the degree of mitral regurgitation at baseline. During the procedure, echocardiography is used to exclude left atrial thrombus, ensure optimal transseptal puncture, select the appropriate balloon size, determine the change in hemodynamics and degree of mitral regurgitation following each balloon inflation, and rapidly identify

complications. Procedural outcomes depend heavily on appropriate patient selection and definitive imaging.

### Introduction

Although there has been a steady decline in the incidence of rheumatic heart disease in industrialized countries, rheumatic mitral stenosis is still a common disease in the developing countries and it is a significant cause of cardiovascular mortality and morbidity.<sup>52</sup>

For treatment of rheumatic mitral stenosis, closed mitral commissurotomy was first described in 1948 and this was followed by open commissurotomy after the advent of cardiopulmonary bypass.<sup>53</sup> In 1984, a Japanese cardiac surgeon named Kanji Inuoe first described the technique of balloon mitral valvuloplasty.<sup>54</sup> Percutaneous mitral balloon valvuloplasty (PMBV) has since proven to be an effective procedure for patients with severe symptomatic rheumatic mitral stenosis, providing hemodynamic and clinical improvement and excellent results in patients with suitable mitral valve anatomical features.<sup>55-58</sup> European Society of Cardiology recommends PMBV as the first-line therapy in rheumatic patients with isolated significant mitral stenosis and feasible valve morphology.<sup>59</sup>

Echocardiography plays an important role in the diagnosis of rheumatic mitral stenosis, determining suitability for PMBV, intra-procedural guidance for PMBV, and postprocedural assessment.

**Table 5. Wilkins Classification for Echocardiographic Grading of Mitral Valve Features**

Grade	Mobility	Subvalvular Thickening	Thickening	Calcification
1	Only tips of mitral leaflets are slightly mobile	Minimal thickening just below the leaflets	Near normal thickness (4-5 mm)	Increased echogenicity in a localized area
2	Normal mobility in the mid and basal parts of the leaflets	Thickening in the chordal structures	Normal in the middle with thickening at the edges	Scattered bright spots at the edges
3	The valve moves forward especially from the base during diastole	Thickening extends to the distal third of the chords	Thickening affects the entire leaflet (5-8 mm)	Brightness reaching the middle parts of the leaflets
4	No or minimal forward movement in diastole	Widespread thickening and shortening of all chordal structures to the papillary muscle	Significant thickening of all leaflet tissue (>8-10 mm)	Intense brightness covering all leaflet tissue

### Diagnosis of Rheumatic Mitral Stenosis and Determining Suitability for PMBV

The characteristic imaging features of chronic rheumatic mitral stenosis include: (1) doming of the anterior mitral leaflet, where the narrowest orifice is at the leaflet tips creating a hockey stick deformity of the anterior mitral leaflet, (2) restricted mobility or immobility of the posterior mitral leaflets, (3) a fish mouth opening appearance of the mitral valve orifice caused by fusion

**Table 6. Padial Method for Echocardiographic Scoring Post- Percutaneous Mitral Valvuloplasty for Severe Mitral Regurgitation**

I-II	Thickening of the valve (score each valve separately)
	1 Leaflet near normal thickness (4-5 mm) or only one thick segment
	2 Leaflet uniformly fibrotic and/or calcified; no thin areas
	3 Leaflet irregularly fibrotic and/or calcified; thinner segments slightly thickened (5-8 mm)
III	Commissural calcification
	1 Fibrosis and/or calcium present only at one commissure
	2 both commissures mildly affected
	3 Calcium in both commissures, one markedly affected
	4 Calcium in both commissures, both markedly affected
IV	Subvalvular Disease
	1 Mild thickening in the chordal structures just below the valve
	2 Thickening extends one-third the length of the chord
	3 Thickening reaches the distal third of the chord
	4 Widespread thickening and shortening of all chordal structures to the papillary muscle
Total score, the sum of all echocardiographic criteria (maximum 16).	

of the commissures, and (4) subvalvular thickening and chordal shortening (Fig. 20, Video 5).<sup>60</sup> Doppler echocardiography is used to estimate the transmitral valve gradients. Adequate mitral valve area assessment is an important step before PMBV. The mitral valve area can be calculated using the pressure half-time method or measured by direct planimetry of the mitral orifice. However, the direct measurement of mitral valve area with planimetry is highly operator dependent and difficult. 2-dimension planimetry may overestimate the orifice area when patient image quality is poor or if the narrowest cross-sectional orifice is not properly identified. The reliability of the pressure half-time method is affected by changes in the preload or left ventricular compliance.

Three-dimensional (3D) echocardiography is superior in quantifying mitral stenosis severity and these 3D echocardiography area measurements are known to correlate strongly with area measurements derived invasively using the Gorlin formula.<sup>61</sup> Multiplanar reformations from 3D echocardiography images can consistently identify the smallest stenotic orifice for area measurements (Fig. 21, Video 6).

Although 3D echocardiography is a very beneficial tool to evaluate mitral valve, it is not widely available in developing countries. Therefore, the mitral leaflet separation index (MLSI) is proposed to reduce the discrepancy. This new index could be a useful surrogate measure of mitral valve area.<sup>62</sup> The MLSI measures the distance between the tips of the mitral leaflets in the parasternal long-axis and apical four-chamber views. The two readings are averaged to produce the MLSI as a reliable measure of mitral stenosis severity. In one study, MLSI index correlated as MLSI of 0.70 mm with MVA <1 cm<sup>2</sup> and 0.92 mm with MVA >1.5 cm<sup>2</sup>.<sup>63</sup> Several studies have reported a good correlation between MLSI and mitral valve area.<sup>63-64</sup> Mitral leaflet separation index is an easy and reliable measurement for the assessment of mitral stenosis before and after PMBV.<sup>65</sup> There was also a significant positive correlation between MLSI and 3D echocardiographic measurement of mitral valve area (r=0.93, P<0.001).<sup>66</sup>

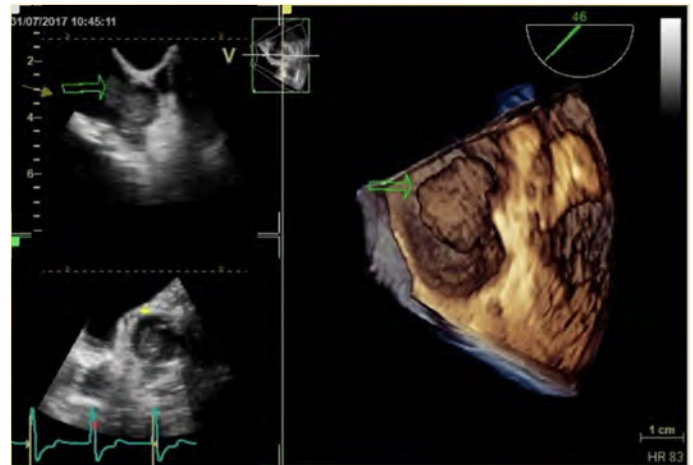


**Figure 22. A large thrombus (arrow) within the left atrial appendage as shown by three-dimensional Transesophageal Echocardiography.**

Echocardiography is also used to determine the severity of mitral regurgitation. For evaluation of mitral regurgitation, mitral valve quantification through 3D-transesophageal echocardiography (TEE) is a simple automated method, easily applicable to patients before PMBV.<sup>67</sup>

When considering intervention for mitral stenosis, we must carefully evaluate the anatomy of the mitral valve to determine the suitability and safety of the PMBV. The first and most widely used echocardiographic scoring system to predict success of PMBV is known as the Wilkins score.<sup>68</sup> Wilkins score takes into consideration the anatomical features of the leaflet, the commissures, and the subvalvular apparatus. The scoring system assigns a point value from 1 to 4 for each of the following: (1) valve calcification, (2) leaflet mobility, (3) leaflet thickening, and (4) subvalvular apparatus degeneration (Table 5). A mitral valve with a score of <8 to 9 with no more than moderate mitral regurgitation is deemed the best candidate for PMBV. In patients with a score of >9 to 10, especially with more than moderate mitral regurgitation, surgical therapy should be advised, except in cases with serious comorbidities. Moderate or severe mitral regurgitation at baseline is considered a contraindication to PMBV.

The development of severe mitral regurgitation following PMBV is an important cause of mortality and morbidity. Especially, significant bilateral or asymmetric calcium patterns in the commissures are associated with the development of significant mitral regurgitation following PMBV.<sup>69</sup> For prediction of severe mitral regurgitation after PMBV, Padial and colleagues refined the Wilkins score to incorporate the commissural calcium pattern (Table 6).<sup>70</sup> They described a new mitral regurgitation-echocardiographic (MR-echo) score that can predict the development of severe mitral regurgitation after mitral balloon valvuloplasty performed by the double balloon technique.

Stenotic mitral valve with a greater extent of commissural fusion may benefit more from PMBV than a valve without any commissural fusion, in which the stenosis is due to rigid leaflets or annular narrowing. In the latter circumstance, the leaflets or subvalvular apparatus may fracture during PMBV, resulting in worsening mitral regurgitation.

Nunes and colleagues demonstrated improved accuracy for predicting success with PMBV and the development of worsening mitral regurgitation using the commissural area ratio and leaflet displacement measurement.<sup>71</sup> These quantitative criteria incorporate both functional and morphologic features of rheumatic mitral stenosis to predict PMBV success and the likelihood of causing severe mitral regurgitation. Independent predictors of outcome were assigned a point value proportional to their regression coefficients: mitral valve area  $\leq 1$  cm<sup>2</sup> (2 point), maximum leaflet displacement  $\leq 12$  mm (3 point), commissural area ratio  $\geq 1.25$  (3 point), and subvalvular involvement (3 point). Three risk groups were defined: low (score of 0–3), intermediate (score of 5), and high (score of 6–11), with observed suboptimal PMBV results of 16.9%, 56.3%, and 73.8%, respectively. The use of the same scoring system in the validation cohort yielded suboptimal PMBV results of 11.8%, 72.7%, and 87.5% in the low-, intermediate-, and high-risk groups, respectively ( $P < 0.0001$ ). The model improved risk classification in comparison with the Wilkins score (net reclassification improvement, 45.2%;  $P < 0.0001$ ). Long-term outcome was predicted by age and postprocedural variables, including mitral regurgitation, mean gradient, and pulmonary pressure.<sup>71</sup>

In addition to measurement of mitral valve area, 3D echocardiography-based score for PMBV has been developed with improved predictive value of success compared with the 2D echocardiography-based Wilkins score.<sup>72</sup> This improvement was achieved by adding evaluation of the mitral commissural regions to the score and by allowing assessment of individual segments of each leaflet to acknowledge the uneven distribution of anatomic abnormalities in rheumatic mitral stenosis.<sup>12</sup>

### Intraprocedural Guidance for PMBV

Prior to PMBV, mitral valve should be evaluated for severity of the stenosis, the regurgitation and for the suitability for the procedure with a complete transthoracic echocardiogram. A transesophageal echocardiogram should be performed immediately prior to PMBV to exclude thrombus within the left atrium or left atrial appendage. Patients with left atrial or left atrial appendage thrombus should not undergo PMBV (Fig. 22, Video 7).

Transesophageal echocardiography or intracardiac echocardiography can be useful for guiding the transseptal puncture. TEE can visualize the transseptal needle and/or catheter within the left atrium and confirm successful puncture of the interatrial septum particularly in patients with severely dilated atria or abnormal interatrial septum anatomy (Video 8). The optimal location for

transseptal puncture for PMBV is in the middle or slightly posterior aspect of the fossa ovalis. TEE is also used to confirm the balloon position across from the mitral valve leaflets and to avoid damaging the subvalvular apparatus. Otherwise, misplacement of balloon beyond the valve may cause chordal rupture.

A critical factor in performing PMBV is selecting the appropriate balloon size. An undersized balloon may not alleviate the stenosis, whereas an oversized balloon may cause excessive damage to the commissures, leaflets, or subvalvular apparatus, leading to severe mitral regurgitation. Mitral annular diameter measured by echocardiography or distance between the 2 commissures in the apical 2-chamber view may be used to select the optimal balloon size.<sup>73</sup>

To assess the success of the procedure and the possible complications, echocardiography should be performed during PMBV. Echocardiographic images must be obtained to determine the transmitral valve gradients and severity of mitral regurgitation after each successive balloon inflation.

### Postprocedural Assessment

After the PMBV procedure, we must assess the leaflet mobility, morphology of the leaflet, transmitral valve gradients, mitral valve area and the presence of mitral regurgitation and pericardial effusion.

Prediction of late favorable results is multifactorial and strongly determined by age, previous symptoms and post-procedural mitral valve area.<sup>74</sup> Immediately after the PMBV, the mitral valve area should be measured by direct planimetry rather than calculated by the pressure half-time method. The pressure half-time method for calculating mitral valve area has been shown to be inaccurate immediately after PMBV before chamber compliance has had sufficient time to adjust to relief of stenosis.<sup>75</sup> The pressure half-time is highly dependent on chamber compliance, which changes dramatically over time after PMBV.

Severe mitral regurgitation after mitral balloon valvuloplasty is a major complication of this procedure. This complication confers an adverse prognosis and frequently requires intensive treatment and urgent mitral valve surgery.<sup>76</sup> The mechanism of severe mitral regurgitation after PMBV is most often due to leaflet tears and the incidence of severe mitral regurgitation has been reported to be between 1% and 9% following PMBV.<sup>56,77</sup> Nunes et al studied mechanisms of mitral regurgitation with 3D echocardiography after PMBV.<sup>78</sup> In this study, significant mitral regurgitation was found in 18.6% of patients following PMBV based on quantitative echocardiographic parameters, with severe mitral regurgitation in 6.7% of patients. Four mechanisms for the development of mitral regurgitation were identified, with major differences in outcomes. Mitral regurgitation resulting from tearing along nonanatomic planes of the valve, especially at the central scallop of the anterior leaflet, was mostly associated with severe hemodynamic impairment requiring emergency surgery. The study concluded that it is not the severity of mitral regurgitation but its mechanism that decides long-term prognosis besides obtained mitral valve area and net atrioventricular compliance.<sup>78</sup>

In conclusion, PMBV is the procedure of choice in symptomatic patients with severe rheumatic mitral stenosis and suitable mitral valve anatomical features. Echocardiography plays a central role in all aspects of PMBV.

**Table 7. Imaging Modalities Efficacy for TAVI (Transcatheter Aortic Valve Implantation)**

	TTE/TÖE	CT	MRI	Fluoroscopy
Aortic stenosis severity	+++	+	++	+
LV function	+++	+	++	-
LV septal thickness	+++	++	++	-
Accompanying valve disease	+++	+	+++	-
Aortic valve annulus diameter	+++	+++	+++	++
Aortic valve anatomy	++	+++	++	-
Valve calcification	++	+++	-	++
Aortic root measurements	++	+++	+++	++
Coronary artery height	±	+++	+++	±
Coronary artery disease	-	++	++	+++
Peripheral artery disease	-	+++	++	++
Peripheral artery calcification	-	+++	-	+

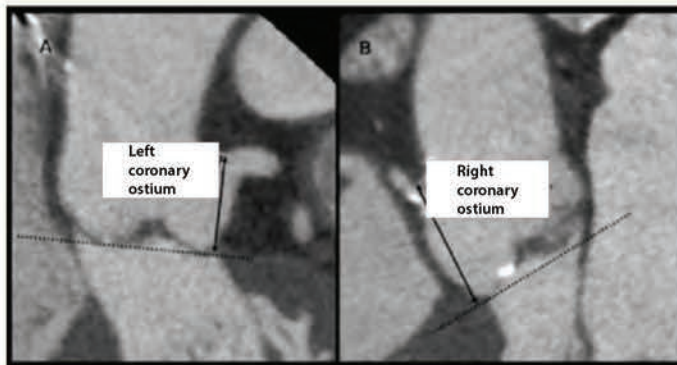


**Figure 23.** Measurement of the distance between the aortic valve annulus plane and the coronary artery ostia.

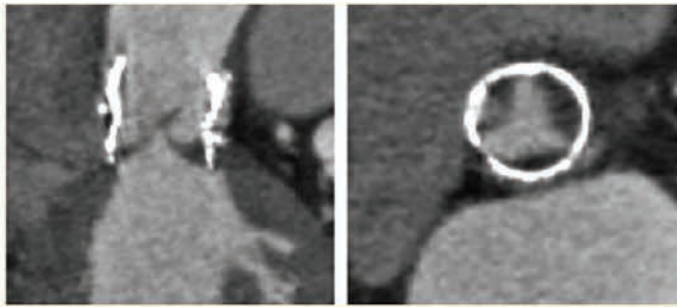


**Figure 24.** Subclinical valve thrombosis with hypoattenuated thickening observed in all three leaflets.

## Imaging Techniques in TAVI Procedures

*Dr. Volkan Kozluca, Dr. Türkan Seda Tan Kürklü,  
Dr. İrem Müge Akbulut Koyuncu, Dr. İrem Dinçer*

Surgical treatment is considered in patients with symptomatic aortic stenosis but one third of these patients are not suitable for this treatment due to reasons that increase the surgical risk (advanced age, frailty, comorbidities). Transcatheter aortic valve implantation (TAVI) appears to be a less traumatic alternative for these patients because of not requiring thoracotomy and cardiopulmonary bypass. In patients with high operative risk, TAVI is superior to medical treatment and noninferior to surgical valve replacement in clinical outcomes.<sup>79</sup>

The support of imaging methods is essential for planning and performing the TAVI procedure. While echocardiography is mostly used to diagnose valve disease, computed tomography (CT) enables vital measurements such as vascular access site, iliofemoral diameters, aortic annulus and coronary height measurements. Fluoroscopy is used to perform coronary angiography before the procedure and aortography for valve alignment during implantation. Echocardiography is also used to monitor possible complications (pericardial fluid, etc.) and valve functions (paravalvular leak, mitral valve function, etc.) after the procedure.<sup>80, 81</sup> Table 7 summarizes the effectiveness of various imaging modalities for TAVI.

### The Role of Multi Detector Computed Tomography (MDCT) in Transcatheter Aortic Valve Implantation (TAVI)

In recent years with the increasing number of detectors, visualisation of the entire cardiac structure with a single breath hold of the patient is possible. The temporal resolution has increased

with the developing dual-origin scanner technology. As a result, MDCT has become the standard procedure for the evaluation of the aortic valve, aortic root, descending aorta and iliofemoral vascular system before TAVI. MDCT has a critical role in obtaining the aortic annulus measurements and choosing the correct prosthesis valve size. MDCT images that are obtained before the procedure are also used to determine the optimal fluoroscopic co-planar projection during valve implantation. In order to make a proper evaluation, MDCT should have a minimum of 64 detectors and should be electrocardiography (ECG) gated.<sup>82, 83</sup>

### Evaluation of the Peripheral Vascular Access

Despite the shrinkage in device profiles over the years, the incidence of major vascular complications related to TAVI is still around 7.9%. As a result, pre-procedural evaluation of the abdominal aorta and the iliofemoral tract with MDCT in terms of vessel diameters, wall calcifications (especially circumferential), minimal luminal diameters, atherosclerotic plaque burden, vessel tortuosity, dissections, complex atheromas, occlusive and aneurysmal disease is crucial. Studies have shown that the evaluation of the peripheral vascular tract with contrast-enhanced MDCT is superior to conventional 2D angiography. MDCT is also superior to conventional 2D angiography in the evaluation of calcification and tortuosity. Standard MDCT evaluation includes 3D volume rendering, curved multiplanar reformat (MPR) and maximum intensity projection (MIP). In 10-15% of the cases, transfemoral access for TAVI is not suitable and alternative access routes like transapical, transaortic, transaxillary, transcarotid and transcaval are used. MDCT is also the standard procedure for evaluation for these alternative routes.<sup>84, 85</sup>

### Evaluation of the Aortic Root and Aortic Valve Anatomy

With current MDCT systems, the aortic root can be evaluated with minimal section thickness (0.5-0.75 mm), allowing oblique reconstruction without sacrificing spatial resolution. With the help of MDCT; the aortic root diameter, distance to coronary ostia, diameters of sinus Valsalva and sinotubular junction and the aortic valve morphology can be evaluated prior to TAVI.

MDCT has become the standard procedure, especially for the measurement of the aortic annulus. The aortic annulus undergoes conformational change throughout the cardiac cycle and is largest at systole. Therefore, the annular measurements should be carried out in the systolic phase and at maximal valvular opening. Aortic annulus measurements are made from the lowest hinge point of the aortic valve leaflets, both on the long and short axis. Accurate annulus measurement is crucial in selecting the correct prosthesis valve size. Incorrect measurements may lead to improperly sized valve implantation and paravalvular regurgitation. In recent years, it has been shown that measurement of the annulus perimeter and cross-sectional area rather than the annular diameter reduces paravalvular aortic regurgitation after the procedure.<sup>86</sup>

MDCT is also useful in the evaluation of the number of aortic valve leaflets and the degree of calcification. The echocardiographic evaluation of valvular calcification may be insufficient due to acoustic shadowing. MDCT, on the other hand, perfectly shows the localisation and degree of aortic valve calcification, owing to its high spatial resolution. MDCT allows reconstruction in the plane of coronary ostia and measurement of the distance

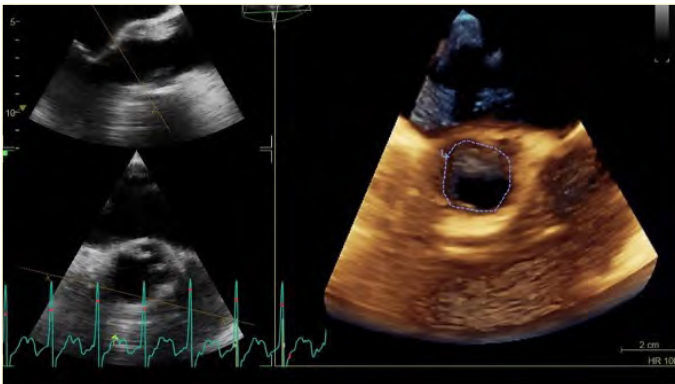


**Figure 25. Manual aortic annulus measurement with 3D multiplanar reconstruction.**

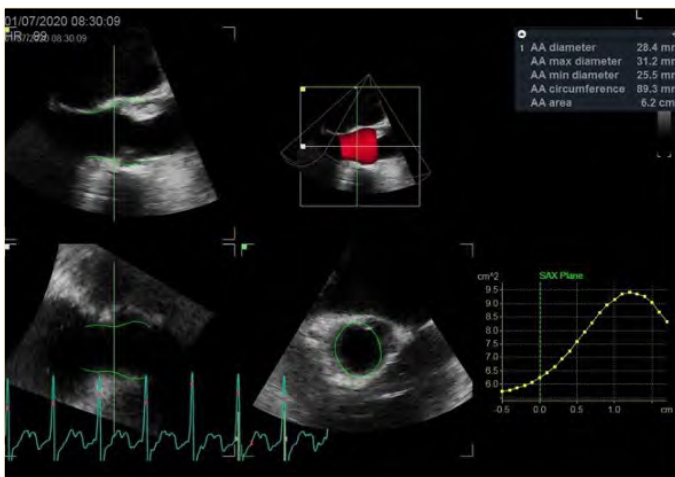


**Figure 26. Semi-automatic aortic annulus measurement with 3D imaging.**

between the annulus and left main coronary artery ostium, owing to the multiplanar and 3D techniques (Fig. 23). As a result, procedural coronary obstruction risk is significantly reduced.<sup>87</sup>

### Evaluation of Concomitant Cardiac Pathologies

MDCT provides complementary information to echocardiography in the evaluation of left ventricular hypertrophy, presence and degree of septal hypertrophy, concomitant mitral regurgitation and biventricular function.

Aortic annulus is in close proximity to the mitral valve apparatus. Most of the non-coronary leaflet and some part of the left coronary leaflet have the same fibrous continuity as the anterior mitral valve leaflet. Intense mitral annular calcification in this region is a major risk factor for the development of paravalvular regurgitation following TAVI. Therefore, evaluation of anterior mitral leaflet is crucial prior to the procedure. MDCT is recommended as the preferred imaging modality for grading accompanying calcifications.

Approximately 15–48% of patients with severe aortic stenosis have at least moderate mitral regurgitation. Although echocardiography is the preferred imaging modality in the evaluation of accompanying mitral regurgitation, MDCT can also be used in calculations such as left ventricular volumes, mitral regurgitant volume, total stroke volume and regurgitant fraction.

Left ventricular thrombus is a contraindication for TAVI. Therefore, it should be ruled out prior to the procedure. Although the main evaluation method is echocardiography, MDCT can also be used in the presence of suboptimal sonographic data.

The risk of development of heart block following TAVI is particularly high after use of self-expandable systems like Medtronic CoreValve (Medtronic, Inc.; Minneapolis, MN). Since the bundle of His penetrates the interventricular septum at the junction of the membranous and muscular septum, measuring the length of the membranous septum in the coronal plane with MDCT before the procedure helps to predict the risk of heart block after the procedure.

Morphological evaluation of the left ventricular outflow tract (LVOT), subannular region and interventricular septum is essential prior to TAVI. Extensive calcification in this region is associated with an increased risk of paravalvular leak and annular rupture after the procedure. Similarly, the presence of significant septal hypertrophy may complicate the positioning of the prosthetic aortic valve and may even constitute a contraindication for the procedure.

LVOT morphology can often be adequately evaluated by transthoracic and transesophageal echocardiography. On the other hand, in the presence of insufficient sonographic data, MDCT measurements can also provide complementary information. At the same time, MDCT provides a more reliable measurement of interventricular septum thickness compared to echocardiography.<sup>82</sup>

### Evaluation of the Coronary Arteries

Evaluation of coronary arteries prior to TAVI is important both to determine the risk of coronary obstruction due to the procedure and to detect concomitant coronary artery disease. Coronary artery obstruction due to TAVI is a rare but serious complication. The left coronary artery is more frequently affected than the right coronary artery. The use of balloon-expandable valves is also a risk factor for coronary obstruction. Several anatomical features have been described that predict a high risk of coronary obstruction due to TAVI:

- Mean sinus valsalva diameter <30 mm
- Coronary ostium-basal leaflet attachment distance <10–12 mm
- Sinus valsalva diameter/annulus diameter ratio <1.25

Patients should be evaluated with MDCT in terms of these anatomical features before the procedure.

The incidence of coronary artery disease in the patient population treated with TAVI is around 40–75%. Routine revascularization of concomitant proximal coronary artery disease is recommended before TAVI. MDCT is increasingly being used as an alternative to invasive coronary angiography in the detection of proximal coronary artery disease. On the other hand, the presence of coronary calcification may interfere with optimal luminal evaluation.<sup>88</sup>

### Long Term Follow-up

Hemodynamically significant valve thrombosis can rarely be seen after TAVI. As a result of the widespread use of MDCT in the post-procedural period, incidental subclinical valve thrombosis has been detected frequently (Fig. 24). The clinical significance of these subclinical valve thromboses, which cannot be dete-

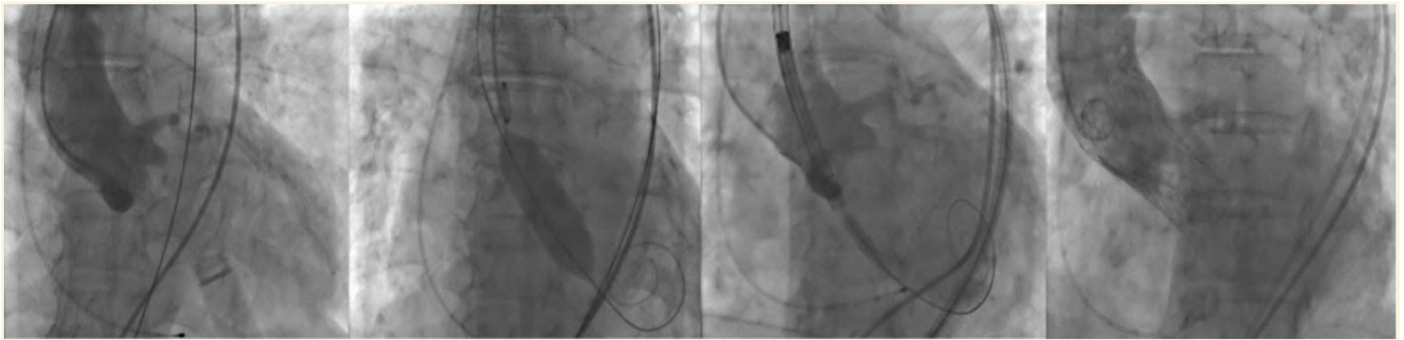


**Figure 27. Use of fluoroscopy in TAVI procedures (From left to right: coplanar angle, balloon aortic valvuloplasty, determination of valve implantation depth, paravalvular leak control).**

cted by echocardiography and are observed as symmetrical or asymmetrical leaflet thickening on MDCT, is unclear.<sup>89</sup> Echocardiography is the main imaging modality in the evaluation of transvalvular and paravalvular aortic regurgitation following TAVI. On the other hand, MDCT can also be used in the quantitative evaluation of regurgitant volumes.<sup>86</sup>

In conclusion, MDCT evaluation prior to TAVI, is essential for providing invaluable anatomical information that optimizes many factors, from proper patient selection to procedural outcomes. Concomitant renal dysfunction, contrast allergy, arrhythmias and pulmonary disease are the main factors limiting the use of MDCT. In the presence of factors, alternative imaging modalities like 3D trans-esophageal echocardiography may be preferred.

### The Role of Echocardiography in Transcatheter Aortic Valve Implantation

TAVI is among the most frequently performed percutaneous procedure worldwide. Echocardiography is used effectively at every stage of the TAVI procedure as an imaging method that has the main role in patient follow-up in the preoperative, intra-operative, and postoperative periods.

Pre-procedural echocardiography is performed to evaluate valve morphology, severity of stenosis, and cardiac response to aortic stenosis. Aortic valve area measurement with echocardiography is commonly performed with the continuity equation. The common error in this method is related to left ventricular outflow tract (LVOT) measurement. LVOT measurement should be performed in early mid-systole. It should be measured from inner edge to inner edge of the point where the right coronary valve attaches to the ventricular septum to the point where the posterior inter-leaflet triangle meets the anterior mitral leaflet. Measurements of under the annulus underestimates the result. Therefore, at the level of the aortic valve measurements of LVOT diameter is more accurate and reproducible.<sup>90, 91</sup> As a result of the developments in three-dimensional (3D) echocardiographic evaluations in recent years, 3D aortic valve area measurement has been demonstrated as an efficient and reproducible method.

The assessment of the valve anatomy, diameter, and geometry of the aortic root should be evaluated prior to operation to decide the valve size. For this reason, multiple imaging methods are used to assess valve and aortic root diameters. Likewise, the location of the coronary ostia and the calcification of the annulus are important considerations that determine the procedure decision. Although

tomography is the essential and gold standard imaging method to evaluate the aortic valve and vascular access before the operation, transthoracic echocardiography (TTE) and transesophageal echocardiography (TEE) are the important imaging modalities in patients who have higher risk for contrast nephropathy. TTE and TEE can be used in several times in the decision-making process before the operation. Although tomography is the gold standard evaluation method in the selection of valve size, manual aortic annulus measurement with 3D echocardiography gives optimal results in patients who cannot undergo tomography (Fig. 25). Apart from 3D manual measurement, Vendor specific semi-automatic measurement methods have been developed (Fig. 26). Previously two-dimensional (2D) measurements were found as insufficient to determine the aortic diameter.<sup>92, 93</sup> Aortic annulus measurements with 3D multiplanar reconstruction has been found to be accurate. In addition, several studies showed the annulus measurements with 3D multiplanar reconstruction was correlated with tomographic measurements. Besides validation studies demonstrated moderate correlation and 10% underestimation with vendor specific measurements compared to tomography.<sup>94</sup> As a result, it is stated that optimal procedural success is achieved with mild or more paravalvular leak with 3D echocardiographic measurement in TAVI candidates who have high contrast nephropathy risk. Apart from the annulus, the aortic root can be accurately measured by echocardiography and the distance of the coronary ostia from the aortic annulus can be measured by 3D multiplanar reconstruction.

During the procedure, the appropriate valve position is determined by using fluoroscopy, aortography and echocardiography. Since TEE can instantly evaluate every stage of the procedure, it can identify acute complications of TAVI. Echocardiography is also the crucial imaging method to decide the valve position, its relationship with the mitral valve, and the presence of paravalvular leak. Due to the fact that the procedure has been performed under light sedation in recent years, TEE is not tolerated. Therefore, the procedure is performed under the guidance of TTE in most centers. TTE is an important imaging method as TEE that can identify all intra-operative complications as well. In particular, the presence of tamponade and paravalvular leak can be clearly determined. The appropriate position of the valve can also be decided with TTE and TEE. It is known that every valve has different annular position. For example, SAPIEN 3 (Edwards Lifesciences, Irvine, CA), should be placed 1–2 mm below the annulus.<sup>95</sup> And, optimal aortic location of Evolut R (Medtronic, Minneapolis, MN) valve is 2–4 mm below the annulus.<sup>96</sup>

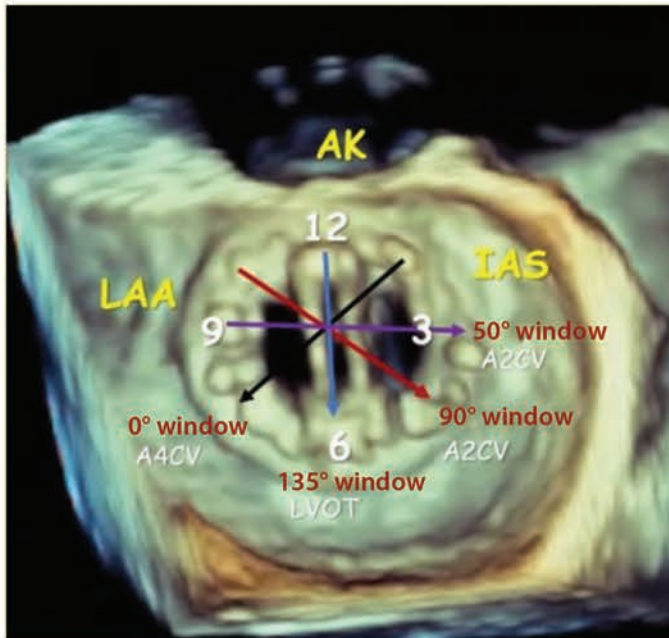


**Figure 28. Three-dimensional echocardiography, clock-face representation of a mitral prosthetic valve. LAA, Left Atrial Appendage; AV, Aortic Valve; IAS, Interatrial Septum; LVOT, Left Ventricular Outflow Tract.**

Immediately after the procedure, the position and shape of the valve movement can be quickly evaluated with echocardiography. While the parasternal long axis view is the best window for valve position, valve shape is best evaluated in parasternal short axis views. The most common complication associated with the procedure is paravalvular leak. It is detected at a rate of about 0-24%.<sup>97</sup> There are many treatment modalities for paravalvular leak such as balloon-in-stent, stent-in-stent or paravalvular leak closure, and the degree of leakage can easily determined by echocardiography which is also used to choose the best treatment option for the leakage. Suboptimal valve opening, deterioration in valve geometry due to severe annulus calcification, and valve localization can be easily determined by echocardiography. The degree of paravalvular leak can be evaluated by many methods. Among them, blood pressure change, Doppler pressure half-time and holodiastolic flow reversal in the descending aorta are the common methods to understand the severity of the leakage. However, one of the most used methods is the evaluation of the aortic annulus in the short axis with colored flow Doppler. More than 30% leakage in aortic annular circumference is considered as severe paravalvular leak. 3D measurement of vena contracta is the novel method to assess the paravalvular leak that gives highly accurate information especially for eccentric regurgitation jets.

After the procedure, the measurement of the valve area is crucial. Valve area can be measured with the continuity equation and Doppler velocity index. Gradient and valve area measurement after the procedure is important in detecting the new pathology during the follow-up.

### The Role of Fluoroscopy in Transcatheter Aortic Valve Implantation (TAVI)

Fluoroscopy is used to detect coronary artery disease and perform percutaneous treatment of coronary lesion in preprocedural period. Fluoroscopy is also facilitate to measure the invasive aortic gradient and valve regurgitation severity. Aortic valve diameter estimation

are not practical unlike in the other imaging modalities, but valve implantation depth measurement can be made precisely.

Lower extremity, abdominal and thoracic aorta and aortic annulus measurements are made with CT for guidance in fluoroscopy. The vascular access site (mostly common femoral artery) is determined with the support of fluoroscopic anatomy and ultrasonographic imaging. The valve is delivered with a guide wire and if the valve is too calcific, balloon valvuloplasty is performed under fluoroscopy. The coplanar angle, the angle at which three cusps aligned, is determined with the information obtained from tomography. Aortography is performed with a guide pigtail catheter placed in the non or right coronary cusp during implantation, depending on the type of valve. Coplanar images are obtained from left anterior oblique views and the optimal implantation depth (3-5 mm below the aortic annulus) is determined. In the 'Cusp Overlap' method, which is an alternative imaging technique, the left and right coronary cusps are overlapped at the right anterior oblique and caudal angle, and this angle allows higher implantation without an increase in paravalvular leak or device embolism risk. The presence of paravalvular leak is evaluated with control aortographic images after implantation. The fluoroscopic approach allows the safe and effective procedure. In addition, it shortens the procedure and hospitalization time. The disadvantages of this approach are radiation exposure and the necessity of using radiopaque materials.<sup>79, 80</sup> Figure 27 shows fluoroscopic images during procedure.

### Imaging in Aortic and Mitral Paravalvular Leaks

*Dr. Kadriye Memiç Sancar, Dr. Gamze Babur Güler*

Prosthetic valve obstruction and regurgitation are the main causes of prosthetic valve dysfunction. Prosthetic valve regurgitation can be either transvalvular or paravalvular. The correct distinction is so important for diagnosis and treatment. While pathological transvalvular leak is accompanied by degeneration, thrombosis and perforation in bioprosthetic valve; obstruction (pannus/thrombus) is expected in mechanical prosthetic valves. During the evaluation of paravalvular leak (PVL), it is necessary to determine symptoms and laboratory

**Table 8. Which findings on transthoracic echocardiography require further evaluation?**

Abnormalities in mitral prosthetic valve structure and movement
Dilated or hyperkinetic left ventricle
Systolic flow convergence in the left ventricle towards the valve
Peak mitral E velocity $\geq 1.9$ m/sn
Left atrial dilatation
Unexplained or recently deteriorated pulmonary hypertension

**Table 9. Determining the severity of paravalvular mitral regurgitation**

Mitral prosthetic valve structure and motion
Color Doppler jet area
Proximal isovelocity surface area (PISA)
Jet density
Pulmonary venous flow pattern

Although validation is limited in prosthetic valves like native mitral valves, numeric parameters can be used: Vena contracta width, regurgitation volume, regurgitation fraction and effective regurgitation area.

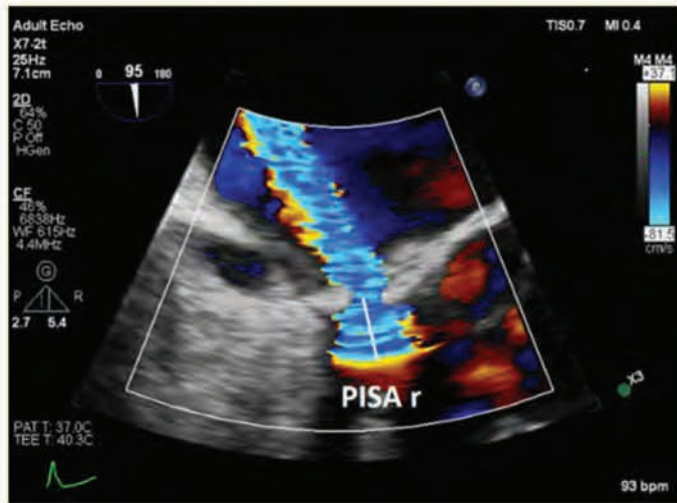


**Figure 29. Mitral mechanical prosthetic valve. Measurement of the radius (r) using the PISA method in a single paravalvular leak.**

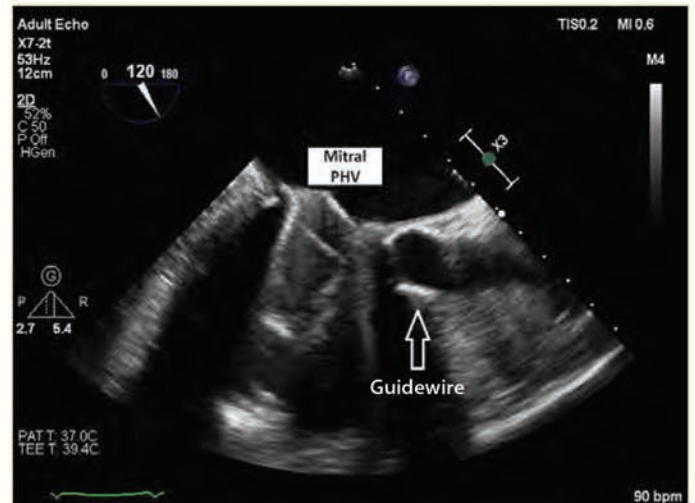


**Figure 32. Mitral mechanical prosthetic valve (PHV). A defect located posteriorly has been accessed via a retroaortic route.**

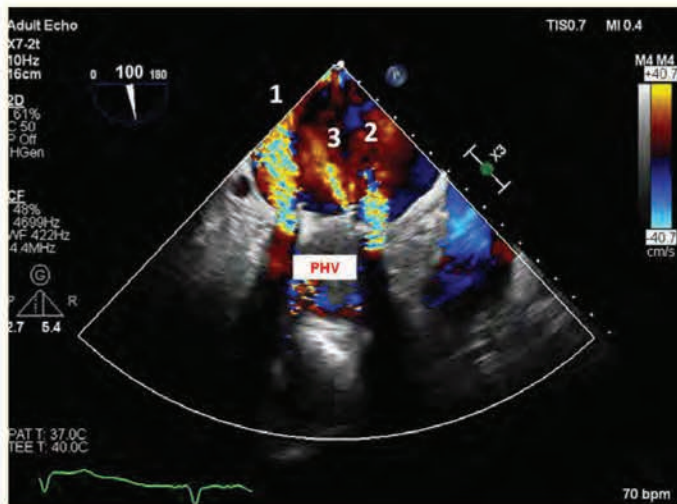


**Figure 30. Mitral prosthetic heart valve (PHV). Three different paravalvular leak jets, seen on two-dimensional echocardiography.**

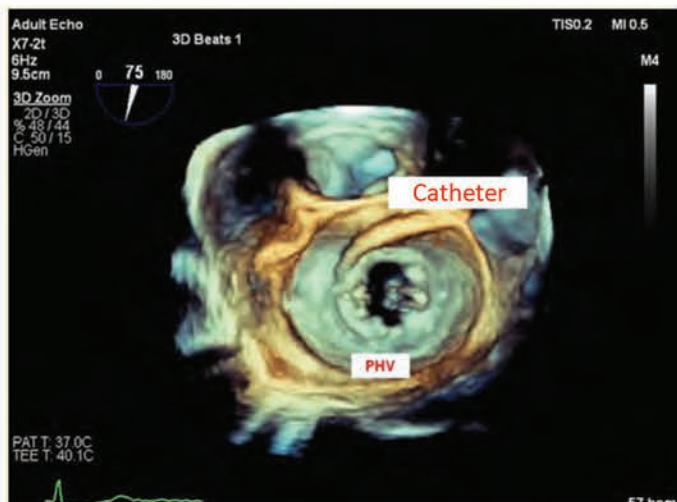


**Figure 31. Mitral prosthetic heart valve (PHV). Placement of a catheter after transseptal puncture in a defect located anterolaterally.**

results of the patients, severity of regurgitation and the appropriate treatment which is medical, surgical or percutaneous closure.

PVL is detected 5–17% in long term follow up period of patients which had history of surgical valve replacement.<sup>99, 100</sup> Paravalvular leak is seen more common in mitral mechanical valves than aortic mechanical valves.<sup>100</sup> Although most PVLs are benign, 1–5% of PVLs are associated with progressive symptoms and clinical worsening.<sup>101, 102</sup> In the last 10 years, the preference of transcatheter aortic valve replacement (TAVR) in patients with high surgical risk makes management of PVL related to TAVR important. TAVR associated PVL is reported as 15% in first generation and last generation TAVR valves.<sup>103</sup> Although PVL rates are higher in self expanding prosthetic valves compared to balloon-expanding valves,<sup>104</sup> nowadays there is still no comparison between two groups.

Prosthetic valve regurgitation is directly related to severity of leak, hemodynamic effects, secondary results (dilatation of left heart chambers, pulmonary hypertension, etc) and related pathologies (vegetation, dehiscence, thrombosis, pannus). While most patients are asymptomatic, previous studies showed that 1–5% of the patients with PVL were symptomatic.<sup>101, 105</sup> Especially new, unexplained, findings of resistant heart failure, hemolysis with or without anemia and changes in auscultation should suggest prosthetic valve dysfunction and require further evaluation. According to 2020 American College of Cardiology (ACC) and American Heart Association (AHA) guideline for the management of patients with valvular heart disease; PVL closure is recommended as class IIa in an experienced heart center, in the case of intractable hemolysis (with or without anemia) or new-onset heart failure in symptomatic patients at high surgical risk who have prosthetic valves.<sup>106</sup>

In this review, we aimed to examine the imaging methods in aortic and mitral PVLs, their contribution to the process from diagnosis to treatment, the differences between aortic and mitral valve; in a way that would be beneficial for our daily practice, in a sequence ranging from echocardiography laboratory to catheter laboratory.

### Approach to Paravalvular Leaks by Using Multimodality Imaging Techniques

#### Evaluation in the Echocardiography Laboratory

Transthoracic echocardiography (TTE) is initial test for diagnosis as easily accessible, non-invasive and most-experienced method.

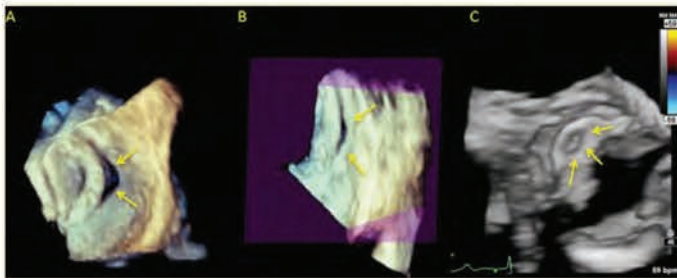


**Figure 33 A-C.** (A) Crescentic, semilunar-shaped defect. (B) Slit-like defect. (C) Oval-shaped defect.

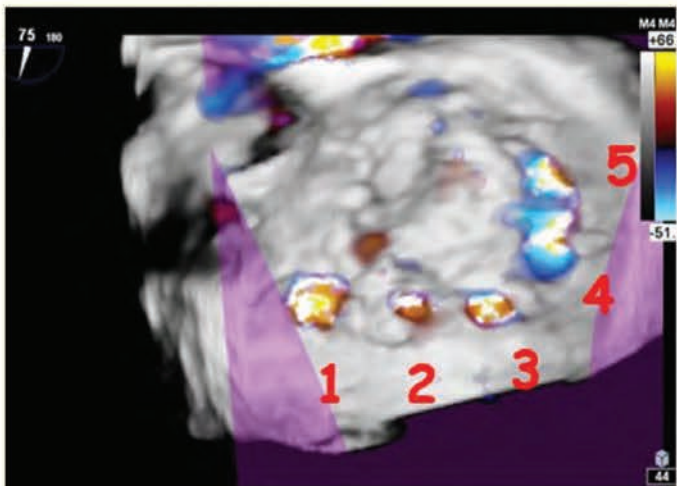


**Figure 34.** Mechanical mitral valve prosthesis (MVR). In three-dimensional echocardiography, five different paravalvular leaks from multiple defects are observed.

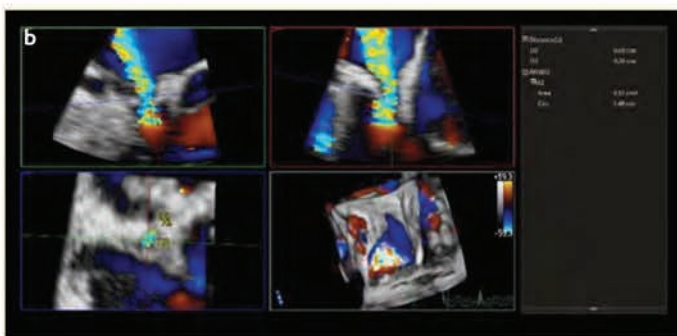
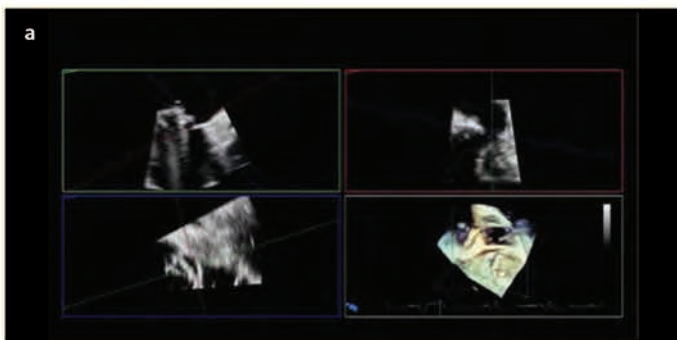


**Figure 35 A-C.** Mechanical mitral valve prosthesis (MVR). (A) Evaluation of the anatomical effective orifice area with the multiplanar reconstruction method. (B) Evaluation of the anatomical effective orifice area with the multiplanar reconstruction method with colour Doppler.

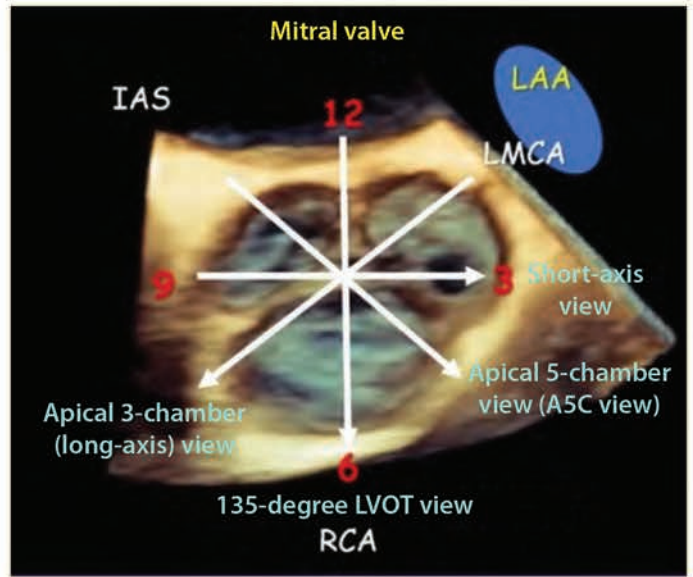


**Figure 36.** Clock-face presentation in aortic valve. LMCA: Left main coronary artery, LAA: left atrial appendage, DTG: Deep transgastric view, IAS: Interatrial septum, LVOT: Left ventricular outflow tract, RCA: Right coronary artery.

Two-dimensional (2D) transesophageal echocardiography (TEE) provides benefits such as transvalvular and paravalvular jets distinction, determining severity, number and location of leaks, evaluation of additional lesions (pannus, thrombosis, vegetation etc.) and detection of hemodynamic results. Three dimensional (3D) echocardiography is so important especially in evaluation of number, location, shape, tunnel length, size and severity of PVL, in the planning of suitability for the interventional procedure and deciding device type and size.

### Evaluation of Mitral Paravalvular Leak

Although defining severity of mitral PVL is recommended in current guidelines, recommendations are similar with parameters of native mitral regurgitation and validation of it is not sufficient.<sup>107, 108</sup> PVL is typically defined as a flow that extends from the left ventricle to the left atrium outside the mitral annuloplasty ring suture. Clock-face representation from the left atrial perspective which is called surgical view (enface view) is used in the evaluation of mitral PVL by 3D echocardiography (Fig. 28). As well as this is important for determining number and location of PVL, it is a crucial definition to use common language between imaging specialist and surgeon or invasive cardiologist. According to this, the aortic valve is located at the 12 o'clock position, the interatrial septum at 3 o'clock and left atrial appendage at 9 o'clock. It is stated that mitral PVLs are most frequently located in anterolateral (10-11 o'clock) and posteromedial (5-6 o'clock) segments.<sup>109</sup> It has been speculated that non-homogeneous distribution of collagen tissue in the mitral annulus, insufficient suture area in the posterior region and mechanical stress in the non-monoplanar mitral annulus is most effective in the posteromedial and anterolateral regions.<sup>110</sup> In addition to this, PVL in the mitral valve can occur anywhere from the valve ring. Thus, it is significant to evaluate the suture ring around the prosthetic valve in multiple windows and using rotational maneuvers (clockwise and counter clockwise) in TEE. Another important point is to confirm the defects detected in 3D echocardiography by using 2D echocardiography. Although there is no issues with the new software; 3D echocardiography, a common used evaluation technique, may show artefact due to arrhythmia, stitching artefacts due to incapacibilities of holding breath, and 'drop-out' artefacts

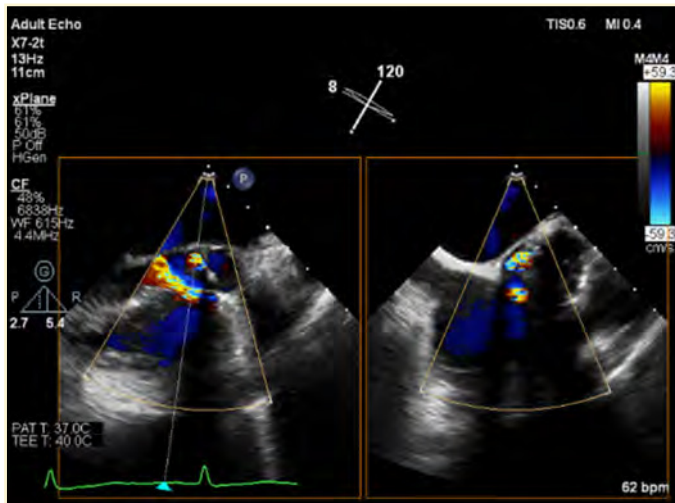


**Figure 37. Aortic prosthesis valve. Evaluation of the exact exit points of the two leaks in the reference window with 3D echocardiography X plane mode.**



**Figure 38. Aortic prosthesis valve. Severe eccentric paravalvular leak (S shaped) where jet width criteria is not beneficial.**

due to the improper adjustment of gain during the evaluation process. These artefacts can lead to misdiagnosis of one or more defects during 3D echocardiographic study. So, it is extremely important that all defects which are detected in 3D echocardiography are determined in expected localization in 2D echocardiography. It may not be possible to evaluate mitral PVL completely in TEE due to acoustic shadowing and reverberation artifacts. In this reason, it is necessary to assess the indirect findings and secondary results that may suggest prosthetic valve dysfunction.

Table 8 summarizes PVL's indirect findings in TEE.<sup>109, 111</sup> It is required to assess by TEE in the presence of one or more of these parameters. Findings of TTE and TEE that are shown at Table 9 are generally used to determine severity of leakage after differentiating transvalvular and paravalvular prosthetic valve dysfunction in TEE.<sup>107, 112</sup> However, it is known that validation of some parameters is limited or absent in prosthetic valve regurgitation like native mitral valve regurgitation. This situation makes the evaluation of PVL even more difficult.

Assessment of mitral valve movement (fixed or limited, also exaggerated movement due to dehiscence and rocking motion) is the first step in evaluating mitral valve regurgitation in TEE. If there is accompanying

lesion (pannus/thrombus/vegetation), its definition is important to determine medical and interventional treatment options. If we examine the echocardiographic parameters used to determine the severity of mitral PVL; vena contracta width is a helpful parameter for the quantification.<sup>112</sup> Prosthetic valve artifacts make it difficult to measure the desired vena contracta, and do not make it possible to measure the vena contracta in the presence of eccentric and multiple jets.

Although proximal isovelocity surface area (PISA) (Fig. 29) is not validated to quantify mitral PVL, widened PISA indicates severe PVL.<sup>108</sup> Regurgitation volume and fraction are not generally recommended because they are not validated in paravalvular leakage.<sup>113</sup> In the case of multiple jets and eccentric jets, PISA formula can not be applied (Fig. 30). Pulmonary venous systolic flow is a useful parameter; although it is specific for severe mitral regurgitation, it is not sensitive.<sup>112</sup> Leak that occurs by finding a pathological way along the side of prosthetic valve ring is usually encountered with eccentric and multiple jets. Thus, conventional methods are insufficient to determine severity.

In TEE examination, it is necessary to create the image plane from the sewing ring level in order to visualize the orifice of PVL defect. Otherwise, a slight angulation from this plane will cause the leak to appear oblique or cause the jet size to be confused with the defect and overestimated. After determining the severity, it is required that the location of the defect, its shape and number should be defined. At this stage, the contribution of 3D echocardiography is very crucial and has no alternative.<sup>114</sup> The clock face mentioned before is very important to be used as a common language in defining location of mitral PVL. Location of the defect is essential for planning for percutaneous closure.

Though the transeptal route can be tried in medially located defects, it is often insufficient; defects that are located anterolaterally are the most suitable for transeptal access (Fig. 31). Loop must be

**Table 10. Determining the severity of paravalvular aortic insufficiency**

Prosthetic aortic valvi structure and its movement
Diameter of left ventricle
Width (especially central) and density of the jet flow
Pressure half time of jet flow
Determination of percentage of peripheral spread of paravalvular jet flow via prasternal short axis view
Diastolic reverse flow in descending aorta

created via retro-aortic route (Fig. 32) or it must be reached apically for medially or posteriorly located defects. Shape of mitral PVL may be serpentine; the defect orifice defined as crescentic (Fig. 33A), slit like (Fig. 33B), oval (Fig. 33C), rounded. As the number of defects increases, determining the number of defects by using 2D echocardiography becomes more difficult. Three dimensional echocardiography is very important in determining the distance between defects as well as making it easier to identify different defects (Fig. 34).

Determination of the size of PVL is crucial for measuring the size of the device during PVL closure process. In order to do that, vena contracta of PVL can be used but 2D calculation is not adequate for a 3D defect. Planimetric measurement of the vena contracta area with 3D TEE is more valuable in the selection of device type and size. From 3D echocardiography modalities, PVL output can be detected simultaneously from different angles with the simultaneous biplane (X-plane/multiplane) mode. With 3D zoom or live 3D modalities, anatomic (Fig. 35A) or colored Doppler formats (Fig. 35B) should be used in order to determine the shape and dimensions of the defect orifice. It has been shown that a major diameter of  $\geq 0.65$  cm of the 3D colored effective regurgitant orifice (ERO) in mitral PVLs has a positive predictive value

of 87.1% and a negative predictive value of 94% in the diagnosis of 3<sup>rd</sup> and 4<sup>th</sup> grade regurgitation.<sup>115</sup> In the same study, it was shown that color Doppler ERO measurement was superior to the anatomical regurgitant orifice in detecting severe PVL. In the evaluation of mitral PVL and in the management of the procedure in the catheter room, 3D echocardiography is much more vital than aortic PVL. Extent of PVL should be measured in catheter labs with balloon because there is a risk of rupture due to calcification of the surrounding tissue.<sup>116</sup>

### Evaluation of Aortic Paravalvular Leak

In aortic PVLs, TTE and TEE images should be evaluated together. If the defect is located on the right coronary cusp side (anterior), it can be easily detected by TTE, thus if it is located on the non-coronary or left coronary cusp side (posterior), it should be evaluated further with TEE.<sup>117</sup> Recommended TEE image windows in aortic PVL analysis<sup>118</sup> are mid-esophageal short and long axis view windows and deep transgastric view windows. In TEE imaging, while locating aortic PVL, clock-face method can be used. Five o'clock corresponds to the commissure between right and left coronary sinus, 8 o'clock corresponds to the commissure between the right and non-coronary sinus and 11 o'clock corresponds to the commissure between the non-coronary and left coronary sinus (Fig. 36). Statistically, aortic PVLs most commonly seen between 7 and 11 o'clock (%46) and between 11 and 3 o'clock (%36).<sup>119</sup> Other than this, PVL localization can be done by using cusp names. In the process of TEE, reporting the localization of coronary arteries and specifying their relations with PVL is crucial in planning of interventional treatment.

Evaluation of aortic PVL should begin with the evaluation of valve movements. Dehiscence, 'rocking' movement, limitation of leaflet movements, accompanying thrombus, vegetation, presence of pannus are the contraindications for PVL closure. At the same time, it is also important to determine the shape of the defect orifice (half-moon or oval) and measure its size with color 3D imaging modes (3D zoom/live 3D/X plane) (Fig. 37). The severity of aortic regurgitation associated with the prosthetic valve can be determined by the parameters and methods shown in Table 10.<sup>107, 109</sup> However, validation of the parameters used in the evaluation of aortic prosthetic valve related regurgitation is limited, as is the case with the mitral valve.<sup>112</sup> When PVLs are frequently eccentric, the jet width measurement has low accuracy. Although the ratio of the width of the jet to the left ventricular outflow tract is the first and most frequently used method in the assessment of severity in practice, it is not possible to accurately evaluate a jet directed to the interventricular septum or anterior mitral valve with this method, (Fig. 38) and its correlation with PVL severity is weak.<sup>112</sup> It is considered as severe paravalvular regurgitation when the pressure-half time (measured by continuous wave Doppler) is <200 ms, and mild regurgitation when it is >500 ms. However, since Doppler measurements of intermediate values are affected by many factors (such as left ventricular compliance, left ventricular pressure, heart rate), it requires evaluation together with other quantitative parameters (vena contracta-flow convergence). When the anatomically regurgitant orifice of the PVL is non-circular, the accuracy of the flow convergence method decreases.<sup>114</sup> Reflected flow in the descending aorta may be misleading, especially in elderly patients, with deterioration of aortic compliance and may cause holodiastolic reverse flow, including in the case of mild PVL.<sup>107</sup> The 2D evaluation, which is important for the evaluation of aortic PVL, is important for carefully visualizing the neck of the jet at the level of the prosthetic suture ring in the short axis image and to determine the circumferential extent of the regurgitation.<sup>112</sup> In the aortic short axis, at the level of the sewing ring, a ratio of the jet neck to the circumference of the sewing ring greater than 30% is significant for severe PVL.<sup>112</sup> However, when applying this

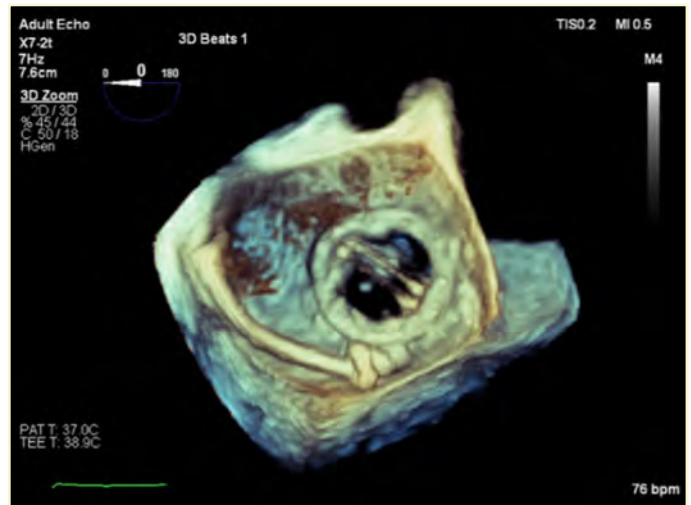


**Figure 39.** In treatment of posteriorly located mitral paravalvular leak, 3D echocardiography is used step by step to determine if the device is perpendicular to the defect.

method; it should be ensured that this ratio is taken from the level of the suture ring, otherwise the angulations will cause an exaggerated measurement of the defect rate.

Approach to the paravalvular insufficiency related to TAVR is totally different. Because the insufficiency flow that develops after surgical aortic replacement occurs with the release of the sutures between the placed valve and the annulus after the removal of calcification in the aortic area during surgery.<sup>120</sup> However, in percutaneously placed valves, the valve is implanted without stitches. Although calcification in the aortic annulus seems to allow full and symmetrical placement of the valve with the transcatheter pathway, the shape of the calcification and the diameter of the aortic annulus may predispose to the formation of PVL.<sup>120</sup>

Transcatheteric aortic PVLs are evaluated via echocardiography in parasternal long and short axis. In fact the evaluation is not different from the PVLs seen after surgery. Despite this, Pibarot et al.<sup>121</sup> has formed a new evaluation for insufficient flow regarded to TAVR procedure. Along with this, a detailed classification has been formed covering; grade determination by cineangiography, invasive hemodynamic evaluation (aortic regurgitant index), evaluation of valve structure and left ventricular diameter by Doppler echocardiography, detailed examination of the properties of the jet (width, density, half-time, multiplicity), calculation of the width and area of the vena contracta, numerical Doppler parameters (regurgitant volume, regurgitant area, effective regurgitant orifice area).

### Use of Other Imaging Methods in Paravalvular Leaks

#### Cardiovascular Magnetic Resonance Imaging

Cardiovascular MR imaging is preferred when TEE and TTE is not sufficient for evaluating the insufficient flow caused by prosthetic valve. Yet this method has restricted usage in clinical practice due to technical complexity and lack of experience. In mechanical valves and stented bioprosthetic valves, the applied magnetic field is often disturbed near the prosthetic ring which causes signal loss. Cardiac MRI enables flow imaging and volume-based measurements, especially in patients with multiple jets whose evaluation with TEE is complex.<sup>122</sup> Cardiac MRI also contributes to the measurement of heart cavities and detailed analysis of the anatomy around the prosthetic valve in stentless valves.

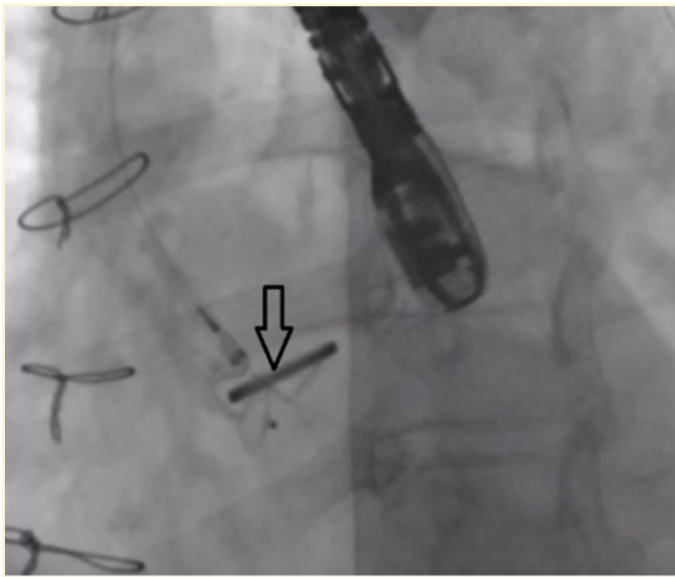


**Figure 40.** Aortic prosthesis valve. In fluoroscopy, a device is inserted into the aortic paravalvular leak and the movement of a single leaflet is severely restricted.

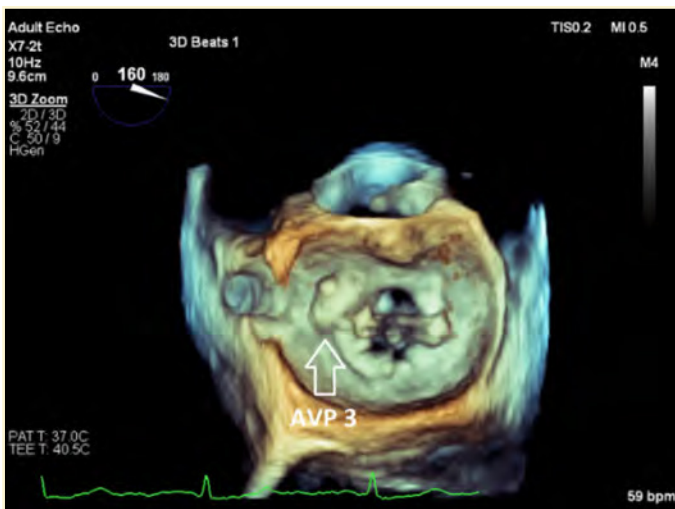


**Figure 41.** Amplatzer Vascular Plug (AVP) III device is inserted into the anterolateral mitral paravalvular leak.

In TAVI related PVLs cardiac MRI has some significant advantages;<sup>121</sup> 1- Regurgitant volume can be calculated independently from number of jets and its morphologies 2- Calculations can be done repetitively. Despite these advantages, there are also studies showing that the rate of moderate/severe PVL is 2-3 times higher with cardiac MR compared to TTE.<sup>123</sup> This has been interpreted as TTE underestimating eccentric, multiple jets, or whereas overestimation of PVL by cardiac MRI due to several technical issues.<sup>123</sup>

### Cardiac Computer Tomography

The main indication for cardiac computed tomography (CT) in patients with significant prosthetic valve insufficiency who could not clearly be evaluated in TTE and TEE is differentiation of pannus and thrombus, evaluation of calcification and valve movements.<sup>107</sup> CT evaluation for aortic prosthetic valve is also recommended in the current guideline.<sup>106</sup> Cardiac CT contributes to the selection of the appropri-

ate method in the closure process by determining the location, size, calcification and characteristics of the surrounding tissue in PVLs with three or four-dimensional reconstruction.<sup>124</sup> In addition to that, a recently developed CT fluoroscopy fusion imaging facilitates access route, wire passage and device insertion during PVL closing procedure. Unfortunately, artefact problems arising from the prosthetic valve that we experience echocardiographically cause difficulties during evaluation of CT as well (such as blooming artefact, beam hardening).

### Cinefluoroscopy (CF)

CF is an imaging method used in the catheter laboratory during closure procedure. Along the procedure, fluoroscopic imaging is complementary to the echocardiographic imaging. Although CF can be used in preop evaluation of PVL, it is a subjective and semi-quantitative method. CF can not determine the anatomical properties of the defect and when we consider radiation exposure and use of opaque materials, it seems rational to use it only during PVL closure.

### Percutaneous Closure in Paravalvular Leaks

#### Intraprocedural Imaging

Percutaneous PVL closure can be done from different entry routes depending on the location of the PVL. Transfemoral arterial access, aortic retrograde pathway (aortic PVL and some medial mitral PVLs) and transapical route are mainly used for PVL closure. Transradial access may be preferred to close small PVLs.<sup>125</sup> Echocardiography guidance with 3D TEE is the preferred imaging modality during mitral PVL closure.<sup>126</sup> For determining the location of the defect and device size, 3D TEE is found to be superior to 2D TEE.<sup>127-129</sup> In addition to that, 3D TEE directs the process in real time, allowing catheter manipulation and reaching the defect with 2D fluoroscopy.<sup>130</sup> 3D echocardiography is the only method by which valve perpendicularity can be checked before the device is released (Fig. 39). If there is a residual defect after device placement, the viewer can re-measure with 3D images for additional device planning. In addition, TEE provides safe transeptal puncture, preventing possible complications (cardiac tamponade or aortic root injury). Although intracardiac echocardiography is not commonly used in our country, it can be used in patients that cannot tolerate the TEE probe even while in general anaesthesia or sedation.<sup>131, 132</sup> Transeptal puncture with transvenous access provides antegrade access to the mitral PVLs. Transeptal puncture should be performed under TEE and fluoroscopy guidance. Gibblet et al.<sup>114</sup> stated in his review on PVL that they preferred a high transeptal puncture for lateral PVLs (6-12 o'clock) and a lower transeptal puncture for septal PVL (12-6 o'clock). The transapical access route is a technique that can be used when it is difficult to reach mitral PVLs via the transvenous or transarterial route, or in the presence of mitral and aortic valve prosthesis.

During the percutaneous closure procedure, it is important to evaluate multiple images taken in one plane or, if possible, to take two orthogonal images simultaneously with biplane fluoroscopy in terms of guiding the procedure.<sup>133</sup> Fluoroscopy is found to be successful in guidance and emplacing of the wire and also in evaluating the valve movements after the device is implanted.<sup>124</sup> Regardless of the path chosen, the aim is to pass through the PVL with the guide wire. At this stage, TEE (2D or 3D) and fluoroscopy are important in deciding whether to pass through the valve or PVL. First, the catheter and then the device placement steps are passed over the wire. At this stage, it is very important to evaluate whether the inserted device affects the movements of the valve (it may affect both closing and opening) (Fig. 40). Monitoring the pericardial effusion throughout the procedure and detecting a new thrombus that may occur on the catheter/wire is the responsibility of the imaging specialist. Since there is a risk of coronary occlusion

for aortic PVLs, especially in defects located on the left coronary cusp side, the device should be checked with aortography before being released. While the contribution of TEE's guidance during the procedure to the success of the procedure is indisputable; the indirect effect on the duration of the procedure, radiation exposure and the use of contrast material cannot be ignored. Success of the procedure can be defined by successful placement of the device, absence of residual defect and absence of newly developed prosthetic valve dysfunction.<sup>133</sup> Clinical success on the other hand is defined related to increase in functional capacity ( $\geq 1$  New York Heart Association) and improved haemolysis.<sup>133</sup>

In PVL closure, there are no specially manufactured devices, the devices are vascular or congenital defect closure devices used in the 'off label' indication. The Amplatzer Vascular Plug III (AVP3; Abbott Vascular) is the most commonly used device for PVL closure worldwide. PVL Device (PLD; Occlutech) and AVP 3 devices (Fig. 41) have the closest shape to the anatomical structure of PVL defects. Off-label AVP 2, AVP 4 and Amplatzer Duct Occluder (St Jude Medical) devices are also used for PVL closure.<sup>134</sup> AVP 2 device is suitable for cylindrical and round leaks, while AVP 4 can be used for serpiginous leaks, especially PVL developing after TAVR.<sup>135</sup> Usually, a single device is sufficient for aortic PVLs.

For the TAVR associated PVLs; balloon post-dilatation, valve in valve or defect closure methods are preferred according to the severity, location and etiology of the PVL instead of closure of the PVL due to the different mechanisms mentioned above.<sup>120</sup> In TAVR associated PVLs there are problems such as irregular tunnels, calcifications, stenting of the valve and difficulty in advancing the device (displacement of the valve). Since the tunnels are small and narrow, smaller devices should be used instead.<sup>117</sup>

### Paravalvular Leaks Prognosis and Follow Up After Paravalvular Closure

There is no specific period suggested for long term follow up imaging after closure of PVL.<sup>136</sup> Prognosis of patients with PVL is related to the reason and severity of the PVL. Mild PVLs have good prognosis in the absence of haemolysis.<sup>137</sup> However, some of the studies reported increased mortality rates (especially worsening of mitral PVL) in patients with moderate PVL.<sup>138</sup> PVL-related haemolysis is associated with poor short-term outcome, even if there is no significant anemia at the time of diagnosis.<sup>139</sup> Mitral PVLs have a worse prognosis than aortic PVLs. Cho et al.<sup>138</sup> followed up 54 patients with mild-to-moderate PVLs for 8 years. Primary end-points were determined as cardiac death, all-cause death, recurrent surgery, and emergency admission due to heart failure. The 8-year event-free survival rate was  $70 \pm 12\%$  in patients with aortic PVL and  $16 \pm 8\%$  in patients with mitral event-free survival rate was  $70 \pm 12\%$  in patients with aortic PVL and  $16 \pm 8\%$  in patients with mitral PVL. For this reason, it is important to evaluate the symptoms that occur during the follow-up of patients with surgical and transcatheter prosthetic valves and to detect the problem earlier with imaging methods.

### Conclusion

A successful closure of PVL starts with an effective imaging. Prior to the PVL closure procedure; location, size, shape, severity and number of the PVL defects are determined with imaging. There are various imaging methods in the diagnosis of PVL. However, there is no optimal method for diagnosis as all methods have their advantages and disadvantages. According to our clinical experience, although the validation of the parameters used to evaluate PVL closure is limited and there are still problems with the devices used for PVL closure, the use of multiple imaging modalities and the experience of the imaging specialist and interventional cardiologist are the most important determinants of procedural.

## The Role of Imaging in the Mitraclip Process

*Dr. Selçuk Opan, Dr. Özge Özden*

Percutaneous intervention in the treatment of symptomatic severe mitral regurgitation (MR) is an alternative to mitral valve replacement and open surgical repair in patients at high surgical risk. With the MitraClip (Abbott Laboratories, Menlo Park, California, USA) device, similar to the Alfieri surgical technique, anterior and posterior mitral leaflets are approximated to create a double MR flow and the mitral valve area is reduced at the same time.<sup>140</sup> This minimally invasive, catheter based approach has revolutionized the treatment of patients at high surgical risk. In the COAPT study, which is a randomized controlled trial, it has been shown that MitraClip-based interventional therapy significantly reduces hospitalizations and total mortality.<sup>141</sup> In current guidelines interventional edge-to-edge repair with MitraClip device is recommended in symptomatic severe MR patients with high surgical risk.<sup>106, 142</sup>

MitraClip procedure is performed under fluoroscopy and transesophageal echocardiography (TEE). Fluoroscopy is primarily used to evaluate the opening angle of the MitraClip arms and TEE is the primary imaging modality for pre-procedural evaluation, procedural guidance, and post-procedural outcome and potential complications. TEE is used to determine the transeptal puncture site, which is one of the key steps for the procedure, to determine the optimal positioning of the MitraClip device, and to evaluate the severity of residual MR just before and after the final insertion of MitraClip. In the first years of MitraClip procedure, two-dimensional (2D) TEE was used as the standard imaging method. Today, with three-dimensional (3D) TEE, which plays a crucial role in most stages of MitraClip application, the possible complication rate is reduced while the procedure time is shortened. Additional to anatomical guidance, 3D TEE offers real-time direct imaging of the mitral valve and adjacent structures. Studies have found that 3D TEE is superior to 2D TEE in guiding many steps in MitraClip application.<sup>143</sup> MitraClip; requires full collaboration between the operator performing the procedure and the cardiovascular imaging specialist responsible for TEE.

### Mitral Valve Anatomy

The mitral valve apparatus, which consists of mitral annulus, anterior and posterior mitral valve leaflets, chordae tendineae and papillary muscles, has a very complex structure. The anatomical description of the valve is made with a segmentation of 6 scallops. While the posterior leaflet consists of P1, P2, and P3 scallops from lateral to medial, the corresponding anterior leaflet scallops are named as A1, A2, and A3 scallops. The posterior leaflet of the mitral annulus, which forms two-third of the annulus, has a wider circumference than the anterior leaflet; but has a shorter leaflet length. While the anterior and posterior leaflets of a mitral valve show complete closure in a normal anatomy, cases where complete closure is not possible present as MR clinically. Although the left ventricular wall is not a defined component of the mitral valve apparatus, it plays a critical key role in functional MR.

Mitral valve disease has many etiologies and mitral regurgitation is basically divided into organic (primary) and functional (secondary) mitral regurgitation. Fibroelastic deficiency, Barlow's disease, rheumatic mitral valve disease, congenital mitral cleft, annulus calcification, infective endocarditis, marantic endocarditis are the main causes of primary MR, while coronary artery disease and dilated cardiomyopathy are the leading causes of secondary MR. Each of these disorder affects the valve apparatus in uniquely different ways.

### Features of the Mitraclip System

The percutaneous edge-to-edge repair system consists of the MitraClip system and the steerable guide catheter (SGC) system that allows its implantation. A guide catheter with a proximal part of 24F and a distal part of 22F is advanced into the left atrium with a transeptal approach

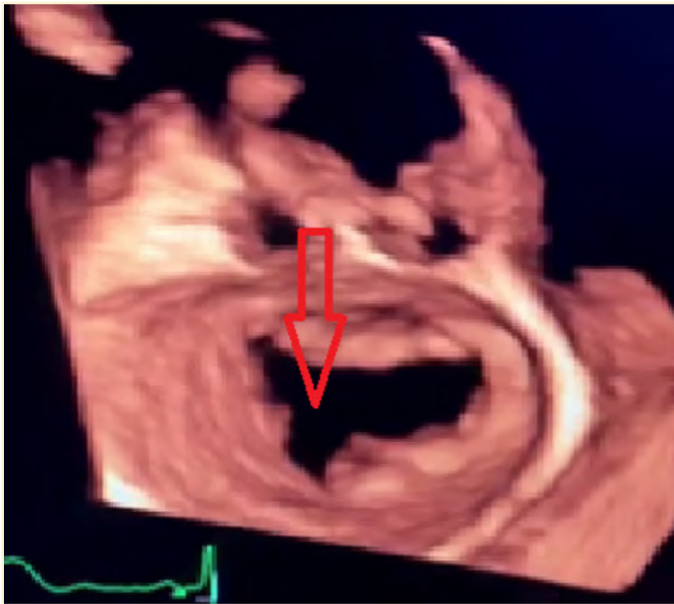


**Figure 42.** A 3D en face TEE image shows the cleft in the posterior leaflet without an optimal valve pathology for the MitraClip procedure.

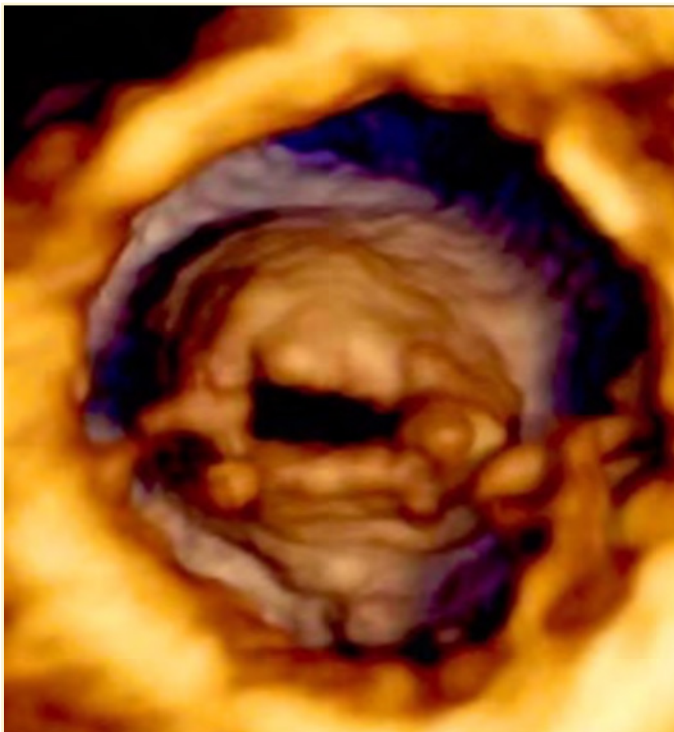


**Figure 43.** 3D TEE image depicted from the mitral valve ventricular face shows rheumatic valve disease commissural fusion with unsuitable valve pathology for the MitraClip procedure.

through a guide wire and dilator. MitraClip is placed at the tip of the clip delivery system (CDS) and advanced into the left atrium over the SGC. Both SGC and CDS can be guided from outside. Thus, MitraClip is positioned perpendicular to the annulus plane at the beginning of the MR flow. MitraClip is a 2-armed, polyester-coated mechanical device that can be opened and closed. Mitral leaflets are grasped by the arms and

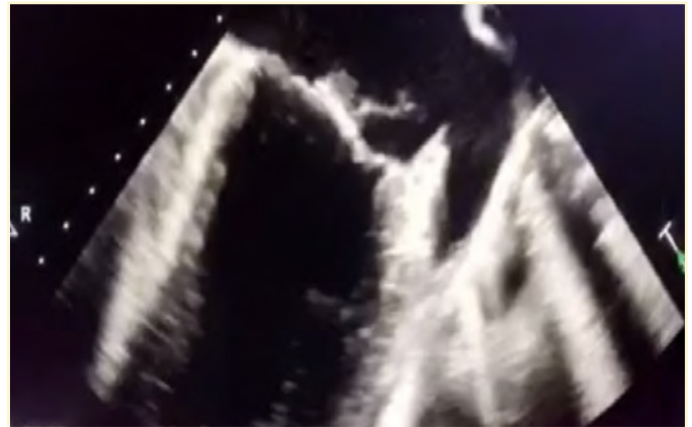


**Figure 44.** Bicommissural 2D TEE image showing vegetation due to infective endocarditis with unsuitable valve pathology for the MitraClip procedure.

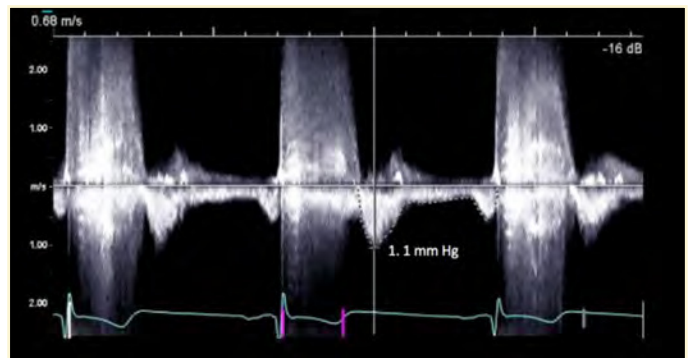


**Figure 45.** Mean gradient on the mitral valve is measured while assessing the suitability for the MitraClip.

fixed between the arms and the grippers by closing the arms. A locking mechanism prevents the MitraClip from opening after fixation.<sup>144</sup>

### Patient Selection

Transthoracic echocardiography (TTE) is the first line imaging modality to determine the severity of MR. While TTE is often sufficient to evaluate the severity of MR, TEE has an important place in the evaluation of the morphological features of the valve and in determining the severity of MR in patients with poor echogenicity. TEE is also very useful in the measurement of eccentric MR jets and pulmonary venous flow, which are difficult to evaluate with TTE. During the quantitative evaluation of MR, the patients should be followed up under appropriate medical treatment. In addition, all treatment options such as percutaneous revascularization and cardiac resynchronization therapy, which may contribute to the reduction of MR severity, should be considered, and MR should be re-evaluated after appropriate invasive treatment options are performed. MR may benefit from transcatheter aortic valve replacement in patients with severe aortic stenosis and high surgical risk. In patients with concomitant severe tricuspid regurgitation, severe pulmonary hypertension or right ventricular dysfunction; clinical results are more limited although the severity of MR is reduced with MitraClip procedure.

In the EVEREST study, which is the index study for MitraClip, patients with severely affected left ventricular structure and functions (left ventricular end-systolic diameter >55 mm or left ventricular ejection fraction <25%) were excluded from the study. On the basis of data obtained from this study, suitable candidates for MitraClip procedure are determined as the ones whose left ventricular structure and functions are

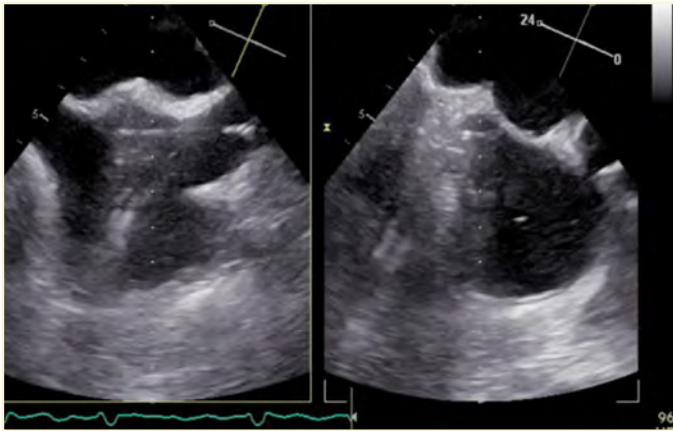


**Figure 46.** Before the transeptal puncture, the superior-inferior orientation is adjusted in the bicaval TEE image and the anterior-posterior orientation is adjusted in the short-axis image.

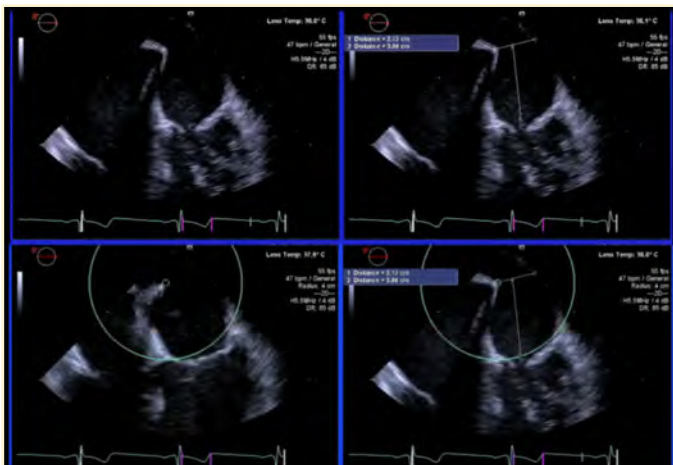


**Figure 47.** Puncture height is adjusted from 0° four-chamber view before transeptal puncture.

not severely affected; with +3 +4 symptomatic chronic MR. In addition, asymptomatic patients with mild to moderate affected left ventricular structure and function (left ventricular ejection fraction 25%–60% left ventricular end-systolic diameter 40–55 mm) or patients with pulmonary hypertension or new atrial fibrillation can be considered as suitable candidates.<sup>145</sup> There are studies showing that MitraClip application can be performed safely with promising results in patients with very low ejection fraction.<sup>146, 147</sup>

### Pre-Procedural Echocardiographic Evaluation

It is important to know the mitral valve morphology well and to recognize the scallops that constitutes the valve from various windows with TEE while choosing the patient. In 0° images (depending on the height of the probe in the esophagus), the A1 and P1 segments can be seen in the upper position, the A2 and P2 segments in the more middle position and the A3 and P3 segments in the lower position. In the 60° intercommissural window, segments P1, A2, and P3 are demonstrated when the image plane precisely crosses both commissures. Clockwise rotation of the probe reveals the A1, A2, and A3 scallops of the anterior leaflet, and counterclockwise rotation shows the posterior leaflet scallopes P1, P2, and P3. By adding 90° to the angle from which the intercommissural window is obtained, a left ventricular outflow tract (LVOT) view and the A2 and P2 scallops are shown.<sup>148</sup> 3D TEE of the mitral valve can give a comprehensive view of the entire mitral valve from a single window in real

time, with simultaneous visualization of all scallops. By providing a direct view of the entire mitral valve from the atrial side with 3D TEE; adjacent structures such as the left atrial appendage and aortic valve can be evaluated in a single window. Percutaneous mitral valve repair aims to grasp the free edges of the anterior and posterior leaflets. Especially deep cleft-like depressions in the posterior leaflet may be associated with severe MR and the presence of these structures may hinder the success of the procedure. 3D TEE is superior to 2D TEE in detecting mitral clefts visible from the atrial and ventricular aspects of the mitral valve (Fig. 42).<sup>149</sup>

In the EVEREST study, MitraClip procedure was limited to A2–P2 scallops with central jets; however today, successful MitraClip application is also performed in pathologies of P1 or P3 segment.<sup>150</sup> The presence of calcification in the 'grasping zone' of the mitral valve is an important limitation for successful implantation of MitraClip. At least 5 mm of distal mitral leaflet tip without calcification should be confirmed in the pre-procedural evaluation. Another point to check is the length of the anatomically shorter posterior leaflet. The posterior leaflet must be long enough to allow it to be safely caught by the MitraClip. The preferred posterior leaflet length is  $\geq 10$  mm, but MitraClip can be applied to the 7–10 mm long posterior leaflet with normal motion. It has been shown that mitral valve anatomy with posterior leaflet less than 7 mm in length is not suitable for MitraClip. Mitral valve area can be reduced by 50% with the first MitraClip and by 30–40% with the second.<sup>151</sup> In order to avoid mitral stenosis after the procedure, mitral valve less than 4 cm<sup>2</sup> is not preferred. In patients with good leaflet mobility, a valve area of 3–4 cm<sup>2</sup> is not an obstacle to the application of MitraClip.<sup>145</sup> It is known that a valve area of less than 3 cm<sup>2</sup> is likely to result in mitral stenosis as a result of MitraClip, and therefore a mitral valve with a valve area of less than 3 cm<sup>2</sup> is also not well suited to MitraClip. In the pre-procedural evaluation of the valve area, 3D TEE and Multiplanar reconstruction (MPR) measurement provide valuable information and are superior to 2D measurements.<sup>143</sup> The presence of a flail mitral valve may adversely affect the success of MitraClip. It is recommended that the flail segment width should be less than 15 mm and the flail gap less than 10 mm. Leaflets that do not meet these conditions may require more than one MitraClip implantation. MitraClip application is not recommended in cases with rheumatic involvement (Fig. 43) and endocarditis sequela accompanied by advanced valve restriction (Fig. 44).<sup>145</sup>

Mitral gradients as well as mitral valve area should be determined before the procedure. The increased flow associated with MR may lead to overestimation of the stenosis. The mean gradient should be measured before the procedure, and if it is 5 mmHg or more, it should be kept in mind that the patient is not suitable for the procedure (Fig. 45) When the indication for intervention of MR is evaluated, a cardiac team consisting of a cardiovascular surgeon, interventional cardiologist, and an experienced echocardiographer with expertise in mitral valve imaging should consider all treatment options. High surgical risk patients with appropriate valve pathology may be candidates for MitraClip.

The MitraClip procedure is divided into the following steps: 1) Transeptal puncture; 2) Advancing the Steerable Guide Catheter into the left atrium; 3) Advancement of the Clip Delivery System into the left atrium; 4) Positioning the MitraClip above the mitral valve; 5) Advancement of MitraClip into the left ventricle; 6) Grasping the leaflets, evaluating the result and releasing MitraClip.

### Transeptal Puncture

Transeptal puncture, which is the first step of the procedure, is one of the most critical stages that determines the success of the procedure. A suitable puncture point allows other steps to be performed quickly and safely. For a successful transeptal puncture, the anatomy of the interatrial septum (IAS) and the corresponding TEE images should be known. A guide wire and a catheter over the wire are inserted into the superior vena cava prior to puncture. The catheter is retracted into the right atrium along the IAS and the tenting image of the catheter towards the left

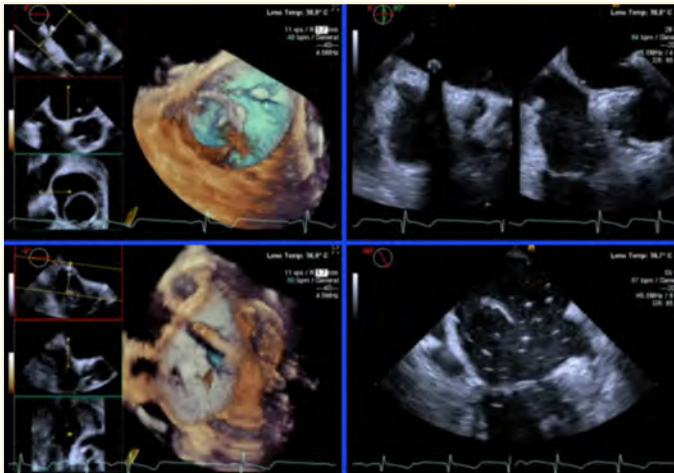


**Figure 48.** 2D and 3D TEE images are used during advancement of the MitraClip over the CDS.

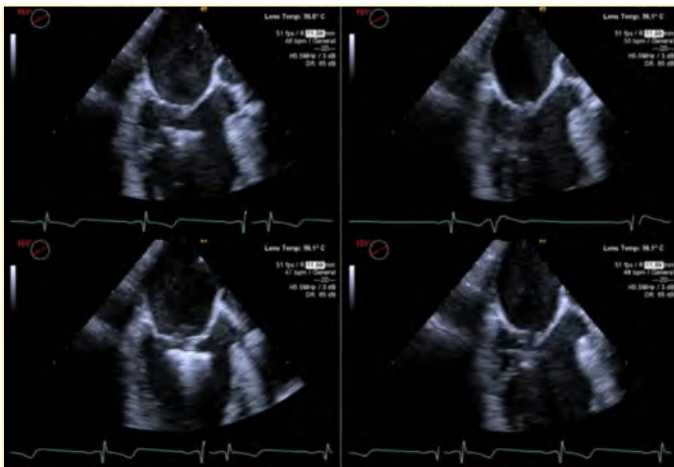


**Figure 49.** Positioning the MitraClip device in the left ventricle in the 2D TEE LVOT view.

atrium provides a visual reference for determining the puncture point. Traditional puncture guided by fluoroscopy would not be an adequate approach for the MitraClip procedure. Three TEE planes are used to define the puncture site. Superior-inferior orientation is adjusted in the 90°–120° bicaval view, while the anterior-posterior orientation is adjusted in 30°–50° short-axis view (Fig. 46). Finally, the distance to the mitral valve plane (puncture height) is determined in 0° four-chamber view. The short-axis view image is very important to avoid aortic puncture.<sup>152</sup>

It is preferred that the optimal puncture point be in the superior and posterior portion of the IAS. The location of the transseptal puncture to be preferred in degenerative and functional MR is different. In degenerative MR, a height of 4–5 cm to the plane of the mitral annulus is preferred. In functional MR, the coaptation line is located below the annular plane. Therefore, the puncture site should be lower and closer to the annular plane. Approximately 3.5 cm above the annular plane is the preferred puncture site in these patients (Fig. 47).<sup>153</sup> Even if patent foramen ovale is present, it is not a preferred puncture point due to its anterior location. Atrial septal defect; cannot stabilize SGC and there is an increased risk of atrial septal rupture. Therefore, even if it is in a suitable location, atrial septal defect is not a suitable transition zone.<sup>154</sup> The puncture point should be confirmed with agitated saline injection after the puncture. An unsuitable puncture site prolongs the procedure time and paves the way for possible complications. Choosing the most suitable puncture

point by using more than one TEE windows while determining the puncture site will facilitate the other steps of the MitraClip procedure.

### Advancing the Steerable Guiding Catheter Into the Left Atrium

Following the transseptal puncture under TEE guidance, the Mullen sheath and dilator are advanced into the left atrium, and a guidewire is placed in the left upper pulmonary vein. Placement of the guidewire in the left atrial appendage is associated with an increased risk of thromboembolism. The position of the wire should be carefully checked with the utility of TEE. The SGC is a large (24F) sheath with its own dilator through which the CDS is advanced into the left atrium. After the position of the wire is controlled, the SGC is advanced into the left atrium with a dilator under the guidance of fluoroscopy and TEE. A perspective showing both the right and left atrial cavities divided by the IAS provides the best view to follow the progression of the SCC from the right atrium to the left atrium.<sup>155</sup> During the passage of the guiding catheter with the dilator the tenting image of IAS is observed.

There is a radiopaque and hyperechoic double ring at the tip of the SGC, which allows it to be recognized. The advancement of the SGC should be carefully monitored under continuous TEE and fluoroscopic monitoring to avoid injury to the free left atrial wall. When the SGC is safely placed in the left atrium, the dilator is withdrawn first, followed by the wire. The use of 3D TEE allows the measurement of the length of the SGC in the left atrium. It is very important to know this length when the SGC needs to be pushed in or pulled back inside the left atrium in the following steps.<sup>154</sup>

### Advancement of the Clip Delivery System Into the left Atrium

The CDS is slowly advanced to the tip of the catheter. At this stage, the movement of the CDS inside the catheter should be carefully monitored with fluoroscopy. At the same time, the position of the catheter along the IAS, whether there is a safe space between the tip of the catheter and the left atrial free wall, and the safety distance from the left atrial appendage should be checked by TEE. Thus, complications such as retraction of the catheter into the right atrium, free wall injury and thromboembolism can be avoided. Three dimensional TEE and X-plane images can be useful for monitoring the catheter tip. Under fluoroscopy guidance, the MitraClip is pushed 1 cm out of the CDS to assess the space in front of its catheter. If friction is not felt and MitraClip motion is not abnormal, the MitraClip is retracted into the CDS and the CDS is advanced into the left atrium with the same length (Fig. 48).<sup>156</sup>

When the CDS reaches the tip of the SGC, the tip of the catheter should be checked in TEE with agitated saline. The CDS is removed through the catheter while the catheter is in a laterally oriented position.

### Positioning of the Mitraclip Above the Mitral Valve

As the CDS is pulled more medially along the aortomitral junction on to the mitral valve, this movement can be observed by counterclockwise rotation of the TEE probe in the range of 35°–55° view and slightly retraction of the probe. During these maneuvers, the atrial protrusion between the left superior pulmonary vein and the left atrial appendage may become an obstacle to the CDS maneuver, and care must be taken not to damage this protrusion. Control is required in at least two TEE planes during this movement. The first plane enables the visualization of the CDS blocked by the atrial protrusion and the second allows the measurement of the distance of the guide catheter to the IAS.<sup>155</sup> A regular cross control is required between these two planes. 3D TEE is very useful in directing the distal part of the CDS to the target in the mitral valve.

After the CDS is positioned on the mitral valve, the arms of the MitraClip device are opened 180° to achieve optimal positioning before the advancement into the left ventricle. The initial target for the first clip

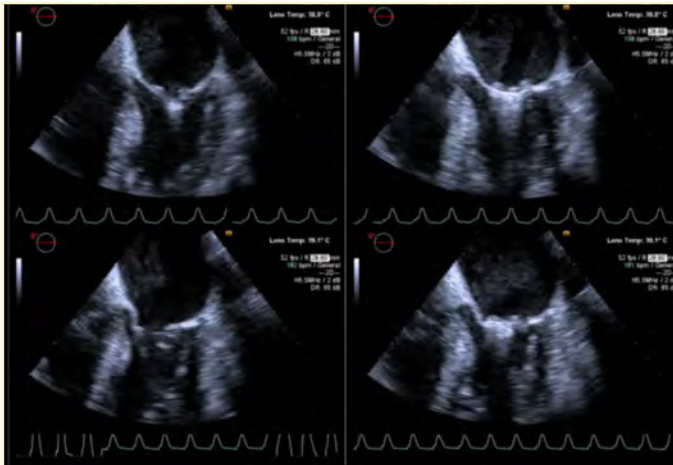


**Figure 50. Demonstration of the leaflet capture phase of the MitraClip device in the 2D TEE LVOT view.**

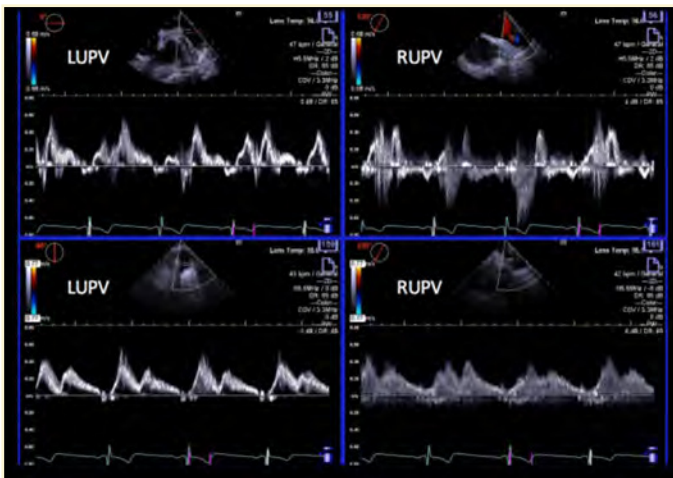


**Figure 51. The disappearance of the systolic flow reversal in the pulmonary veins and the predominance of the S' wave in the upper left and right upper pulmonary veins by TEE with the decrease in the severity of MR.**

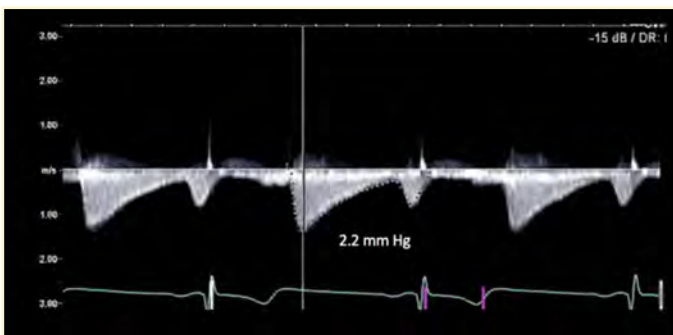


**Figure 52. Mean gradient of the mitral valve measured after MitraClip implantation.**

depends on the expected number of clips to be used. The tip of the MitraClip should be directed towards the largest proximal isovelocity surface area (PISA). If more than one MitraClip is planned to be used, a 'medial to lateral' approach should be followed.<sup>156</sup> When the MitraClip is opened on the mitral valve, two special conditions need to be checked.

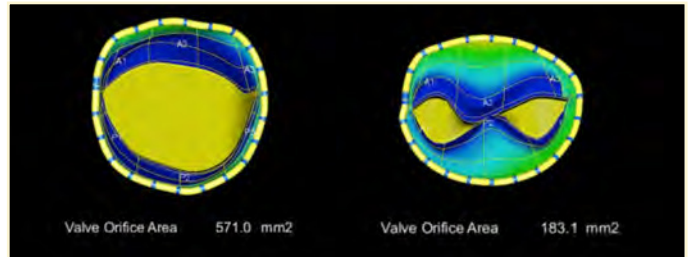


**Figure 53. The orifices developed after MitraClip are measured planimetrically with 3D TEE: The new areas are added to each other arithmetically.**

The first is the perpendicular position of the CDS axis to the mitral valve plane. The second situation is when the MitraClip arms are in the open position, a perfectly perpendicular angle to the coaptation line should be maintained. Medial-lateral position of MitraClip is evaluated in the intercommissural view at 40°-60° mid-esophageal, while anterior-posterior positioning is performed in the LVOT view at 135°-150°. MitraClip alignment can be performed by monitoring these two planes simultaneously in X-plane imaging. In the correct position, MitraClip arms should not be visible in the intercommissural view, and both MitraClip arms should be visualized in full length in the LVOT view.<sup>152</sup> At this stage, MitraClip positioning can be performed by reducing probe manipulation with 3D TEE. In addition, TTE short-axis images at the level of the mitral leaflets can be used in cases where TEE windows are not sufficient.

### Advancement of Mitraclip Into the Left Ventricle

In routine practice, it is recommended to advance the MitraClip into the left ventricle while the arms of the clip are open. However, during the advancement from the left atrium into the left ventricle, the carefully adjusted orientation of the MitraClip may be distorted. It is often preferred to advance the closed MitraClip by holding breath by anesthesia in the LVOT image, under the mitral leaflets, in the region of the regurgitant jet.<sup>157</sup> Under the guidance of fluoroscopy and TEE, advancement along the mitral valve should be observed. Advancement of the MitraClip into the left ventricle is best followed in X-plane imaging, where the intercommissural view and the LVOT view can be evaluated simultaneously. The arms of the MitraClip, which were closed during the transition, should be opened again below the coaptation line. The 2D transgastric short-axis view allows the MitraClip alignment to be visualized relative to the coaptation line. 3D TEE from the atrial face allows for careful monitoring of subtle movements under the valve, and this window is very useful in confirming the perpendicular position of the MitraClip to the coaptation line. If any changes for the MitraClip position are required, these should be minimal to avoid entanglement in the chordae. If significant movements are required, the MitraClip should be retracted into the left atrium where it can be safely manipulated.<sup>148</sup> Correct orientation of the MitraClip dividing the MR jet in intercommissural and LVOT views, vertical alignment to the coaptation line, and verification that both mitral leaves move freely over the arms of the MitraClip are critical for successful grasping of the mitral valve leaflets.

### Grasping of the Leaflets, Evaluation of the Grasping of the Leaflets and Release of the Mitraclip

Two-dimensional TEE is the basic imaging method to be preferred during the grasping of the mitral leaflets by MitraClip. The image obtained with 3D TEE can not provide sufficient resolution at this stage.<sup>155</sup> In LVOT imaging with 2D TEE, the MitraClip arms are positioned at 120° angle and pulled back until the leaflets are firmly captured (Fig. 49, 50).

Capture of the posterior leaflet can be observed in LVOT view, and capture of the anterior leaflet can be observed in four-chamber view.<sup>154</sup> Entanglement of the chordae tendinea between the arms of the MitraClip adversely affects the success of the procedure; this can be checked

in intercommissural view. If sufficient leaflet tissue is captured between the grippers and arms, MitraClip is gradually closed and the remaining amount of regurgitation is monitored with color Doppler. Excessive distortion of the mitral valve should be avoided. Initial echocardiographic results of valve grasping with MitraClip should be evaluated under general anesthesia. The essential point to be considered here is that similar hemodynamic conditions as maintained in the first echocardiographic evaluation of the patient should be met during the final measurements. Providing hemodynamically similar conditions is especially important in functional MR.<sup>155</sup> In addition, the initial color and gain settings of the device should be preserved. A reduction in MR should be confirmed by TEE before MitraClip is released from the CDS. The total amount of new double regurgitation jets depicted in color Doppler in 2D TEE may lead to overestimation of MR.<sup>158</sup> With the improvement in the severity of MR, it is expected that the systolic flow reversal observed in the pulmonary veins will disappear and the S' wave will become dominant (Fig. 51).

Optimal evaluation after MitraClip procedure has prognostic significance. The echocardiographic evaluation performed for native MR cannot be applied exactly because of the artifacts created by the clip and the morphological changes in the valve after MitraClip procedure. Although parameters such as color Doppler, transmitral flow and regurgitant volume have been shown to be unuseful, other parameters are promising. Although it is difficult to evaluate 3D vena contracta area, it provides valuable prognostic data during follow-up together with the pulmonary vein flow pattern. However, no validation study has been conducted on this subject yet. More studies and standardization in this area are of utmost importance.<sup>159</sup>

After MitraClip implantation, the mitral valve gradient should be evaluated to exclude significant valve stenosis. Assessment of mitral gradient have similar sensitivity to double orifice planimetric measurements.<sup>160</sup> A mean gradient of up to 5 mmHg is considered acceptable (Fig. 52).

Planimetric measurement of the mitral valve can be done on short-axis transgastric images and 3D TEE by arithmetic addition of both orifice areas to each other (Fig. 53).

The final orifice area and geometry are precisely evaluated by 3D TEE. If the result after MitraClip implantation is not satisfactory, the MitraClip can be reopened and repositioned to achieve a more optimal position. If the residual MR is satisfactory; MitraClip is released from the transport system and, CDS and SGC are retracted. TEE is used to ensure that the system does

**Table 11. Tricuspid Regurgitation**

Primary	Secondary
1. Rheumatic	1. Pulmonary hypertension accompanying RV remodeling due to left heart origin
2. Infective Endocarditis	2. Dilated Cardiomyopathy
3. Iatrogenic (device lead endomyocardial biopsy)	3. Annular dilatation (associated with AF)*
4. Congenital (Ebstein anomaly, major artery transposition)	4. RV volume loading (shunt/high output)
5. Others (carcinoid syndrome, endomyocardial fibrosis, drug use, radiation, trauma)	

\*: Isolated TV is defined for cases accompanied by AF with left ventricular EF >60%, systolic pulmonary artery pressure <50 mmHg, no accompanying left-side valve disease, and normal-appearing tricuspid valve leaflets.

not contact the atrial structures during the system retraction. Repeated hemodynamic, angiographic and echocardiographic evaluations are performed. The degree of any shunt after transseptal puncture is also assessed.

**Conclusion**

MitraClip procedure is an important therapeutic option of severe MR in patients with high risk for surgical mitral valve repair or rep-

**Table 12. ACC/AHA Guidelines for Tricuspid Valve Grading**

Stage	Description	Valve Hemodynamics	Hemodynamic Outcomes	Clinical Symptoms and Signs
B	Progressive TV, central jet covers less than 50% of RA	Width of Vena Contracta <0.7 cm	ERO <0.40 cm <sup>2</sup>	Regurgitant volume <45 mL
C	Asymptomatic Severe TV, central jet covers more than 50% of RA	Width of Vena Contracta >0.7 cm	Dilated RV and RA, increased RA c-V wave	Venous pressure increase, no symptoms
D	Symptomatic Severe TV, same as Stage C with symptoms	The central jet occupies more than 50% of the right atrium Vena contracta width >0.7 cm, ERO >0.40 cm <sup>2</sup> Regurgitant volume >45 mL Dense, triangular-shaped CW Doppler signal Systolic flow reversal in the hepatic vein	Venous pressure increase, dyspnea on exertion, fatigue, ascites	ERO >0.40 cm <sup>2</sup> , Regurgitant volume >45 mL

The c-V wave indicates a positive systolic wave, ERO stands for effective regurgitant orifice; RA is the right atrium; RV is the right ventricle, and TY denotes tricuspid insufficiency.

lacement. It is of utmost importance to select the best patient with a precise clinical and echocardiographic analysis for the success of this procedure. 3D echocardiography is useful not only for

**Table 13. Qualitative and Quantitative Echocardiographic Measurements Defining Severe TR According to the ESC Guidelines**

Qualitative	Abnormal/flail
Tricuspid valve morphology	Very large central jet or eccentric wall-impinging jet
Color Doppler regurgitant jet	Early peaking, dense, triangular-shaped signal
CW Doppler signal of the regurgitant jet	
Semi-quantitative	
Vena contracta width (mm)	> 7 <sup>a,b</sup>
PISA radius (mm)	> 9 <sup>c</sup>
Hepatic vein flow	Systolic flow reversal
Tricuspid inflow	E-wave dominant ≥ 1 m/s <sup>d</sup>
Quantitative	
EROA (mm <sup>2</sup> )	≥ 40
Regurgitant volume (mL/beat)	≥ 45
Chamber/vessel enlargement	RV, RA, inferior vena cava

CW, continuous wave; EROA, effective regurgitant orifice area; PISA, proximal isovelocity surface area; RA, right atrium; RV, right ventricle; TR, tricuspid regurgitation. a: Nyquist limit 50-60 cm/s. b: Preferably biplane. c: Baseline Nyquist limit adjusted to 28 cm/s. d: In the absence of other causes increasing right atrial pressure.

preprocedural mitral valve evaluation, but also for intraprocedural guiding, postprocedural complication and assessment of procedural success.

**Table 14. Proposed 5-Stage Tricuspid Regurgitation Classification**

Parameter	Mild	Moderate	Severe	Massive <sup>a</sup>	Torrential <sup>a</sup>
Qualitative					
TV morphology	Normal/Abnormal	Normal/Abnormal	Abnormal, flail, large coaptation defect		
TR jet by color Doppler	Mild, central	Moderate	Very large central jet or wall-impinging eccentric jet		
TR jet CW Doppler signal	Faint, parabolic	Dense, parabolic	Early-peaking dense / triangular	Peak TR velocity <2 m/s	-
Semi-quantitative					
VC width (mm) <sup>b</sup>	<3	3–6.9	7–13.9	14–20	>21
PISA radius (mm)	<5	6–9	>9	-	-
Hepatic vein flow	Systolic dominance	Systolic blunting	Systolic flow reversal		
Tricuspid inflow	Normal	Normal	Dominant E wave (≥1 cm/s)		
Quantitative					
EROA (mm <sup>2</sup> ) by PISA	<20	20–39	40–59	60–79	≥80
EROA (mm <sup>2</sup> ) by quantitative Doppler	-	-	75–94	95–114	≥115
EROA (mm <sup>2</sup> ) by 3D echo	-	-	75–94	-	≥115
Regurgitant volume (mL) by PISA	<30	30–44	45–59	60–74	≥75

a: Further studies are required; b: Biplane measurement is recommended. CW, continuous wave; EROA, effective regurgitant orifice area; PISA, proximal isovelocity surface area; TV, tricuspid valve; TR, tricuspid regurgitation; VC, vena contracta.

## Role of Imaging in Transcatheter Tricuspid Edge-to-Edge Repair

**Dr. Gökhan Kahveci, Dr. Emir Derviş**

Moderate or severe tricuspid regurgitation (TR) is a valve disorder, which is observed more frequently in increasing ages and affect about 4% of the patients aged 75 years or more.<sup>161</sup> TR is also associated with increased mortality and morbidity due to contribution to development of right heart failure irrespective of left ventricular (LV) systolic functions and pulmonary hypertension.<sup>161, 162</sup> The Etiology is of secondary origin in 90% of the patients with TR1.<sup>161</sup> In patients with primary or secondary pulmonary hypertension, leaflet tethering and annulus dilatation as a result of right ventricular (RV) remodelling due to pressure or volume overload are associated with the development of secondary TR.<sup>106</sup> In addition, there is a subgroup of patients with isolated TR because of annulus dilation. This situation is usually associated with atrial fibrillation in the absence of LV pulmonary hypertension and LV systolic dysfunction.<sup>163</sup> Causes of primary TR include infective endocarditis, rheumatic valve disorders, carcinoid syndrome, blunt chest trauma, myxomatous disease, congenital disease (Ebstein anomaly), endomyocardial fibrosis, iatrogenic etiologies (pacemaker leads, endomyocardial biopsies) (Table 11).<sup>106</sup>

TR severity is evaluated with multiple qualitative and quantitative parameters that are recommended by ESC and ACA/ACC guidelines. In patients with anatomically normal tricuspid valve (TV) trace and mild TR that does not cause any physiological consequences can be observed with transthoracic echocardiography (TTE). However, severe TR is associated with poor long term outcomes.<sup>164</sup> Regurgitation could be seen more severe especially in primary disorders of the tricuspid apparatus.<sup>106</sup> Table 12 shows the stages of TR in AHA/ACC guidelines.

Table 13 show echocardiographic criteria of severe TR which is recommended in ESC guideline.<sup>142</sup>

However with the percutaneous tricuspid valve repair studies there is a trend towards to revise the severity of TR grading, because there are difficulties in explaining the improvements in TR degree after the intervention with the current TR classification.<sup>165</sup> For example, in the SCOUT (Percutaneous Tricuspid Valve Annuloplasty System for Symptomatic Chronic Functional Tricuspid Regurgitation) trial, quantitative EROA decreased by  $-0.22 \pm 0.29$  mm<sup>2</sup>. However, pre-pro-

cedure EROA was  $0.85 \pm 0.22$  mm<sup>2</sup>, and post-procedure EROA was  $0.63 \pm 0.29$  mm<sup>2</sup>. Therefore, current TR severity grading schemes do not take into account the "torrential" nature of TR in the patients who were enrolled in these trials. In the SCOUT study, although TR grading decreased from "severe TR" to "severe TR" according to the current definition, patients quality of life parameters improved and their forward stroke volume increased.<sup>166</sup> To better characterize, the TR severity was proposed increasing the grades to include massive and torrential.<sup>165</sup> The proposed new TR grading scheme was summarized in Table 14.

Except grading and understanding the etiology of TR, the effects of TR on RV functions should be evaluated with echocardiography. In patients with TR undergoing left sided valve surgery, tricuspid annulus diameter should be measured. An annular diastolic diameter >40 mm (or >21 mm/m<sup>2</sup>) is associated with increased risk of persistent or progressive TR after mitral valve surgery.<sup>167</sup> Pulmonary artery systolic pressure is calculated from maximal TR velocity. Assessment of RV functions poses a challenge due to the geometric structure of RV which is affected by volume status and needs appropriate image acquisition.<sup>168, 169</sup> Normal RV systolic function could be defined with some parameters: Tricuspid annular plane systolic excursion (TAPSE) >16 mm, tricuspid valve systolic annular velocity >10.0 cm/s, and RV end-systolic area <20.0 cm<sup>2</sup> or fractional area change >35%. Alternative to echocardiography, cardiac catheterization can be performed to evaluate pulmonary vascular resistance and cardiac MRI regurgitation volume and RV functions can be evaluated.<sup>106</sup>

## Treatment

### Medical Therapy

Patients with severe TR usually have right HF symptoms or signs like peripheral edema and ascites. Diuretics can be used to decrease volume overload (Class 2a-C-E0). HF symptoms can be alleviated with loop diuretics, however their use is restricted because with using excessive diuretics may worsen the low-flow syndrome.<sup>106</sup> Aldosterone antagonists may be helpful, especially in patients with hepatic congestion. However, medical therapy is limited in patients with stage C and D groups described by the ACC guideline. Guideline directed medical therapy is useful for secondary TR related to HF with reduced LVEF. In selected patients with pulmonary hypertension, specific pulmonary vasodilators reduce pulmonary hypertension and pulmonary vascular resistance; as a result this may decrease secondary

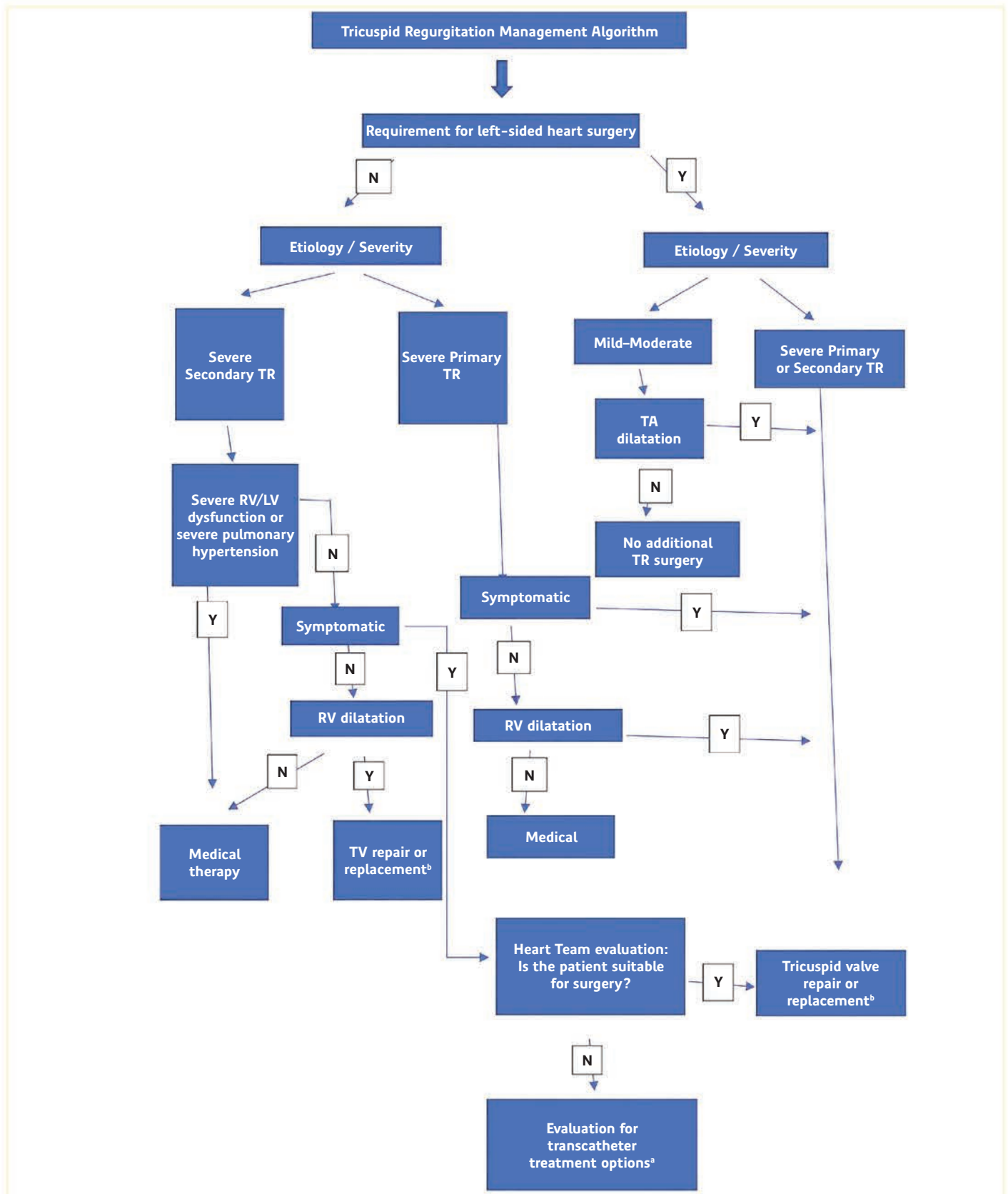


Figure 54. Management algorithm for tricuspid regurgitation as recommended in the ESC guidelines. (a) The anatomical suitability of the tricuspid valve (TV) for transcatheter procedures should be assessed by a Heart Team including specialists in tricuspid valve interventions (considering coaptation gap, presence of lead-associated TR, tethering height, and jet location). (b) If repair is not feasible, valve replacement is preferred. Y, yes; N, no; LV, left ventricle; RV, right ventricle; TA, tricuspid annulus; TV, tricuspid valve; TR, tricuspid regurgitation.

TR severity and RV afterload (Class 2a- C-EO).<sup>170, 171</sup> Restoration of normal sinus rhythm should be considered in patients with TR attributable to annular dilation associated with AF (Sinif 2a- C-EO).<sup>172, 173</sup>

### Invasive Management

TV interventions are underutilized in clinical practice and are often delayed for intervention.<sup>174</sup> Appropriate timing of the intervention is important to avoid the risk of end organ damage and irreversible RV failure, which is associated with increased risk of surgery. In ESC guide-

**Table 15. 2021 ESC Guidelines for Tricuspid Valve Insufficiency Treatment**

Recommendation	Class	Level
In patients undergoing left-sided surgery with severe primary TI	1	C
Surgical treatment is recommended if RV dysfunction is absent in symptomatic patients with isolated severe TI	1	C
Consider surgical treatment in patients undergoing left-sided surgery with moderate TI	2a	C
Surgical treatment should be considered in mildly symptomatic or asymptomatic patients with isolated severe TI and suitable for surgery with RV dilation	2a	C
In patients undergoing left-sided surgery with severe secondary TI, surgical treatment is recommended	1	B
Consider surgical treatment in patients undergoing left-sided surgery with mild or moderate TI and a dilated annulus	2a	B
In the presence of severe secondary TI (regardless of prior left-sided surgery), consider surgical treatment if there is RV dilation or symptoms without RV or LV dysfunction	2a	B
In patients who cannot undergo surgery as decided by a heart team, consider transcatheter treatment at specialized centers for severe symptomatic secondary TI	2b	C

LV: Left ventricle; RV: Right ventricle; TK: Tricuspid valve; TY: Tricuspid insufficiency; 2D: Two-dimensional. a Recommendation class; b Level of evidence; c Recurrent left-sided valve dysfunction must be excluded in patients who have previously undergone left-sided surgery; d Transcatheter procedures can be applied in experienced centers as decided by the Heart Team in patients with suitable tricuspid valve anatomy where an increase in quality of life or survival is expected.

lines, surgery is recommended in symptomatic patients with severe TR (Class 1-C). In selected asymptomatic or mild symptomatic patients with severe TR who are appropriate for surgery, intervention should be considered when RV dilation or dysfunction occurred (Class 2a-C).

Surgery is recommended in patients with severe TR who are planned for left sided valve surgery (Class 1-B). Surgery should be considered in patients undergoing left sided valve surgery with mild or moderate TR and diastolic tricuspid annulus >40 mm (or >21 mm/m<sup>2</sup>) measured by 2D echocardiography (Class 2a-B).<sup>142</sup> Surgical TV repair does not increase perioperative risk during left-sided surgery. On the contrary TV repair promotes reverse remodelling of RV and increase functional status when patient has annular dilation even in the absence of severe TR.<sup>167, 175, 176</sup>

Patients with new-onset or worsening secondary TR have increased postoperative risk in reoperation due to delayed referral or accompanying poor clinical condition.<sup>177</sup> In order to improve prognosis even in this challenging scenario, treatment of severe TR should be considered in case of RV dilatation or decreased RV systolic function, even if the patient is not symptomatic (after exclusion of left-sided valve dysfunction, severe RV or LV dysfunction and severe pulmonary vascular disease/ hypertension) (Class 2a-b).

In addition if it is possible,annuloplasty with prosthetic ring is preferred option to valve replacement.<sup>167</sup> Valve replacement may be necessary if there is severe annular dilatation or intrinsic valve pathology.<sup>142</sup> Figure 54 and Table 15 show recommendations of ESC guidelines for the TR treatment.<sup>142</sup>

In the ACC/AHA guidelines, TV surgery is recommended in patients with severe TR (Stages C and D) undergoing left-sided valve surgery (Class 1-B-NR). TV surgery is beneficial in patients with progressive TR (stages B) undergoing left-sided valve surgery, when annulus diameter is >40 mm or in patients with signs and symptoms of RV failure (Class 2a- B-NR). In patients with primary severe TR (stage D) isolated TV surgery can be beneficial in order to reduce symptoms and recurrent hospitalizations (class 2a- B-NR). In patients with severe secondary TR (stage D) related with annular dilation (in the absence of pulmonary hypertension or left-sided disease) who are poorly responsive to medical therapy, isolated TV surgery can be beneficial in order to reduce symptoms and recurrent hospitalizations (class 2a- B-NR). In asymptomatic patients with severe TR (stage C) when progressive RV dilation or systolic dysfunction occurs, isola-

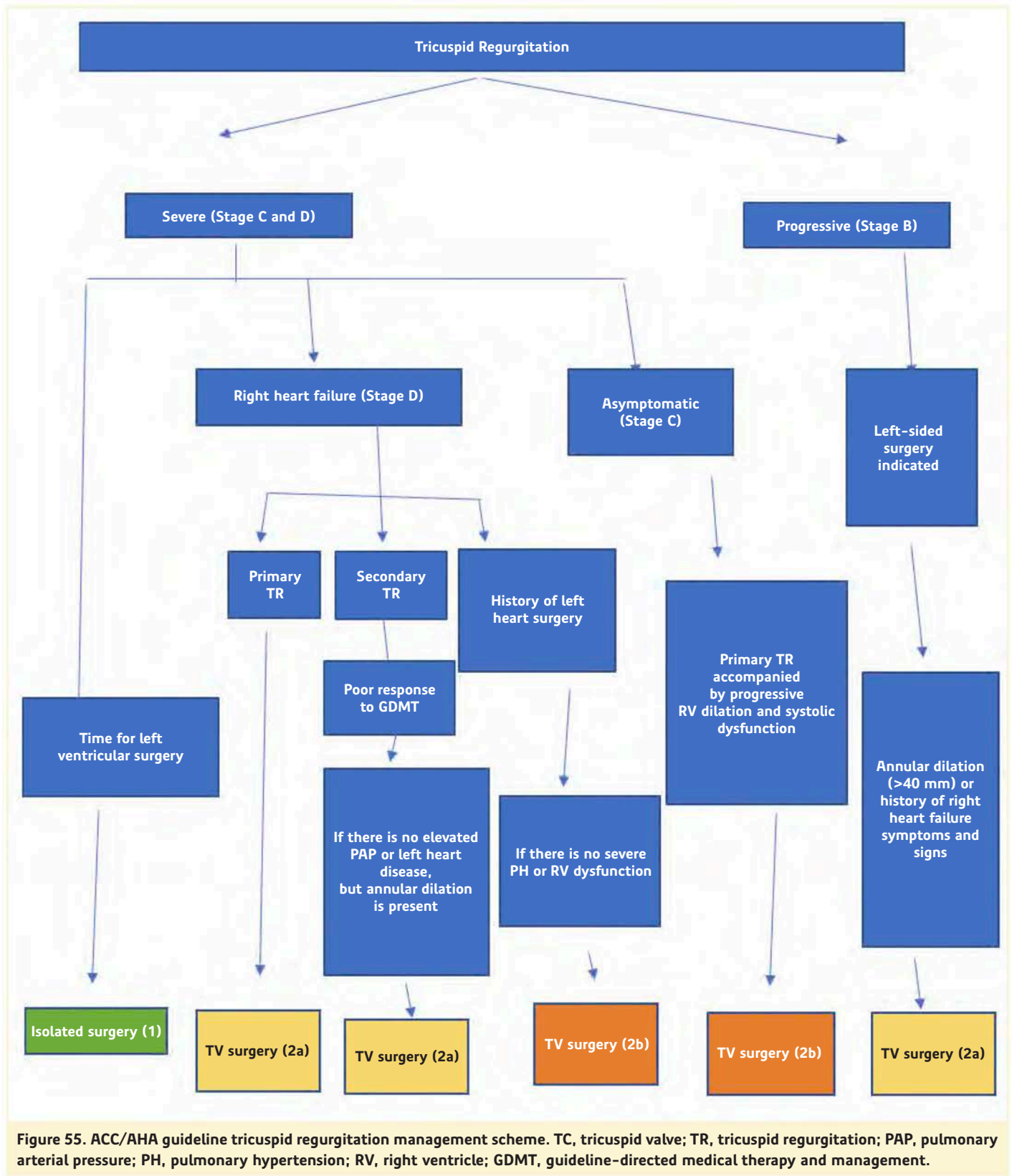
**Table 16. TRI-SCORE: Risk Factors and Scoring for In-Hospital Mortality Post Isolated Tricuspid Valve Surgery**

Risk Factor	Score
Age >70	1
NYHA functional capacity III-IV	1
Right heart failure symptoms	2
Daily furosemide dose >125 mg	2
Glomerular filtration rate <30 mL/min	2
Elevated total bilirubin	2
Left ventricular ejection fraction <60%	1
Moderate/severe right ventricular dysfunction	1
<b>Total</b>	<b>12</b>

a: In the study, moderate/severe right ventricular dysfunction is defined as TAPSE <17 and/or tissue Doppler systolic peak annular velocity of 9.5 cm/s and/or visually significant reduced fractional area change.

ted TV surgery may be considered (Class 2b C-LD). In patients with severe TR (stage D) who have previously undergone left-sided valve surgery, reoperation with isolated TV surgery may be considered in the absence of severe pulmonary hypertension or severe RV systolic dysfunction (Class 2b- B-NR).<sup>106</sup> In Figure 55, recommendations of ACC/AHA guidelines for invasive management of TR is illustrated.

Isolated TV surgery is reported to be a high risk surgery with 10% mortality.<sup>178-180</sup> In a study performed in France, early and mid-term outcomes of patients who underwent isolated TV surgery were investigated.<sup>181</sup> Although isolated TV surgery was found to be associated with high mortality in this study, preoperative clinical (NYHA class 3/4, RV failure signs), echocardiographic findings (moderate/severe RV dysfunction or dilation) and laboratory markers (lower glomerular filtration rate) rather than the TR etiology were associated with mortality and morbidity. Therefore, the main reason for the high mortality in TV surgeries is that the most patients presented with advanced stages of the disease and with impaired kidney and liver functions.<sup>181</sup> It is obvious that both Society of Thoracic Surgeons (STS) and logistic EuroSCORE/EuroSCORE II risk scores are not designed for TV surgeries. This study revealed the necessity of specific risk model which could predict mortality for TV surgery. Dreyfus et al.<sup>182</sup> developed a new risk model, which is named as TRI-SCORE, to predict in hospital mortality after isolated TV surgery (Table 16). In this risk model, there are 8 different variables and the expected mortality over a maximum of 12 points increases from 1 point to 9 points, from 1% to 65%.



In the study, the risk score  $\leq 3$  was accepted as low risk, 4–5 as medium risk,  $\geq 6$  points as high risk.<sup>182</sup> According to these results, TV intervention can be considered before the patient’s performance decreases and at the late and hopeless stage of the disease. In addition, patients defined as high-risk TV surgery in the past were conservatively

managed. However, with developing transcatheter technologies and published studies with satisfactory results, such symptomatic high-risk patients can be referred to transcatheter intervention. According to ESC guidelines, transcatheter interventions may be considered by the Heart Team at experienced Heart Valve centers in symptomatic,

inoperable, anatomically eligible patients (Class 2b–C).<sup>142</sup> Nowadays, the most preferred transcatheter intervention is edge-to-edge repair of the valve.<sup>183</sup> In some retrospective analyzes, edge-to-edge repairs have been shown to significantly reduce the TR severity and improve symptoms.<sup>184, 185</sup> The 1-year follow-up results of the prospective, multicenter, international, single-arm TRILUMINATE study, in which TriClip (Abbott, Chicago, IL, USA) device was used as edge-to-edge repairing system, showed that a durable repair with significant reduction in TR were associated with improvements in quality of life and functional capacity; reduced rates of hospitalization and low mortality in a fragile population at high risk; and positive structural and functional right ventricular reverse remodeling over time.<sup>186</sup> From August 1, 2017 to November 29, 2018, a total of 85 patients who had symptomatic moderate or greater TR and high surgical risk and no indications for left sided or pulmonary valve correction and received successful edge-to-edge repair by TriClip tricuspid valve repair system, were included in this study. Patients were excluded from the study if they had systolic pulmonary artery pressure of more than 60 mm Hg measured by echocardiography, a previous tricuspid valve procedure, cardiovascular implantable electronic devices (either pacemaker or implantable cardioverter defibrillator leads) which would inhibit proper TriClip placement. In this study, only patients with coaptation gaps of less than 10 mm were included.<sup>187</sup> TR severity was assessed according to five-class grading scheme (mild, moderate, severe, massive, and torrential).<sup>165</sup> The primary safety endpoint was a composite of major adverse events at 6 months, including cardiovascular mortality, myocardial infarction, stroke, new onset renal failure, endocarditis requiring surgery, and non-elective cardiovascular surgery for tricuspid valve repair system-related adverse events post procedure. The primary efficacy endpoint was a reduction in tricuspid regurgitation severity by at least one grade at 30 days. At 30 days, 71 (86%) of 83 patients had at least one grade reduction in tricuspid regurgitation severity.<sup>187</sup> At 1 year, 87% of subjects had sustained TR reduction  $\geq 1$  grade.<sup>186</sup> In this study, after TV edge-to-edge repair, significant improvement in quality of life, clinical status and reduced hospitalization rates was observed. Clinical improvements occurred mostly within first month after the procedure. There was no significant difference in NYHA class and 6 minute walk distance between 30 days and 1 year. At 6 months, three (4%) of 84 patients experienced a major adverse event. Cardiovascular death occurred in two patients and in one patient new onset renal failure was observed. In other clinical safety end points, in five (7%) of 72 patients, a single leaflet device attachment occurred (three anterior, two septal) without clinical findings or worsening of tricuspid regurgitation. In 9 patients major bleeding and new onset atrial fibrillation was observed in one patient. Tricuspid stenosis (mean 5.3 mm Hg) developed in 6 patients requiring no further intervention. No cases of stroke, myocardial infarction, or device embolisation were reported within 6 months. There were no cases of endocarditis or device related adverse event requiring non-elective cardiovascular surgery. In conclusion, TriClip repair system has been found to be safe and effective in patients with moderate or greater TR and has been associated with excellent repair durability and a sustained and marked clinical benefit with reduced rates of hospitalization and low mortality after 1 year in a fragile population at high risk.<sup>186</sup> However, selection and evaluation of the patients, who are suitable for percutaneous TV repair, is important to increase the success of the intervention. In this regard there are echocardiographic and clinical parameters to consider. According to instructions for use TriClip device is indicated for patients whose TV anatomic coaptation gaps are  $\leq 10$  mm, and who are at high risk for TV surgery, do not have severe mitral regurgitation or severe pulmonary hypertension (systolic pulmonary artery pressure  $>60$  mm Hg) and are symptomatic despite medical therapy.<sup>188</sup> Contraindications include rheumatic TV disease, active endocarditis and presence of

thrombus of intracardiac origin or in femoral veins or vena cava.<sup>188</sup> In addition, device is not approved for TR associated with congenital valve lesions. The required minimum leaflet insertion (6 mm for smaller and 9 mm for larger devices) defines the minimum mobile

**Table 17. Predictors of Success and Exclusion Criteria for Echocardiography During Procedures**

Success Predictors	Exclusion Criteria
Coaptation gap $<7$ mm	
Leaflet length $>7$ mm	
Tethering height 10 mm	
Mean tricuspid pressure gradient $<3$ mmHg	
Echocardiographic exclusion criteria	
Inadequate visualization of the valve	
Rheumatic/congenital etiology	
Active endocarditis	
Intracardiac thrombus	
Severe leaflet and annular calcification	

leaflet length. It is recommended that pre-implantation transvalvular mean gradient should be  $\leq 3$  mm Hg because leaflet grasping may cause valvular stenosis. (mean pressure gradient of  $\geq 5$  mm Hg should be considered as a significant risk factor for creating tricuspid valve stenosis).<sup>188</sup> In the Edwards PASCAL user manual, which is another edge-to-edge repair system approved for use in Europe, echocardiographic contraindications are stated as poor visualization of the TV, intra-cardiac mass, thrombus or vegetation. In addition, the operator is advised to consider the anatomical structures described: non-degenerative TV diseases, moderate to severe signs of calcification in the grasping area, severe calcification in the annulus or subvalvular apparatus, presence of cleft or perforation in the grasping area, and as well as leaflet mobility length  $<8$  mm.<sup>188</sup> Optimal echocardiographic criteria for percutaneous tricuspid edge-to-edge repair are still in development. In a substudy of TriValve registry it has been shown that baseline RV size and functions, as well as estimates of systolic pulmonary pressure did not predict clinical outcomes.<sup>189</sup> Nevertheless, coaptation gap ( $\leq 7$  mm), regurgitation jet in central or antero-septal location, and tethering height ( $\leq 10$  mm) are associated with higher procedural success and improved survival.<sup>185</sup> Table 17 summarizes the echocardiographic markers that affect the success of the procedure and echocardiographic exclusion criteria.<sup>188</sup>

## Echocardiographic Imaging

### Pre-Procedural Evaluation

#### Tricuspid Valve Anatomy

The TV is the largest and most apically positioned of cardiac valves with a normal orifice area between 7 and 9 cm<sup>2</sup>.<sup>190</sup> TV peak trans-tricuspid diastolic velocity is lower than 1 m/s with mean gradients of 2 mm Hg due to the low pressure difference and large surface area between the RA and RV.<sup>191</sup> The TV can be divided into 4 components similar to mitral valve: TV leaflets, papillary muscles, chordal attachments, and annulus (with attached atrium and ventricle).<sup>191</sup>

#### Tricuspid Valve Leaflets

Although TV usually consist of 3 leaflets of unequal size, it may consist of 2 or more than 3 leaflets.<sup>190, 192</sup> Leaflets are defined as septal, anterior-superior and inferior according to the anatomical position of the body.<sup>191</sup> However, the nomenclature was made as septal, anterior and posterior. The anterior leaflet has the widest and longest radial length, with a larger surface and greater range of motion. The posterior leaflet, which has the shortest circumferential diameter, may

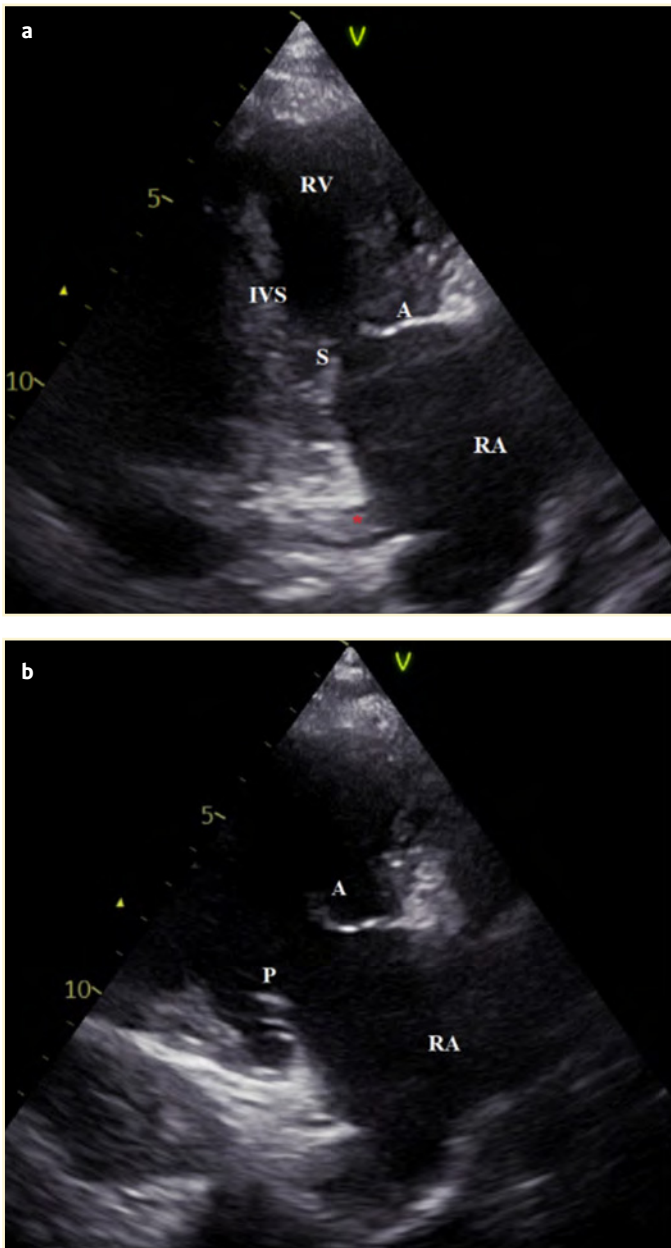


**Figure 56. A, B. Parasternal inflow windows. (A) Anterior and septal leaflets are observed when the coronary sinus ostium (\*) or IVS is observed. (B) Anterior and posterior leaflets are observed when the probe is angled inferiorly and slightly to the right and no IVS is seen. A, anterior; IVS, interventricular septum; P, posterior; RA, right atrium; RV, right ventricle; S, septal.**

consist of multiple scallops. Septal leaflet has the shortest radial length and is the least mobile.<sup>193</sup> Although the anatomical markers of the leaflets may vary according to the size and shape of the annulus, the commissure between the posterior and septal leaflet is usually located near the entrance of coronary sinus to the right atrium. The commissure between the septal and anterior leaflet is usually adjacent to the non-coronary sinus valsalva of the aortic root. The antero-septal commissure is the longest, as the anterior and septal leaflet are the largest circumferentially.<sup>193</sup> The coaptation of TV is located at the level of annulus or just below it, with the coaptation length of 5 to 10 mm.<sup>194</sup> This long coaptation length acts as a reserve, allowing the annulus to expand slightly before the malcoaptation occurs.<sup>193</sup>

## The Papillary Muscles and Chordae

There are 2 distinct papillary muscles, anterior and posterior, and a third variable papillary muscle. The anterior papillary muscle is the largest papillary muscle and support both anterior and posterior leaflets with chordae. Posterior papillary muscle, which is bifid or trifid, support with chordae to posterior and septal leaflets. Septal papillary muscle may show variations and be small, multiple, or absent in 20% of normal patients. The chordae may extend directly from the septum to the anterior and septal leaflets. Accessory chordae can attach directly to right ventricular free wall and as well as to moderator band.<sup>193</sup>

## Tricuspid Annulus

The normal tricuspid annulus is D-shaped and consists of nonplanar two distinct segments: a large C-shaped segment corresponding to the RV and RA free wall, and a relatively straight segment that corresponds to the septal leaflet and ventricular septum. The tricuspid annulus has a complex and dynamic structure that allows it to change under loading conditions. Unlike the mitral annulus, the semilunar valve corresponding to the tricuspid annulus has no fibrous continuity.<sup>193</sup> In healthy group, the circumference and area of the tricuspid annulus are  $12 \pm 1$  cm<sup>2</sup> and  $11 \pm 2$  cm<sup>2</sup>, respectively.<sup>190</sup> In addition, during atrial systole and also during late systole/early diastole, there is a significant increase in the annulus area ( $29.6 \pm 5.5\%$ ) and circumference.<sup>190</sup> The posteroseptal annulus is more ventricular, while the anteroseptal part is more atrial.<sup>167, 196</sup> In secondary TR, the annulus expands towards the posterior free wall and laterally and becomes more spherical and planar.<sup>197</sup> Dilation of the septal segment of the annulus is limited due to its relationship with the fibrous skeleton of the heart.<sup>198</sup>

## Transthoracic Echocardiography

Because of the complex structure of the TV, it is difficult to visualize the 3 leaflets in a single 2D plane. Therefore, it is tried to evaluate the structure of the valve and the pathophysiology of the regurgitation jet by using some anatomical markers from multiple different views. For example, the commissure between the anterior and septal leaflet is adjacent to the non-coronary cusp of the aortic valve, while the coronary sinus is adjacent to the commissure between the posterior and septal leaflet.<sup>199</sup> The first TTE view in the evaluation of the tricuspid valve.

## Parasternal Long Axis of the Right Ventricular Inflow View

From the parasternal long-axis (LAX) view, the transducer is angled inferiorly and to the right (toward the right hip) to produce the parasternal inflow view. If the coronary sinus ostium or the muscular interventricular ventricular septum appears, then the leaflets imaged are the anterior and septal ones. With the transducer angled more acutely inferiorly and to the right with no IVS seen, the anterior and posterior leaflets are imaged (Fig. 56A-B).<sup>200</sup>

## Parasternal Short Axis View

Rotation of the transducer about 90° from the parasternal long-axis view will yield the short-axis view, where the anterior tricuspid valve leaflet is generally seen. Septal leaflet can be seen if the image plane is tilted towards the left ventricular outflow tract.

## Apical 4 Chamber

In 4 chamber view, typically septal leaflet and posterior or anterior leaflet can be observed. With slight anterior angulation, anterior and septal leaflet can be seen. With slight anterior angulation, anterior and septal leaflets can be evaluated with a slight visualization of

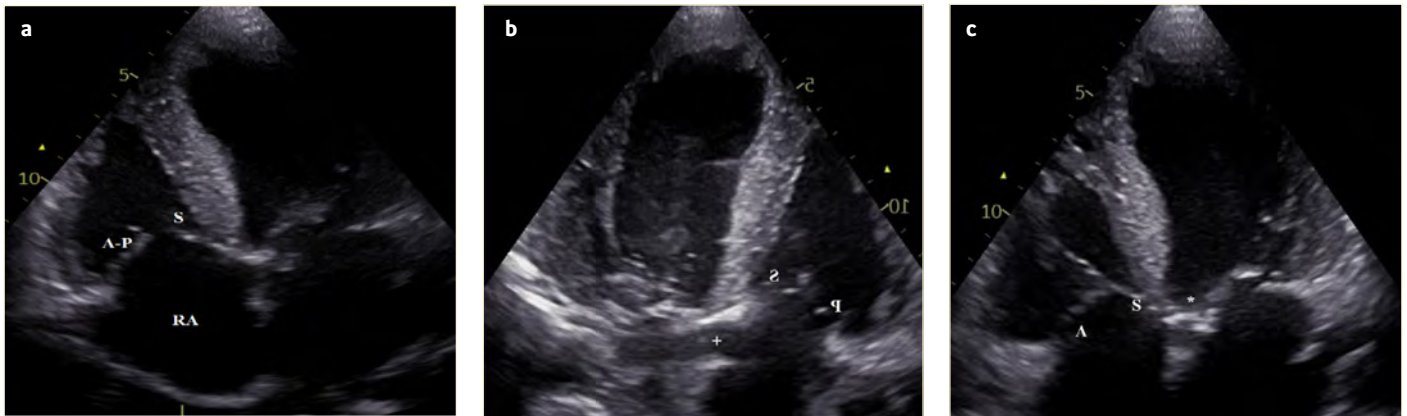


**Figure 57.** In the apical 4-cavity window, anterior or posterior leaflet is observed together with the septal leaflet. With slight posterior angulation, septal and posterior leaflets are observed with observation of the coronary sinus (+), whereas with anterior angulation, anterior and septal leaflets are observed with observation of the LVOT (\*) entrance. A, anterior; P, posterior; RA, right atrium; S, septal.

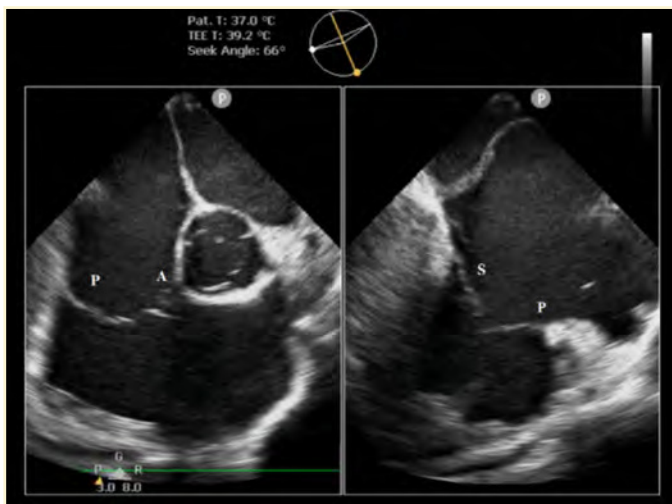


**Figure 58.** Anterior and posterior leaflet is observed in the midesophageal commissural window. Biplane imaging of the posterior leaflet shows the septal and posterior leaflet. A, anterior; P, posterior; S, septal.

the aorta, and septal and posterior leaflets can be evaluated with angulation posteriorly and viewing the coronary sinus (Fig. 57A-C).

Recent ASE guidelines recommend performing the right ventricular examination from apical 4-chamber, right ventricular-focused apical 4-chamber and modified 4-chamber views.<sup>21</sup>

Septolateral tricuspid annulus measurement should be performed in end diastole. Tricuspid tenting height and area should be performed in end systole.<sup>190</sup> In addition, vena cava inferior size and respiratory changes should be examined through the subcostal view for RA filling pressures.

### 3D Echocardiography

Three-dimensional echocardiography greatly improved the accuracy of images, identification of TV leaflets, evaluation of associated anatomical structures, and mental reconstruction of multiple 2D planes.<sup>201</sup> Lang et al.<sup>12</sup> have recommended that the interatrial septum should be placed inferiorly (at the 6 o'clock position) regardless of ventricular or atrial orientation for image standardization. Three-dimensional images can be obtained from the apical, subcostal, or parasternal axis. The view, in which axis has the best acoustic

visual quality, is used while getting 3D images.<sup>202</sup> In order to obtain a good 3D acquisition, it is important to obtain 2D images in which the demarcation of TV can be seen clearly.<sup>190</sup> In order to maximize the spatial resolution and volume velocity, the pyramidal imaging volume should be reduced to the lowest point, including the distinctive anatomical markers where all leaflets are seen. In order to increase the temporal resolution, the number of beats taken can be increased. However, the greater number of beats increase the probability of stitching artifacts, due to patient and/or operator movements.<sup>12</sup> With 3D imaging of the valve, accurate leaflet location, where the regurgitation jet occurs and further anatomical landmarks can be evaluated. In addition, since the tricuspid valve is anteriorly located, it is likely to obtain better 3D images with TTE rather than with TEE.<sup>203</sup>

### Transesophageal Echocardiography

Before the procedure, the anatomy of the tricuspid valve and the structure of the regurgitation should be evaluated with TEE. Biplane imaging of all views simultaneously is essential in understanding of TV anatomy.<sup>203</sup> The tricuspid valve is evaluated with multilevel imaging which starts from the mid-esophageal view, and from the distal esophagus and transgastric view.

#### Mid-Esophageal View

With 4-chamber view, the septal and typically the anterior leaflet can be evaluated; simultaneous biplane imaging may help clarify which leaflet is imaged because the anterior leaflet is typically seen adjacent to the aorta. As we increase the transducer angle to 30° with retroflexion, the posterior leaflet may be seen. Then probe is proceeded to about 60 to 70°, which yields a "commissural" view, where the anteroseptal and posteroseptal commissures can be evaluated using biplane imaging (Fig. 58). At 90°, anterior and posterior leaflets can be observed. With biplane imaging either leaflet can be visualized with septal leaflet.<sup>203</sup> Superior and inferior vena cava and interatrial septum are observed with bicaval view. In this view Eustachian valve, Chiari network structures, pacemaker leads/ ICD leads or intra atrial anatomy (ASD/PFO) or implants that could possibly interact with the device should be evaluated.

#### Distal Esophageal View

Right sided anatomy can be evaluated more clearly by advancing the probe slightly into distal esophageus, where there is no left atrium in view. At 0° in the distal esophageal view, the anterior and posterior leaflets can be observed. Anterior and septal leaflet are evaluated at 90°.

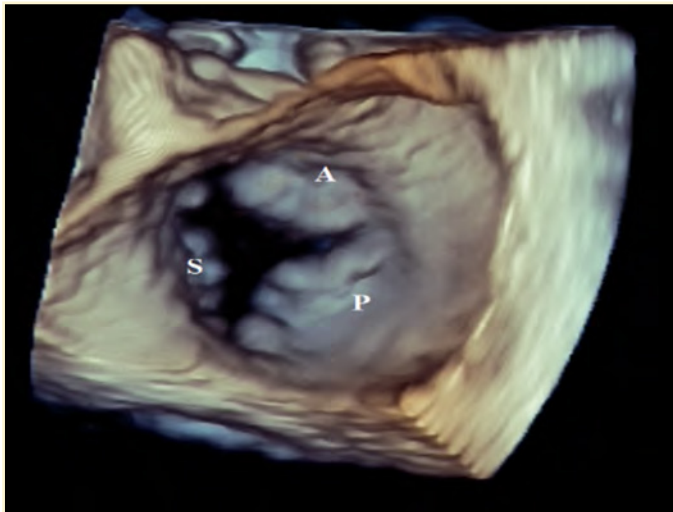


**Figure 59.** Evaluation of tricuspid valve anatomy with three-dimensional imaging. A, anterior; P, posterior; S, septal.



**Figure 60.** Visualization of all 3 leaflets in a transgastric short axis window. This is the only window in which all 3 TK leaflets are visualized simultaneously with 2D. A, anterior; P, posterior; S, septal.

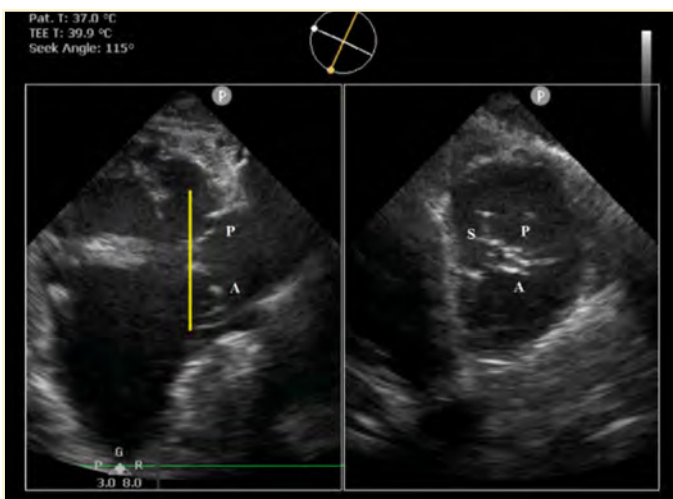


**Figure 61.** With biplane imaging from the tip of the posterior and anterior leaflets in the transgastric RV inflow window, all 3 leaflets can be clearly observed.



**Figure 62.** Transportation of the clip system through the bicaval window into the right atrium.

### Transesophageal 3D Imaging

Multiple 3D TEE data sets from multiple probe positions should be collected for the evaluation of the valve and annulus, as long as the 2D images are of sufficient quality (Fig. 59). Care should be taken to include anatomical markers such as aortic root and interatrial septum in optimal imaging. Full volume 3D images should be obtained from the modified bicaval view will help to define the leaflets and anatomy according to the relationship of the TV with the aorta and interatrial septum. In addition, 3D images can be obtained from distal esophageal views to obtain better images due to the absence of left heart structures. If satisfactory images can not be obtained, attempts should be made from shallow and deep transgastric views. Information about the anatomy and severity of the TR can also be obtained from Doppler imaging in 3D views.

### Transgastric Views

It is the most important view to analyze the tricuspid valve regurgitation and to plan for edge-to-edge repair treatment strategy. For optimal evaluation, all 3 leaflets, coaptation zones and coaptation gaps should be clearly visualized.

When the heart is in the distal esophagus, after the probe is positioned at 0° in the middle of the screen, the probe is slowly advanced into the stomach, after the liver is seen, the anterior and posterior leaflet of the tricuspid valve is observed with right flexion and ante-flexion. As we increase the transducer angle to 20–40° all 3 leaflets can be visualized (Fig. 60). The septal leaflet is near the septum and the anterior leaflet can be seen in the far field, while the posterior leaflet is in the near field. Biplane imaging can be used to observe specific leaflets, as a consequence we can evaluate among which leaflets TR is located and malcoaptation occurs (Fig. 61). In this view, leaflets, which are device targeted, can be determined and according to this, strategy will be planned.

### Intraprocedural Imaging

Demonstrating the TV leaflet anatomy, the location of the regurgitation jet, and the leaflet capture process multiplan by TEE are vital in the procedure. During the procedure, multiplan images from all levels should be actively obtained as previously mentioned and the TV and TR should be visualized in 3D views.

Two leaflets will be clipped as anterior and septal or posterior and septal, and the targeted TR jet at the beginning of the procedure, should be clearly demonstrated, especially through the trans-

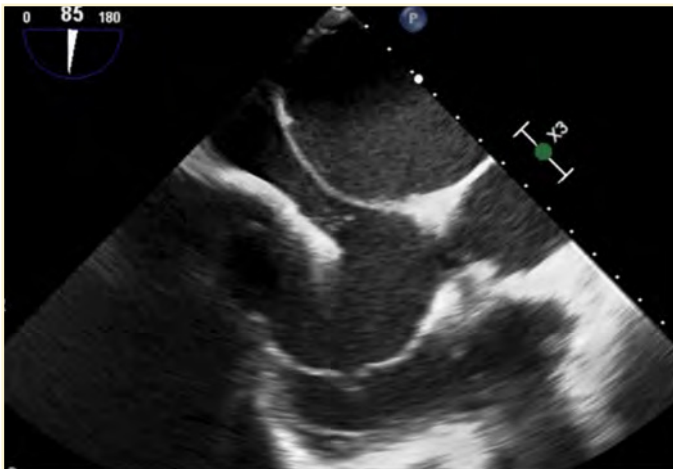


**Figure 63.** Coaxial guidance of the triclip system to the tricuspid valve through a modified bicaval window.

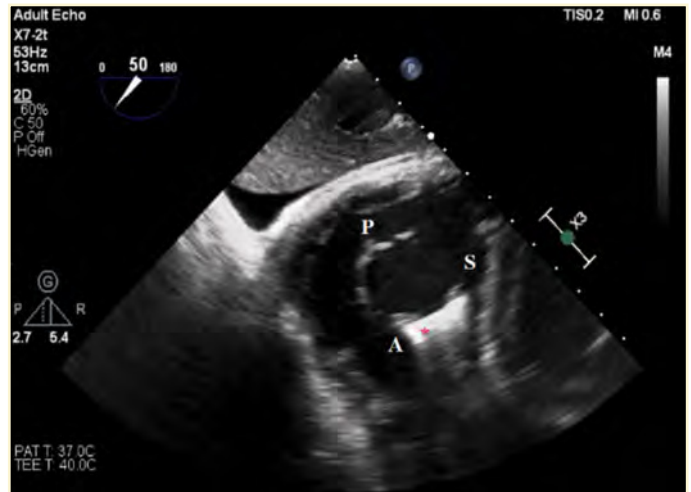


**Figure 66.** Transgastric short axis window showing the Triclip system positioned perpendicular to the anterior and septal leaflet. A, anterior; P, posterior; S, septal.

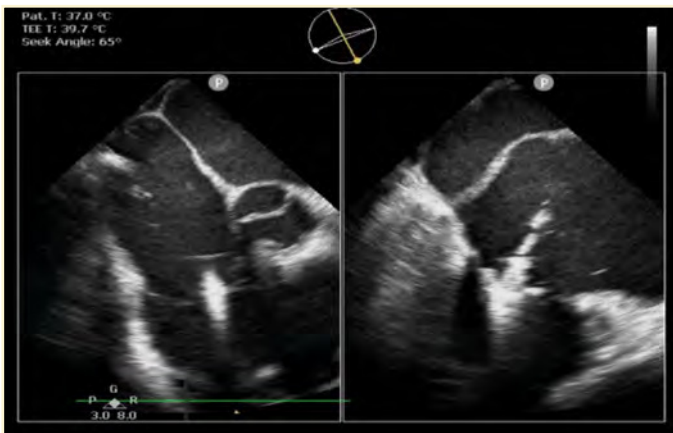


**Figure 64.** Advancement of the TriClip system in the intercommissural window in an anteroseptal orientation in the direction of the TV. Biplane is used to simultaneously demonstrate the system in the anterior and septal leaflet neighborhood.

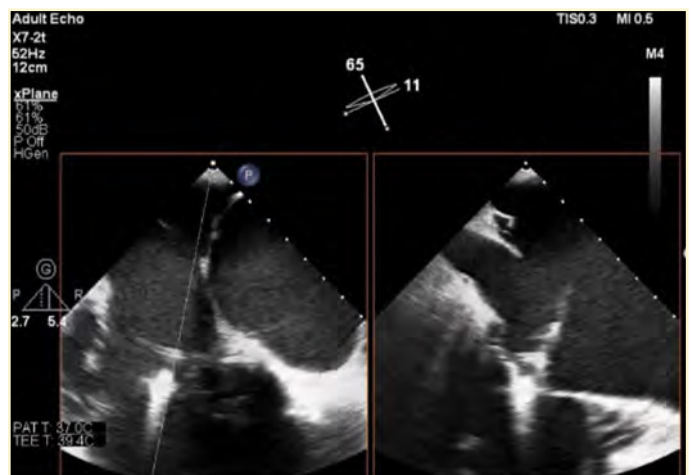


**Figure 67.** Demonstration of leaflet capture using biplane in the intercommissural window.

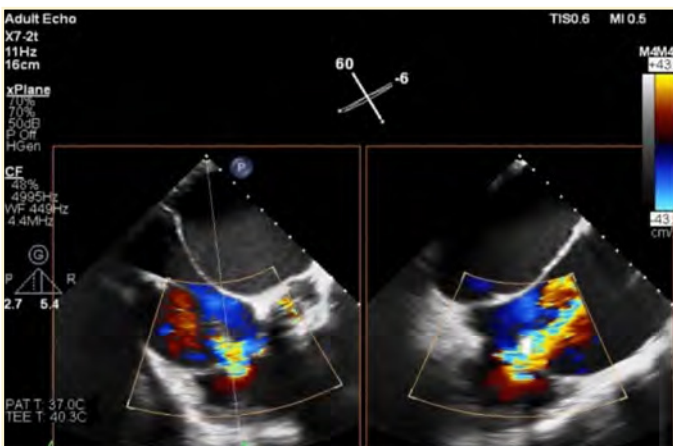


**Figure 65.** Use of color Doppler during device orientation.

gastric short axis view. Orienting the clip delivery system to the tricuspid valve is the first step (Fig. 62, 63). The device should be moving toward the TV along the right atrial wall and bicaval view

guides this step. The most important point of this process is to avoid damage and possible perforation to the interatrial septum. The system may be directed towards the inferior of the interatrial septum while clip advances to TV and since the system is in a rigid structure, the septum may be damaged as a result of pushing the system further.<sup>199, 203, 204</sup> Intercommissural view or distal esophageal view at 60–80° is used to guide the delivery system toward the TV (Fig. 64, 65). The clip system must be coaxial to TV during transition. In commissural view with biplane imaging we can optimize the delivery system trajectory to TV and adjust the clip position with making rotation at the targeted TR. In transgastric short axis view, the coaptation site of all 3 leaflets can be optimally visualized (Fig. 66). This view is especially very important for navigating the clip system to the right ventricle and monitoring its rotation simultaneously. If the coaptation site can not be clearly demonstrated in a single axis, multiplane imaging should be used. In addition, optimal position of the clip should be verified with 3D imaging.

During grasping the targeted leaflets, both arms of the clip should be clearly demonstrated with multiplane imaging (Fig. 67). By set-

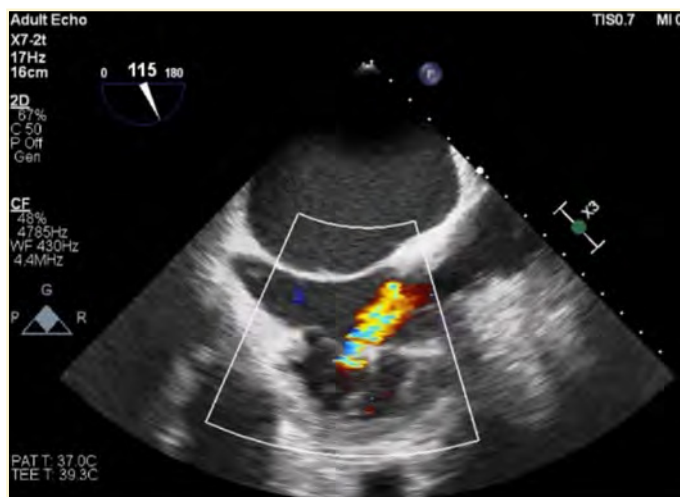


**Figure 68.** Demonstration of regression of regurgitation jet after procedure in a modified bicaval window. In this patient, 2 clip systems were used between the anterior and septal leaflets.

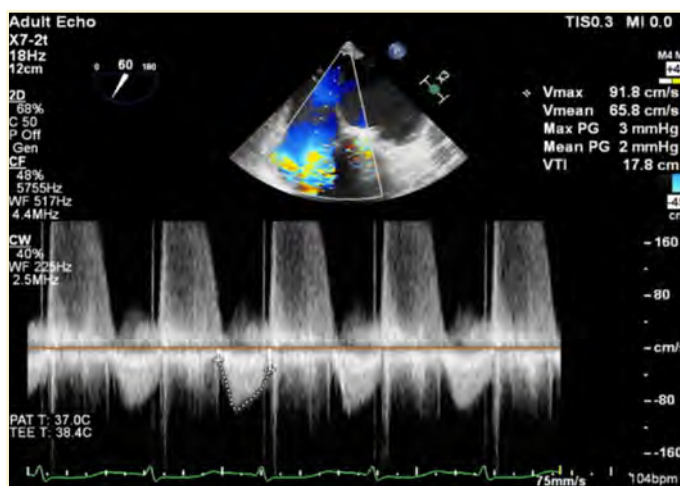


**Figure 69.** CW Doppler measurement after clip implantation showed that the mean gradient over the tricuspid valve was less than 4 mmHg.

ting the primary view as commissural view, the clip can be easily positioned along the septal commissure. For anteroseptal grasps, the secondary plane should be directed anteriorly (toward the aorta), and for posteroseptal grasps, the secondary plane should be directed posteriorly (away from the aorta). After clip placement, adequate leaflet grasping must be demonstrated before clip release. We can demonstrate from multiple views to ensure restriction of the leaflet motion near the clip on 2D imaging, an adequate tissue-bridge from 3D imaging, and reduction of TR by color Doppler (Fig. 68).<sup>204</sup> After clip insertion, acceptable mean transvalvular gradient should be below 4 mm Hg (Fig. 69).<sup>203</sup>

## Conclusions

Severe TR is associated with poor long term outcomes and increased mortality. In this respect, the evaluation, follow-up and classification of TR are important. Transcatheter methods can significantly improve the quality of life and reduce the hospitalization rates of patients who are not suitable for surgical intervention.

## Use of Transesophageal Echocardiography in Percutaneous Left Atrial Appendage Closure

*Dr. Büşra Güvendi Şengör, Dr. Alev Kılıçgedik*

Atrial fibrillation is the most common arrhythmia, the prevalence of which reaches 13% at the age of 80 or older and it is responsible for 15–20% of all ischemic strokes.<sup>205, 206</sup> Although oral anticoagulant therapy provides a reduction in ischemic strokes and mortality, it may not be a proper option for every patients due to the bleeding risk and narrow therapeutic range. In these patients, percutaneous closure of left atrial appendage (LAA), an important source of cerebral thromboembolism, appears an alternative treatment option.<sup>207</sup> Transesophageal echocardiography plays a significant role in pre-procedure assessment, guidance during the procedure and follow-up. In this review, perioperative echocardiographic evaluation for the most frequently used three devices (Watchman, Amulet, Lambre) are summarized.

Left atrial appendage anatomy. Left atrial appendage (LAA) is a tubular, blind-ended pouch connected to the main trunk of the left atrium. In 70% of the patients, LAA has a bent or spiral axis and varies greatly in size and shape.<sup>208</sup> Since LAA orifice is often ovoid-shaped, it has one large and one small orifice diameter. The anatomical orifice differs from landing zone, which is important for most devices, and separated from the left pulmonary veins by a structure known as the Marshall ligament or coumadin ridge. The orifice is followed by the region of neck, body and apex, respectively.<sup>209</sup> Anatomically, LAA is divided into three regions as the orifice, the neck and the lobar region.<sup>210</sup> It has usually 2 lobes (54%), and its inner surface has complex indentations formed by pectinate muscles. Morphologically, the shape of LAA is classified into four types: chicken wing (48%), cactus (30%), wind-sock (19%) and cauliflower (3%). While the chicken wing is the most common morphology, the cauliflower is the most commonly associated with embolic events.<sup>211</sup> The chicken-wing morphology is a cause of procedural challenge regardless of the device to be selected due to variable size and shallower depth.<sup>209</sup>

## The Percutaneous Closure of the LAA

### Pre-Procedural Assessment

The percutaneous closure of the LAA largely depends on the accurate determination of the anatomical structure. An accurate measurement of the LAA dimensions is also crucial to select the appropriate device. Choice of the proper device is the key of procedural success. Choice of a small device size may cause embolization and peri-device leaks, while choice of a large device may result in tamponade or obstruction of the left upper pulmonary vein. Therefore, the accurate measurement of the landing zone and orifice diameter play a significant role in performing procedure safely and successfully.<sup>212</sup>

Transesophageal echocardiography (TEE) is the main imaging modality used to evaluate anatomy of the LAA and its relationship with surrounding structures, to decide on the appropriate device and size, to investigate thrombi and to identify probable anatomical contraindications. Fluoroscopy can be used during the procedure in addition to two or three dimensional (2D or 3D) TEE as well as CT or MRI can be used for further assessment of the LAA before the procedure.<sup>211</sup> It should be noted that dehydration due to fasting and sedation before the procedure may show LAA measurements less than they are, therefore, it is recommended that the diameters of the LAA should be measured when the patient is euvolemic and LA pressure is  $\geq 12$  mm Hg. Before the procedure, the administration of 500–1000 cc of saline is also recommended.<sup>213</sup> To select the proper size of device, measurements

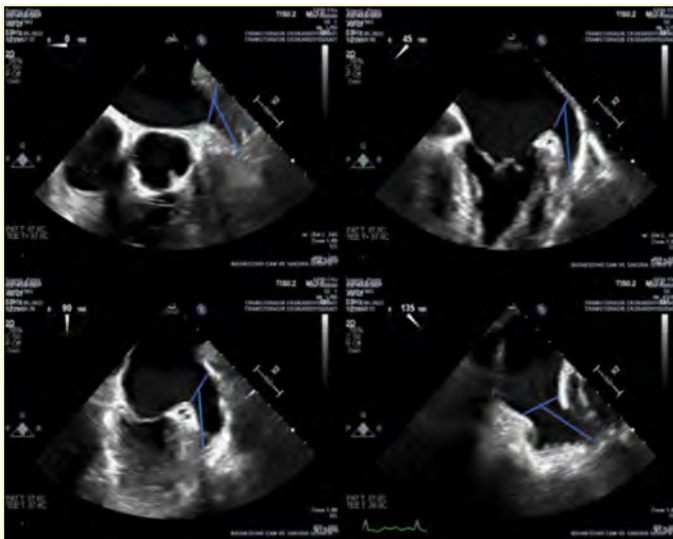


**Figure 70.** The measurements for the WATCHMAN device (Horizontal line shows landing zone for the WATCHMAN device, perpendicular line shows the LAA depth.)

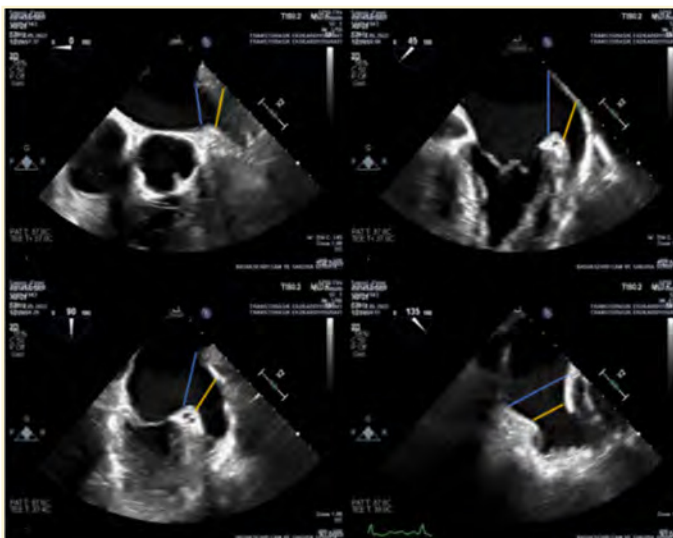


**Figure 71.** The measurements for the Amulet device (Yellow line shows the landing zone for the Amulet device).

should be made when the LAA size is the widest, that is, at the end of ventricular systole and under normal left atrial filling pressures.<sup>211, 213</sup> TEE images should be evaluated from at least 4 different mid-esophageal planes, which are typically at  $\sim 0^\circ$ ,  $\sim 45^\circ$ ,  $\sim 90^\circ$ , and  $\sim 135^\circ$ . The LAA is the most anterolateral structure of the heart. The correct position of the TEE probe at mid-esophageal level, at  $50^\circ$ – $70^\circ$  with a slight retroflexion provides the best long-axis image (the longest depth) of the LAA. In this plane, mitral annulus, the circumflex (CX) artery (at the medial of the LAA), limbus or coumadin ridge (at the lateral and superior) and the left upper pulmonary veins (at the lateral) can be viewed. If the LAA is more anteriorly located, its long axis can be viewed at  $0^\circ$ – $45^\circ$  and if it is more laterally located, it can be best viewed at  $70^\circ$ – $90^\circ$ . The short axis of the LAA (the shortest depth) is best viewed from  $135^\circ$ . Although it is challenging to image with a 2D probe, accurate position can be achieved by biplane imaging from  $45^\circ$  with a 3D probe.<sup>213</sup> Because of the oval shaped of the orifice, it should be taken into account that the LAA orifice can be measured wider at  $135^\circ$  than at lower angles.<sup>214</sup> This TEE image and measurements determine the

success of the device deployment because this location is the most common place for peri-device leaks after implantation. The choice of a suitable percutaneous closure device depends on the accuracy of the landing zone measurements. The selected device size should be several mm larger than the landing zone measurements to obtain a secure and stable device location. The maximum length of the fixing lobe should be additionally measured to ensure that the selected device has the appropriate area for deployment. Different measurements should be made in accordance with manufacturer's recommendation for different device designs.<sup>212, 215</sup> The angle among the orifice, the neck and the lobes should be evaluated before the procedure, because this may affect the location of septal puncture. The number of additional lobes and their initial parts should be investigated.<sup>211</sup>

Currently, in Turkey, there are three percutaneous closure devices, named the WATCHMAN, Amulet ve LAmBRE, in our country. The WATCHMAN is a self-expandable system with an outer diameter of 14 Fr, which consists of a nitinol frame covered by polyethylene fabric and 10 fixation bars. More data has been available about the WATCHMAN than the other closure systems. The Amulet is a second generation self-expandable system with an outer diameter of 14.4–16.5 Fr, which consists of a fixed size cover disk, lobe and stabilization hook. Its design is based on the first generation of the AMPLATZER cardiac plugs. Amulet has a slightly larger disk than first-generation devices, which provides better closure of the LAA. The middle part and the lobe are longer than the first-generation plugs, and there are more stabilization wires around the device to improve flexibility and stability of the device. The LAmBRE, increasingly used in recent years, is a self-expandable system, made of a nitinol mesh and polyester membrane with an outer diameter of approximately 10 Fr. The LAmBRE is composed of a hook-embedded umbrella, a cover disk which isolates the LAA and a thin cylindrical part to connect other parts. The umbrella part has 8 small distal hooks and 8 U-shaped ends, which allow better fixation of the device.<sup>215</sup>

The LAA evaluation for the WATCHMAN and LAmBRE is performed with 2D TEE from  $0^\circ$ ,  $45^\circ$ ,  $90^\circ$  ve  $135^\circ$  to find the widest landing zone and depth of the LAA.<sup>209</sup> The landing zone for the WATCHMAN is measured from the top of the mitral valve annulus or the inferior part of the LAA orifice at the level of the CX artery, to 2 cm below of the left upper pulmonary vein. The depth of the LAA is obtained by drawing a perpendicular line to this measurement (Fig. 70). The landing zone, measured from all angles with 2D TEE, may not have been in the same plane, this limitation could be overcome with 3D multiplanar reconstruction (MPR) mode. By aligning two different long axis views of the LAA with 3D MPR, a short axis view is obtained, therefore, landing zone diameter can be more accurately measured.<sup>209</sup> The device is selected according to the largest landing zone diameter, more than 8–20% of the largest diameter is determined as a device diameter. The WATCHMAN device can not be used if the LAA orifice is too small ( $<16.8$  mm) or too wide ( $>30.4$  mm), if the LAA depth is too shallow (less than the diameter of the widest diameter of the orifice) and if the depth of secondary LAA lobe is too close to the LAA orifice.

Echocardiographic assessment for the Amulet is performed from  $0^\circ$ ,  $45^\circ$ ,  $90^\circ$  ve  $135^\circ$  with 2D TEE, as in the WATCHMAN device. However, it is recommended to focus on the smallest landing zone diameter from long axis views ( $30^\circ$ – $60^\circ$ ) and the widest landing zone diameter from short axis views ( $120^\circ$ – $150^\circ$ ).<sup>209</sup> The measurements for the device size are different from the measurements established for the WATCHMAN. The diameter of the LAA orifice is the line between pulmonary vein–coumadin ridge and the CX artery. The landing zone diameter is measured from the 10–12 mm distal to the neck of the LAA perpendicular to this line, the depth of the main lobe is measu-

red based on the expected axis of the device (Fig. 71).<sup>210</sup> Although the device selection is mainly based on the experience and choice of the operators, the LAmBRE system should be considered first, if the patients have chicken wing morphology or multilobulated LAA or if the groin complications during the transportation are foreseen.<sup>215, 216</sup>

Peri-procedural assessment. During the procedure, 2D and 3D TEE is the most valuable imaging method and it supports fluoroscopy. TEE plays a great role in evaluating the presence of the thrombi before transseptal puncture, guiding the puncture, verifying the location of the catheter and sheath during the procedure, positioning and placement of the device.

### Transseptal Puncture

The location of the transseptal puncture is probably the most important stage affecting positioning and placement of the device. The transseptal puncture is performed from a more inferior and posterior of the fossa ovalis due to anterolaterally located LAA. Therefore, the sheath position becomes more co-axial to reach the LAA. Bicaval view (90°–110°) is the initial imaging for superior and inferior orientation, after tenting in the mid and inferior of the fossa ovalis, anteroposterior assessment is performed at 45°. After the appropriately performed transseptal puncture, the wire and catheter system are parked in the left upper pulmonary vein.

### Imaging During the Placement of the WATCHMAN Device

The procedure begins with baseline evaluation with 2D and 3D TEE. During the procedure, thrombi should be excluded in the LAA and the measurements should be repeated with fluoroscopy to select the appropriate size and device.<sup>217</sup> The presence of intra-cardiac thrombi and pericardial effusion, characteristics of the inter-atrial septum and the LAA are evaluated. Measurements of the LAA body and orifice are made again. Valve diseases, movable aortic atheromas and intracardiac shunts are investigated. After transseptal puncture, the WATCHMAN device system, 14 Fr, is advanced to the LA with a pigtail catheter under the guidance of 2D and 3D echocardiography. After puncture, 2D and 3D TEE allows to view the entire catheter from the LA through the LAA. Therefore, it can be seen passing the tip of the catheter through the septum, how far the catheter is from the septum or how much of it is in the LA. A probable injury of the interatrial septum and atrial free wall can be prevented. After the guide catheter is advanced to the LAA orifice, a pigtail catheter is advanced through the guide catheter into the LAA and contrast angiography is performed for fluoroscopic evaluation of the LAA. Meanwhile, a large number of bubbles are noted in the LAA with 2D and 3D echocardiography. Then, the guide catheter is properly inserted in the LAA and the pigtail catheter is removed. The WATCHMAN device system is advanced.<sup>218</sup> Four 'PASS' criteria must be met prior to device release. These criteria are defined as **P**osition, **A**nchor, **S**ize, **S**eal.

**Position:** The device shoulder, the curved part inside the LAA ostium, should not protrude too far from the LAA.

**Anchor:** The Tug test is performed under TEE. The device is retracted and it should return to the original position when it is released.

**Size:** A compression grade of the device should be 8–20% from images at 0°, 45°, 90° ve 135° with 2D TEE.

**Seal:** The peri-device leaks are evaluated under 3D TEE. The narrowest cross-section of the leak, vena contracta (VC), is measured from the plane where the device is closest to the LAA wall. If the VC of the leak is <5 mm, it is acceptable, but, if the VC is >5 mm, the device should be repositioned or replaced with a larger device. It is recommended to evaluate the leakage with a low Nyquist limit (20–30 cm/s) and the peripheral spread of the leakage can be assessed with 3D TEE.

### Imaging During the Placement of the Amulet Device

The wire is advanced to the left upper pulmonary vein after the transseptal puncture. The guide catheter is advanced to the LA through the wire. For the Amulet devices, there are two guide catheter options, 12 Fr and 14 Fr, depending on the size of the preferred device. After the catheter is advanced to the LA, the wire is retracted and the catheter is directed to the LAA. The catheter tip is placed in the landing zone of the LAA, the Amulet device is advanced through the catheter, and the lobe of the device is partially opened. After the lobe of the device is placed exactly in the landing zone, the remained disk of the device is opened if its angle and position are appropriate.

Before the device release, the following a number of checks are carried out:

The lobe of the device should be rubber-shaped.

It should be shown that there is a certain degree of decoupling between the device lobe and the disk.

The device disk should be concave relative to the LA body.

The axis of the device lobe should be perpendicular to the axis of the LAA neck.

At least 2/3 of the device lobe should be positioned at the distal of the CX artery.

Tug test should be performed for device stability.

Peri-device leaks can be evaluated with a low Nyquist limit (35–45 cm/s) for the Amulet device. The presence of the defects <3 mm in diameter or multiple jets (the sum of leaks <3 mm) are considered to be small leaks, while 3–5 mm leaks are considered medium, >5 mm leaks are defined as large leaks.<sup>209, 210</sup>

### Imaging During the Placement of the LAmBRE Device

The LAmBRE device has a stabilization system, consisting of anchors and hooks which targeted the trabecula and the pectinate muscles of the LAA.<sup>215, 219</sup> The risk of LAA perforation is the lowest in this device due to its structure.<sup>219</sup> The guide catheter of the device is positioned proximal to the LAA, and the umbrella is inserted. The stability of the device is confirmed by the Tug test, and it is confirmed whether the device completely closes the LAA orifice with contrast study and TEE. The LAmBRE device has advantage due to having many options of different sizes, therefore, it can be able to use in all anatomical types of the LAA (multiple lobes, wide orifice, relatively small depth) with a LAA orifice larger than 12 mm.<sup>215, 216, 219</sup>

The use of 2D and 3D TEE helps to evaluate leaks after device placement and to recognize complications. The device size should not be less than the largest LAA diameter, it should be selected 2–6 mm larger according to the anatomy of the LAA, the manufacturer's recommendations and the operator's experience.<sup>215</sup> The correct positioning of the device is also crucial. Placing the device too deeply prevents the closure of the proximal lobes, while its more proximal positioning may result in embolization due to reduced stabilization.<sup>211</sup> After device placement, the mitral valve apparatus adjacent to the device, the left upper pulmonary vein and the CX artery must be examined carefully for probable compression. The presence of a link between the LA and the LAA should be checked with colour Doppler at a low Nyquist limit. Complications such as pericardial effusion, tamponade, iatrogenic atrial septal defect and possible thrombi should be explored by echocardiography before the procedure is terminated.<sup>211, 219</sup>

Follow up. After the procedure, TTE is recommended to exclude device embolization and pericardial effusion before discharge. TEE is usually used to evaluate device embolization, erosion, thrombus formation or peri-device leaks at 1, 3, 6 and 12 months. At 1 year, TTE is preferred for follow up if there is no suspicion of complications.<sup>211</sup> The atrial septal defect secondary to the transeptal puncture should be re-evaluated during each examination. After the WATCHMAN device is placed, endothelialization occurs approximately within 45 days. Following 45 days of placement of WATCHMAN and Amulet device, an echocardiographic examination is performed, the device position and stabilization is evaluated.<sup>209</sup> Although the absence of peri-device leak by complete closure of the LAA is the most important determinant of procedure success, peri-device leaks are common after procedure and  $\leq 3$ –5 mm leaks may be acceptable. Leaks that occur during the procedure may continue to increase or new leaks may develop during follow up. On the case of peri-device gap is  $>5$  mm, it is recommended to continue anticoagulation.<sup>220</sup>  
<sup>221</sup> The presence of any thrombus on the device should be checked.

## Conclusion

Percutaneous closure of the LAA is a new and developing treatment option used to prevent embolic events in eligible patients with non-valvular AF. 2D and 3D TEE are the most frequently used imaging method to determine eligible patients before the procedure, to choose proper devices and sizes, to monitor during and after the procedure and they have a significant role in guiding the intervention.

## Imaging in the Process of Septal Alcohol Ablation in Patients with Hypertrophic Cardiomyopathy

*Dr. Mert Pehlivan Altın, Dr. Selcen Yakar Tülüçe*

Hypertrophic cardiomyopathy (HCM) is defined as left ventricular (LV) hypertrophy that cannot be solely explained by loading conditions. Left ventricular hypertrophy is often accompanied by myocardial fibrillar misalignment, interstitial fibrosis and intramural small vessel disease. Its prevalence is 1:500 and it is actually a relatively common cardiomyopathy. While there is an autosomal dominant cardiac sarcomere protein gene mutation in 50–60% of the cases, there is a sporadic mutation in 40–50% of the cases.<sup>222</sup> Although patients may be asymptomatic, they can present with different clinical conditions such as heart failure, arrhythmia and sudden cardiac death. Symptoms such as chest pain, dyspnea, palpitations, presyncope and syncope can be observed in the course of the disease. These symptoms generally develop due to LV diastolic and systolic dysfunction of varying degrees, dynamic LV outflow obstruction, myocardial ischemia and arrhythmias. In 1/3 of the patients with HCM, no pressure gradient is detected in the LV outflow tract (LVOT), while a gradient is detected during rest or with exertion in the remaining cases.<sup>223</sup>

Hypertrophic cardiomyopathy is a disease with a reported annual mortality rate of 3–4%, and the aim of treatment in patients with symptomatic obstructive HCM is to increase functional capacity, reduce the degree of LVOT obstruction, improve diastolic filling and increase survival.<sup>224</sup> Considering that the presence of a significant gradient in the LVOT is an important factor in the pathophysiology of dyspnea, angina and syncope as the main symptoms of the disease, the importance of reducing the LVOT pressure gradient with treatment could be better understood. The initial treatment of LVOT obstruction is medical, and beyond that, alcohol septal ablation (ASA) and surgical myectomy are the other main modalities. With the ASA procedure performed in angiography laboratories, the dec-

reased LVOT area due to hypertrophy can be increased, the severity of mitral regurgitation can be reduced and the coronary flow reserve can be increased.<sup>225–227</sup> Decreasing the LVOT gradient reduces LV afterload, resulting in an increased cardiac stroke volume. As a result of these hemodynamic changes, the diastolic pressure in the aorta increases, while the LV diastolic pressure decreases, thus increasing the coronary filling pressure. In addition, hemodynamic and echocardiographic studies have also revealed that myocardial relaxation indicators, especially active relaxation, are improved after ASA, resulting in an improvement in diastolic functions.<sup>225–230</sup>

It has been shown earlier that the obstruction can disappear after myocardial infarction in patients with LVOT obstruction.<sup>231</sup> The idea for the first catheter-based treatment to reduce the LVOT gradient in patients with HCM was created by Sigwart, Kuhn et al.,<sup>232</sup> when they noticed that systolic wall motion decreases when the coronary artery perfusing the septum is occluded with a balloon. In 1995, for the first time, Sigwart<sup>233</sup> performed ASA percutaneously and reported positive results in 3 patients. Initially, this method was questioned in terms of long-term results, considering that it might increase myocardial scar burden in this patient group who already had the risk of malignant ventricular tachycardia.<sup>234, 235</sup> Especially with the use of myocardial contrast echocardiography, ASA has begun to be performed in many parts of the world as a less invasive alternative to myectomy.<sup>236</sup> Echocardiography-guided ASA, which was first described by Faber and his team and Seggewiss et al., has become a treatment method performed in many centers around the world today.<sup>237</sup> The aim of this article is to review the basic and current imaging methods used in the selection of suitable patients for the ASA procedure, during and after the procedure.

## Preoperative Imaging

### Evaluation of the anatomy

Previously, ASA was recommended for patients with an interventricular septum thickness of 17–30 mm. In recent publications, it has been shown that ASA is also effective and safe with thinner septum thickness (15–16 mm).<sup>238</sup> Especially with septal thicknesses  $<16$  mm, myectomy treatment is more likely to cause both iatrogenic ventricular septal defect and a high residual LVOT gradient due to inadequate myectomy.<sup>239</sup> In patients with septal thickness  $>30$  mm and in cases with intense septal scarring, the possibility of benefiting from ASA is low.<sup>222</sup> Because obstruction may also be at the midventricular level, especially in the younger patient population with massive septal hypertrophy, extended myectomy may provide more symptomatic relief by reducing or eliminating obstruction at all levels. Certainly, measuring the septal thickness alone is not sufficient when performing preoperative cardiac imaging. Since LVOT obstruction may also be related to the length of the mitral valves, the submitral chordae under the mitral valve, papillary muscle number, hypertrophy and insertion abnormalities (Fig. 72, Video 9, 10), the obstruction mechanism may need to be evaluated with other imaging methods such as transesophageal echocardiography and cardiac magnetic resonance imaging, when necessary,<sup>240</sup> since determining the level of contribution of abnormalities other than septal thickness in the LVOT obstruction mechanism will guide which invasive septal reduction treatment method should be selected.

### Pressure Gradient

Obstructive type HCM is diagnosed in patients with a LVOT gradient  $\geq 30$  mmHg, and latent type obstructive HCM in patients with a resting gradient  $<30$  mmHg and a gradient  $\geq 30$  mmHg with provoca-

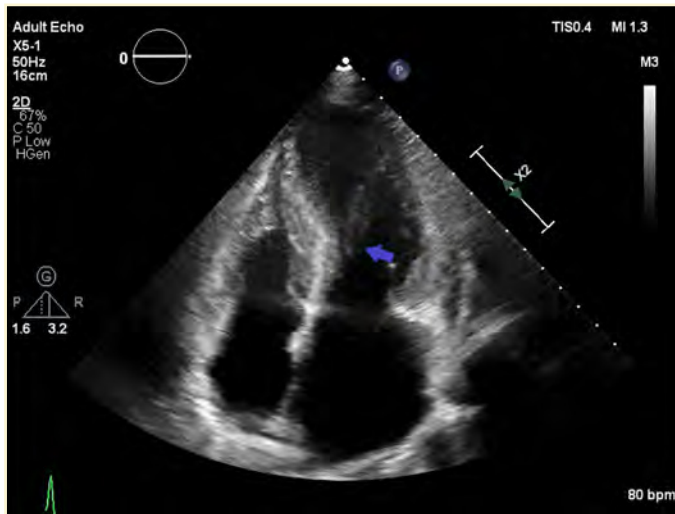


**Figure 72. Apical 4-chamber window echocardiographic image of false tendon (blue arrow) attached to the left ventricular outflow tract; therefore, the patient was not considered suitable for ASA and was treated surgically. ASA: Alcohol Septal Ablation.**

tion. For a HCM patient to be a candidate for ASA or surgical myectomy treatment, the patient should be symptomatic (NYHA class III) despite negative inotropic agents recommended in the guidelines, and the LVOT gradient evaluated at rest or during provocation should exceed 50 mmHg (Table 18).<sup>222</sup> In other words, the threshold

**Table 18. Optimal Patient Characteristics for Septal Alcohol Ablation**

Persistent severe symptoms despite optimal medical treatment NYHA class III/IV
Dynamic LVOT obstruction due to systolic anterior motion of the mitral valve Peak gradient >50 mmHg with rest or provocation
Ventricular septum thickness >15 mm
No intrinsic mitral valve disease
No accompanying cardiac surgery required e.g., no coronary bypass or valve replacement needed
NYHA: New York Heart Association class of heart failure; LVOT: Left ventricular outflow tract.

of LVOT gradient to diagnose obstructive type HCM and the threshold of LVOT gradient for referring a patient to an invasive procedure are not the same;<sup>223</sup> but some centers set a resting gradient  $\geq 30$  mmHg and a provocation gradient  $\geq 50$  mmHg as a threshold to refer patients to ASA therapy.<sup>239</sup>

### Electrocardiography

Both ASA and surgical myectomy procedures might cause damage to the cardiac conduction system, resulting in atrioventricular (AV) block and a need for a permanent pacemaker. Therefore, it is very important to evaluate the cardiac conduction system before the procedure. Typically, patients undergoing ASA develop a right bundle branch block by surgical myectomy patients develop a left bundle branch block postoperatively; therefore the presence of a contralateral bundle branch block before the procedure is an important predictor of future complete AV block development and the need for a permanent pacemaker.<sup>241</sup> For this reason, the presence of a left bundle branch block before the procedure in patients who will undergo ASA or a right bundle branch block in patients who will undergo surgical myectomy is considered as a relative contraindication to these procedures in a few publications.<sup>238</sup>

### Peroperative Imaging

A diagnostic heart catheterisation might be done at a preceding session or immediately before ASA. Measurement of the intraventricular gradient aims at concluding the diagnosis and site of significant obstruction (LVOT versus midventricular) and should be performed both at rest and during provocative manoeuvres (e.g. strain phase of Valsalva, after an extrasystole). Before the procedure, coronary angiography is also performed in order to exclude concomitant presence of a coronary artery disease and to identify the septal artery or branch that is most likely to supply blood to the septal area where LVOT obstruction occurs (anterior mitral leaflet contact area). For this purpose, femoral artery and vein are punctured using the standard Judkins technique, through the femoral approach, a 6F temporary pacemaker is placed in the apex of the right ventricle, a 5F/6F 'pigtail' or 'multipurpose' catheter is placed in the LV, and a 6F/7F guiding catheter is placed in the ascending aorta.<sup>242</sup> Usually, the target artery for the ASA is the first major septal artery or a branch of it originating from the left anterior descending artery (LAD). Since many variations can be encountered in perfusion of the interventricular septum, as in the blood supply of other cardiac structures, it would be more appropriate to consider the perfusing area where the LVOT obstruction occurs as the target vessel for alcohol ablation during transthoracic echocardiography performed using intracoronary echocontrast agent or bubbled mixture. During the transthoracic echocardiography procedure, the initial LVOT gradient is also evaluated and recorded. After the target septal artery is determined, the left main coronary artery is engaged with a well-supporting catheter, and a 0.014-inch coronary guidewire is placed in the predicted target septal artery. Then, a balloon catheter (1.5–2.5 mm, preferably  $\leq 10$  mm long) with a diameter that will completely occlude the target septal artery when inflated is sent over this guidewire. This balloon catheter is in the over-the-wire (OTW) system, unlike the quick-change monorail balloon catheter system used in routine coronary interventional procedures. The OTW system has two lumens along the length of the balloon catheter, one that extends to the balloon and inflates it, and the other that allows the passage of the wire. Thus, after the target septal artery is completely disconnected from the proximal LAD coronary vascular network using the inflated balloon catheter, this system allows administration of contrast agent or alcohol via the catheter lumen to the area supplied by the target septal artery after the wire is pulled back. After the OTW balloon is inflated without protruding into the LAD, the 0.014 inch wire is withdrawn. Angiographic contrast agent is given to the septal artery through the lumen where the wire is removed, and the presence of possible backflow into the LAD and collateral connections of the septal artery are evaluated angiographically. Myocardial contrast echocardiography can be performed when it is confirmed that there is no backflow to the LAD and no collateral connections with other cardiac structures. Since coronary angiography is a lumigraphic method, the area supplied by the ballooned septal artery cannot be clearly distinguished angiographically. For this reason, the possibility of the septal artery not supplying blood to the septal myocardial area adjacent to the LVOT obstruction may cause unsatisfactory procedural success or the possibility of supplying blood to areas outside the target area (papillary muscle, etc.) may lead to complications, before alcohol injection in the ASA, it is vital to determine the myocardial area supplied by this septal artery using myocardial contrast echocardiography. The decision to inject alcohol into the evaluated septal artery can only be made after myocardial contrast echocardiographic evaluation.



**Figure 73.** During myocardial contrast echocardiography, contrast enhancement of the basal septum (blue arrow) is observed in the apical 5-chamber window.

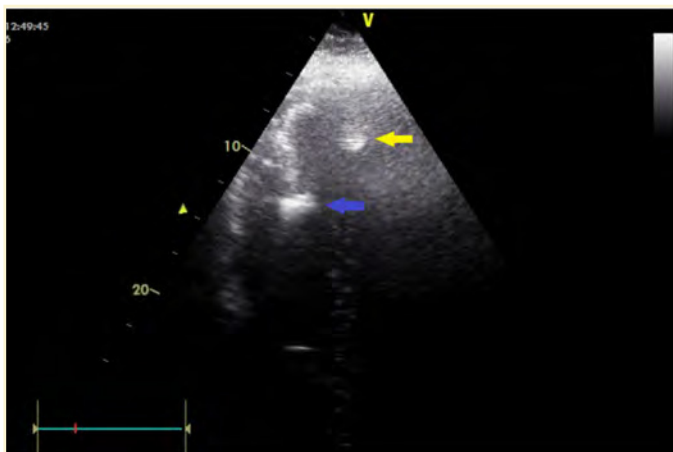


**Figure 74.** During myocardial contrast echocardiography, apical 4-chamber window shows contrast enhancement in both the septum (blue arrow) and papillary muscle (yellow arrow). Other septal arteries were also evaluated due to the presence of enhancement in the papillary muscle, and the patient was not considered suitable for ASA due to recurrent enhancement in cardiac structures outside the septum. ASA: Alcohol septal ablation.

Echocardiographic contrast agents are prepared by mixing the dry powder in the vial with physiological saline and then shaking for 30–60 seconds.<sup>243</sup> The dilution rates of different contrast agents in dry powder vials with physiological saline are different according to the manufacturer's recommendations. For example, one of the most commonly used agents, "Levovist" (Berlex Laboratories, Montville, NJ) (concentration 450 mg/ml), was used as a suspension of approximately 1.0–1.5 ml during the ASA procedure and contains microspheric bubbles with a diameter of 7–8  $\mu\text{m}$  containing air with a shell that is made of galactose stabilized with palmitic acid, which can pass into the capillary mesh.<sup>244</sup> There are also publications stating that instead of dedicated contrast agents, as a simple and inexpensive method, 3 ml of intravascular contrast (which we use during angiography) + 2 ml of saline + 1 ml of air, with the help of two injectors in the 3-tap vascular access may be

mixed and the mixture obtained can be used in contrast echocardiography during the procedure.<sup>245</sup> Another alternative that can be used in cases when access to dedicated contrast agents is limited is a cold rinsed GelaFundin 4% solution (Braun, Melsungen, Germany) and it is suggested that it may be superior to dedicated contrast agents.<sup>246</sup>

While the balloon of the OTW balloon catheter is in the inflated position, 1–2 ml of diluted echocardiographic contrast agent (e.g., Definity, Lantheus Medical Imaging, North Billerica, MA; Optison, GE Healthcare, Milwaukee, WI; Levovist, GE Healthcare, Milwaukee, WI, Montville, NJ; SonoVue, Bracco, Milan, Italy) or, since dedicated contrast agents aren't available in Türkiye, the bubbled mixture consisting of intravascular contrast + saline + air prepared as mentioned above is administered into the septal artery, and thereafter 1–2 ml of saline solution is given for washing the lumen and simultaneously echocardiographic imaging is performed (Fig. 73, Video 11).<sup>245, 247</sup> Before contrast administration, a 2 $\circ$  harmonic setting should be used for better echocardiographic image quality and a low mechanical index setting (<1) to reduce contrast bubble destruction.<sup>248</sup> Contrast material dispersed within the septal artery perfusion area causes a hyperechoic appearance on echocardiography and draws the boundaries of the area where the infarct will occur as a result of alcohol administration. Transthoracic echocardiography is the most commonly applied imaging technique used in most centers for evaluation of contrast distribution. It is very important to evaluate the borders of myocardial contrast distribution from multiple windows, including the apical four and three chambers, and parasternal long and short axis, immediately after contrast agent administration during the procedure.<sup>247</sup> It may be necessary to re-administer echo-contrast agent or bubbled mixture to different septal branches in order to better determine the area where the mitral apparatus contacts the interventricular septum.<sup>240</sup> There are also studies suggesting that intramyocardial contrast echocardiography using 3D TTE might be more successful in reducing periprocedural complications since it provides simultaneous assessment with multiple views. When using 3D-TTE during the procedure, the highest possible frame rate (frame rate at least 30 Hz) in the sector width to contain both the right ventricle and LV cavities should be set in single-beat 'full volume' mode on apical images. In multiplanar sections, it is possible to evaluate whether there is sufficient contrast in the targeted area with off-line analysis. If the targeted septal area is not filled with enough contrast, if more than 1/3 of the septal length is filled, or if the interventricular septum adjacent to the right ventricle or the right/left ventricular free wall, papillary muscles are contrasted, then the contrast-administered septal branch should be considered inappropriate for the procedure (Fig. 74).<sup>248</sup> If the hyperechoic myocardial area includes the area adjacent to the LVOT obstruction, the area where the anterior mitral leaflet contacts the septum as a result of systolic anterior motion, and there is no more opacification of the tissues (LV anterior wall, right ventricular free wall, papillary muscles, etc.) outside the target septal area, the ASA is completed by injecting pure alcohol into the target area with 1 ml fractions.<sup>249</sup> Otherwise, the existing septal artery should be abandoned and another septal artery should be evaluated for ASA with myocardial contrast echocardiography. Continuous fluoroscopic, hemodynamic and electrocardiographic monitoring is performed during alcohol injection. However, when contrast enhancement is not observed in the appropriate anatomical area, if the appropriate anatomic region is still not detected by repeated contrast echocardiography despite switching to another septal artery or branch, the procedure is terminated without ethanol administration and the patient is considered ineligible for the ASA procedure. Intravenous analgesia is also applied in patients who are found to be suitable for alcohol injection, as chest pain will develop during the procedure.

The amount of alcohol used depends on the center. While it has been suggested in the Euro-ASA registry that 1.5–2.5 mL of ethanol is the most appropriate dose in terms of both efficacy and safety, which is evaluated as periprocedural atrioventricular (AV) block development, in a study by Kashtanov et al., 3 ml of standard alcohol was used in 150 HCM patients during the ASA procedure, regardless of perforator artery width and interventricular septum thickness, and they suggested that 3 ml of alcohol use was safe during the 15-year follow-up period. However, the number of patients with 15-year follow-up was limited and the need for a permanent pacemaker was relatively high.<sup>250</sup> In another study conducted in patients with septal thickness  $\geq 30$  mm, an average of  $2.7 \pm 1.3$  ml of alcohol was used in patients with septal thickness  $\geq 30$  mm, while  $2.2 \pm 0.9$  ml of alcohol was used in the group of patients with septal thickness  $< 30$  mm.<sup>239</sup> There are also centers that recommend the use of 1 ml of alcohol per 1 cm of septal thickness. It is worth mentioning that even septal branches with a thickness  $< 1$  mm may need to be ablated, especially those perfusing the areas where the mitral valve contacts the septum. As the infarct area increases, the frequency of arrhythmia due to scarring may increase, so it is important to use the optimal amount of alcohol. Another point to be considered is that the alcohol injection should be done slowly (1 ml/minute).<sup>240</sup> Usually 1 ml insulin syringes are suitable for this slow injection. A  $> 50\%$  decrease in the LVOT gradient measured invasively during the procedure immediately after alcohol injection into the appropriate septal perforating artery is considered as a successful procedure. If this goal is not achieved, it is recommended to repeat the alcohol injection into the same septal artery first, and if this is not successful, another septal artery (or branch) should be evaluated for alcohol ablation. The severity of the LVOT gradient and the degree of mitral regurgitation is also evaluated by the imaging team using TTE. After the alcohol is injected, the balloon is kept in an inflated state for about 10 more minutes, ensuring that the tissue contact continues, while at the same time preventing the

pacemaker cable is left in place and the rhythm is monitored.<sup>240, 242, 244, 251, 252</sup> Wall thickness and gradients are evaluated on the first postoperative day, before discharge, after three to six months and at the end of the first year.<sup>242, 245, 251, 253</sup> A gradient of  $> 50\%$  decrease in LVOT, which is associated with myocardial stunning and is considered a success criteria immediately after alcohol injection during the procedure, remains stable in some patients throughout all these echocardiographic follow-ups. The situation in which the pressure gradient is always low as in the early postoperative period is called the monophasic pattern. In some patients who have a successful ASA procedure, the gradient rises to the pre-procedural high level in the first 3 days, followed by a return to the successful low gradient level within the first 3 months, and this is called the triphasic pattern.<sup>251</sup> In this group of patients with a triphasic pattern, the gradient increase seen in the first 3 days is associated with edema of the ablated area or hypercontractility of other intact segments.<sup>254</sup> The subsequent slower and permanent decrease in gradient is the result of septal scarring, thinning and left ventricular remodeling.<sup>252</sup> Post-procedure septum thickness decreases by an average of 0.4–0.7 cm, and although it is stated that this reduction is usually completed in the first 3 months, there are also publications stating that it may take up to a year.<sup>242, 254</sup> On the other hand, it can be seen that the decrease in the gradient may improve in some cases in parallel with this septal thinning in the long term. Therefore, to evaluate the success of the procedure, not only the evaluations made in the first months, but also the echocardiographic evaluation at the end of the 1-year follow-up should be taken into account.<sup>240</sup> It has been shown that the degree of mitral regurgitation and the systolic pulmonary artery pressure decreased in the echocardiographic follow-ups of patients.<sup>255</sup> Therefore, it should be kept in mind that an adequate follow-up period is required before deciding to re-intervene.<sup>242</sup>

**Table 19. Potential Complications During or After the Procedure**

Conduction abnormalities (1 <sup>st</sup> –2 <sup>nd</sup> degree or complete AV block)
Mortality seen in early or late phases
Ventricular fibrillation
LAD dissection
Anterior myocardial infarction due to alcohol spreading to LAD
Pericardial effusion
Coronary artery spasm
Cardiogenic shock
Pulmonary embolism
Cerebrovascular event

AV: Atrioventricular; LAD: Left anterior descending artery.

spread to other branches.<sup>244</sup> After the LVOT pressure target is achieved, the balloon is deflated and the procedure is terminated by repeating the coronary angiogram to assess whether the septal artery is occluded and the LAD is patent.<sup>242</sup> Attention should also be paid to the development of pericardial fluid or cardiac tamponade both during and after the procedure. Complications that may occur during or after the procedure are given in Table 19.

### Postoperative Imaging

After the procedure, patients are followed in the intensive care unit. The intensive care follow-up period is at least 24–48 hours, and the length of stay in intensive care and hospitalization varies according to the protocols applied by the clinic. In addition, during the intensive care follow-up or in the first 24–48 hours of follow-up, the temporary

### Perioperative Echocardiography

**Dr. İrem Dilara Can, Dr. Halenur Sarıbaş, Dr. Elmas Kaplan, Dr. Ertan Andaç Al, Dr. Omac Tüfekçioğlu**

Perioperative transesophageal echocardiography (PTE) is used for monitoring and diagnosis in cardiac and non-cardiac surgical procedures. During the operation; volume status, ischemia detection, the need for inotropic /vasopressor therapy, and basic structural heart diseases can be easily evaluated with PTE.<sup>256</sup> PTE includes classical transesophageal echocardiography and epicardial echocardiography with a sterile nylon coating on the transthoracic probe.<sup>257</sup> Transesophageal echocardiography is relatively safe and has a mortality of  $< 1$  in 10,000 patients and morbidity in 2–5 patients in 1,000 patients.<sup>258, 259</sup> There were no known complications associated with use of epicardial echocardiography.<sup>257</sup>

### Evaluation of Left Ventricular Global and Regional Functions

Evaluation of left ventricular (LV) function is the most common indication for PTE. It is used in both cardiac and non-cardiac operations. Global longitudinal deformation is evaluated with LV linear and volumetric measurements. As indicated in the ASE and EACVI guidelines, 4-chamber, 2-chamber, and long axis images taken at the middle esophageal level are used to determine global and segmental functions over the 17-segment LV model.<sup>21</sup> Left ventricular mid-segments are also evaluated from transgastric short axis images.<sup>256</sup>

### Evaluation of Right Ventricular Global Functions

Right ventricular (RV) function assessment is the second most used indication for PTE. There are many operations that may affect RV function. Evaluation of RV function is important for liver transplantation

among non-cardiac operations. In cirrhotic patients, it may increase LV filling pressure and pulmonary artery pressure due to high flow and increased preload. The chronic ongoing hyperdynamic state due to cirrhosis can cause enlargement of the right heart and even right heart failure. It should be kept in mind that the possibility of underlying porto-pulmonary hypertension may also contribute to the formation of right heart failure.<sup>260</sup> Absolute RV function should be evaluated in heart transplantation, LV assist device implantation, pulmonary vascular surgeries, and many cardiac surgical procedures involving the left heart.<sup>256</sup> RV and right atrial (RA) size should be measured. Both qualitative and quantitative parameters of the RV should be measured using multiple acoustic windows. The most frequently used parameters are: Fractional area change for RV systolic function, tissue Doppler imaging-derived tricuspid lateral annular systolic velocity wave, M-mode-derived tricuspid annular plane systolic deviation, RV wall longitudinal deformation, and RV index of Doppler and myocardial performance with at least one or a combination of RV function. RV systolic pressure calculated using the tricuspid regurgitation jet and RA pressure based on inferior vena cava size and collapse should be reported.<sup>21</sup>

### Hypovolemia

Hypovolemia is a common cause of hemodynamic instability in the perioperative period. The first echocardiographic findings in hypovolemia are decreased left ventricular diastolic size. The most used echocardiographic parameters in the diagnosis and follow-up are LV end-diastolic diameter and LV end-diastolic area obtained in the transgastric midpapillary short axis image. Volume resuscitation or positive inotropic support of the hypovolemic patient should be followed up with PTE.<sup>21, 256</sup>

### Pulmonary Embolism

There is an increased risk for acute pulmonary embolism (APE) after both surgery and trauma. Therefore, although it is not the gold standard, PTE is used for the diagnosis of APE. With PTE, the thrombus in the right heart can be seen directly, but visualization of the thrombus in the pulmonary artery may not always be possible. It may not always be possible to visualize the thrombus in the pulmonary artery. However, RV dysfunction (eg, RV dilatation, RV wall hypokinesia) and atypical regional wall motion abnormalities of the RV free wall provide important clues to diagnose hemodynamically significant APE.<sup>256</sup>

### Mitral Valve Surgery

Due to the complex anatomy of the mitral valve, PTE is an absolute necessity in mitral valve stenosis and mitral regurgitation (MR) that requires mitral valve surgery. Anatomical and hemodynamic severity of valve pathology should be determined preoperatively.

In the evaluation of mitral stenosis, it is necessary to distinguish between rheumatic and degenerative etiology. It is important to determine the valve area planimetrically with multimodality imaging methods, especially considering that patients may also have low-flow low-gradient physiology. In addition, evaluation of valve calcification, especially annular calcification is required. Other pathologies accompanying mitral stenosis (other valve pathologies) should be evaluated.

The Carpentier classification based on mitral leaflet mobility is used in the preoperative assessment of mitral regurgitation. It is generally used to classify the mechanism of MR and to identify cases that are suitable for the surgical team. Type I MR occurs with normal mitral leaflet movement, usually mitral annular dilatation, or mitral leaf-

let perforation. Type II MR occurs in the setting of excessive mitral leaflet movement and due to mitral valve prolapse or flail leaflet (jet directed away from the affected leaflet). Type III MR involves mitral leaflet motility and is divided into type IIIa, which includes both systolic and diastolic leaflet restriction, and type IIIb (jet towards the affected leaflet), which is associated with limited leaflet movement during systole. Type IIIa MR is seen in rheumatic or calcific degenerative mitral valve disease, type IIIb MR is seen in LV dilatation or LV wall motion disorder (with leaflet tethering).<sup>261</sup> In mid-esophageal 5-chamber or long axis views, the lengths of the posterior and anterior mitral leaflets in mid-diastole, the ratio of anterior and posterior leaflet heights measured from the mitral annulus to the coaptation point at the end of systole, the distance from the coaptation point of the mitral leaflets to the interventricular septum at the end of systole (C-septal distance) and the angle between the mitral valve and the annular planes of the aortic valve should be measured.<sup>21, 261</sup> Anterior leaflet systolic anterior movement (SAM) is a serious complication after mitral valve repair. Independent pre-operative predictors of SAM include thick basal interventricular septum (>15 mm), short C-sept distance (<25 mm), narrow aorto-mitral angle (<120°), anterior displacement of papillary muscles, and ratio between anterior and posterior leaflet lengths >1.3.<sup>21</sup>

PTE can be used during cannulation in minimally invasive or robotic surgery. It should be visualized that the femoral venous catheter passes through the RA through the inferior vena cava and enters the superior vena cava. In addition, it is observed that the arterial cannula entering from the femoral artery reaches the aortic root and is located 2–4 cm more distal from the sinus valsalva, and the aorta is fully endovascularly occluded (cross-clamp) during cardioplegia. PTE plays an important role in the placement of a coronary sinus catheter, and any persistent left superior vena cava should be detected. Especially in patients with persistent left superior vena cava, adequate flow will not be provided during retrograde cardioplegia. Care should be taken to avoid trauma to the interatrial septum, fossa ovalis, and right atrial appendage during placement of the venous cannula, and to monitor aortic injury during placement of the large-bore arterial cannula.<sup>21, 261</sup>

Valve evaluation after mitral repair is evaluated after aortic cross-clamp removal, adequate LV filling volume, adequate elevation of systolic pressure, and heart rate control (<100/min). Evaluation of mitral valve repair includes: (1) residual MR, (2) iatrogenic mitral stenosis (mean gradient <6 mmHg, especially after Alfieri-type intervention), (3) SAM (considering adequate volume expansion and heart rate control in evaluation), (4) LV function, (5) lateral and posterior wall motion disorder in newly developed LV (circumflex artery trauma due to posterior annuloplasty), (6) iatrogenic aortic regurgitation (due to retraction of NC or LC aortic cusps due to their proximity to the mitral valve), and (7) very rare iatrogenic fistula formation from LV to coronary sinus, RA or RV. If the mitral valve is replaced with a metallic prosthetic valve, in the post-pump evaluation; It should be evaluated in terms of (1) paravalvular leak, (2) opening of the cusps, and (3) any coronary artery damage.<sup>21, 261</sup>

### Aortic Valve Surgery

Aortic stenosis usually develops with rheumatic, degenerative or congenital etiologies. In calcific stenosis, the preference is to replace the aortic valve with a metallic prosthetic valve. Annulus diameter should be evaluated with PTE. If the annular diameter is <2.0 cm, the probability of patient-prosthesis mismatch after the operation is high. LV outflow obstruction due to basal septal hypertrophy and anterior angula-

tion of the aortic root at the pump outlet should be investigated. A LV end-diastolic diameter <42 mm, a hyperdynamic and asymmetrical hypertrophic LV (IVS/posterior wall >1.45) are independent predictors of LV outflow tract obstruction after aortic valve replacement.<sup>262</sup>

Paravalvular aortic insufficiency in prosthetic valves is corrected by stopping the heart again if necessary, depending on its severity. In biological stentless prosthetic valves, which have paravalvular leakage and vena contraction <3 mm, correction is not usually needed, since the pump outlet is likely to improve after protamine, but it is also checked again after protamine administration. If the vena contracta is larger than 3 mm in contraction, paravalvular insufficiency is corrected by re-entering the pump before protamine administration.<sup>263</sup> Aortic root tears, fistula formation from the LV outflow tract to the RA (Gerbode), mitral valve disorders due to its anatomical proximity, interventricular septum dissection, and fistula formation from the aorta to the RV or LV are among the complications that can develop, although they are rarely seen.<sup>261</sup>

A classification like the Carpentier classification used for mitral valve is used in the repair of aortic regurgitation (AR): Type I (normal cusp motility), type II (increased cusp motility) or type III (limited cusp motility). In type I AR, cusp mobility is normal, but there is AR due to dilatation of the aortic root complex (annulus, root, or sinotubular junction) or perforation of the aorta, most commonly resulting in central regurgitation. In type II AR, there is an excessive cusp mobility resulting from prolapse or flail, typically resulting in eccentric AR directed away from the affected tip. Cushion prolapse may occur in tricuspid aortic valves (most commonly the right valve is involved), but more commonly occurs in bicuspid valves where the attached cusp is most affected, although both valves may be prolapsed. It is suitable for pulp prolapse, pulp plication or resuspension repair techniques. In type III AR, calcification, fibrosis or post-inflammatory or degenerative changes can be seen. Type III AR is the least suitable type for repair. Bicuspid valves are often unsuitable for repair because the annulus is enlarged, and the cusps are asymmetrical.<sup>21, 261</sup>

When the pump becomes off after aortic insufficiency repair; the presence of more than mild residual AR, coaptation tips being below the annular plane, coaptation length <4 mm, and effective cusp height <9 mm have all been shown to be predictors of significant recurrent AR within 2 years.<sup>264</sup>

## Other Uses of PTE

PTE plays an important role in the implantation of left ventricular assist devices (LVAD). Contrast studies are required for the evaluation of the patent foramen ovale during the operation. Due to the left atrial suction effect that develops after actively working LVAD, the oxygenated blood from the RA can pass to the left system. Aortic regurgitation is also important in the evaluation, as it will cause blood to be continuously taken from the LV and returned from the aorta with the aortic cannula after the LVAD. It is valuable for the prevention of complications in the evaluation of thrombus in the LV and left atrium. It should be checked that the LV cannula position is correctly implanted towards the mitral valve. After activating the LVAD, the interventricular septum position and RV function are also checked.

PTE has important uses in tricuspid and pulmonary valve operations, heart and lung transplantation operations, insertion and removing external circulatory support systems and assessment of cardiac masses.<sup>265</sup> PTE is an indispensable tool for the follow-up and treatment of structural disorders of the heart and hemodynamic deterioration in modern operating rooms.

## Kaynaklar

1. Ntaios G, Papavasileiou V, Sagris D, et al. Closure of Patent Foramen Ovale Versus Medical Therapy in Patients With Cryptogenic Stroke or Transient Ischemic Attack: Updated Systematic Review and Meta-Analysis. *Stroke*. 2018;49(2):412-418. [Crossref]
2. Pristipino C, Sievert H, D'Ascenzo F, et al. European position paper on the management of patients with patent foramen ovale. General approach and left circulation thromboembolism. *Eur Heart J*. 2019;40(38):3182-3195. [Crossref]
3. Mojadidi MK, Meier B, Tobis JM. Patent Foramen Ovale Closure for Stroke, Myocardial Infarction, Peripheral Embolism, Migraine, and Hypoxemia. 1st ed. Academic Press, Elsevier Inc; 2020.
4. Silvestry FE, Cohen MS, Armsby LB, et al. Guidelines for the Echocardiographic Assessment of Atrial Septal Defect and Patent Foramen Ovale: From the American Society of Echocardiography and Society for Cardiac Angiography and Interventions. *J Am Soc Echocardiogr*. 2015;28(8):910-958. [Crossref]
5. Mahmoud AN, Elgendy IY, Agarwal N, Tobis JM, Mojadidi MK. Identification and quantification of patent foramen ovale-mediated shunts: echocardiography and transcranial Doppler. *Interv Cardiol Clin*. 2017;6(4):495-504. [Crossref]
6. Mojadidi MK, Roberts SC, Winoker JS, et al. Accuracy of transcranial Doppler for the diagnosis of intracardiac right-to-left shunt: a bivariate meta-analysis of prospective studies. *JACC Cardiovasc Imaging*. 2014;7(3):236-250. [Crossref]
7. Yamashita E, Murata T, Goto E, et al. Inferior Vena Cava Compression as a Novel Maneuver to Detect Patent Foramen Ovale: A Transesophageal Echocardiographic Study. *J Am Soc Echocardiogr*. 2017;30(3):292-299. [Crossref]
8. Ayan K, De Boeck B, Velthuis BK, Schaap AJ, Cramer MJM. Lipomatous hypertrophy of the interatrial septum. *Int J Cardiovasc Imaging*. 2005;21(6):659-661. [Crossref]
9. Hotda MK, Krakczyk-Ozóg A, Koziej M, et al. Patent Foramen Ovale Channel Morphometric Characteristics Associated with Cryptogenic Stroke: The MorPFO Score. *J Am Soc Echocardiogr*. 2021;34(12):1285-1293.e3. [Crossref]
10. Rana BS, Thomas MR, Calvert PA, Monaghan MJ, Hildick-Smith D. Echocardiographic evaluation of patent foramen ovale prior to device closure. *JACC Cardiovasc Imaging*. 2010;3(7):749-760. [Crossref]
11. Roy DA, Sharma R, Bunce N, Ward D, Brecker SJ. Selecting the optimal closure device in patients with atrial septal defects and patent foramen ovale. *Interv Cardiol*. 2012;4(1):85-100. [Crossref]
12. Lang RM, Badano LP, Tsang W, et al. EAE/ASE recommendations for image acquisition and display using three-dimensional echocardiography. *J Am Soc Echocardiogr*. 2012;25(1):3-46. [Crossref]
13. Salaun E, Carles S, Bigand E, et al. High Radiation Exposure of the Imaging Specialist During Structural Heart Interventions With Echocardiographic Guidance. *JACC Cardiovasc Interv*. 2017;10(6):626-627. [Crossref]
14. Meier B. Closure of patent foramen ovale: technique, pitfalls, complications, and follow up. *Heart*. 2005;91(4):444-448. [Crossref]
15. Hoffman JI, Christianson R. Congenital heart disease in a cohort of 19,502 births with long-term follow-up. *Am J Cardiol*. 1978;42:641-647. [Crossref]
16. Bartel T, Müller S. Device closure of interatrial communications: pericardial-interventional echocardiographic assessment. *Eur Heart J Cardiovasc Imaging*. 2013;14(7):618-624. [Crossref]
17. Fraker Jr TD, Harris PJ, Behar VS, Kisslo JA. Detection and exclusion of interatrial shunts by two-dimensional echocardiography and peripheral venous injection. *Circulation*. 1979;59(2):379-384. [Crossref]
18. Baumgartner H, De Backer J. The ESC Clinical Practice Guidelines for the Management of Adult Congenital Heart Disease 2020. *Eur Heart J*. 2020;41(43):4153-4154. [Crossref]
19. Kitabatake A, Inoue M, Asao M, et al. Noninvasive evaluation of the ratio of pulmonary to systemic flow in atrial septal defect by duplex Doppler echocardiography. *Circulation*. 1984;69(1):73-79. [Crossref]
20. Rufino Nascimento LG, Dehant P, Jimenez M, Dequeker JL, Castela E, Choussat A. Calculation of the pulmonary to systemic flow ratio using echo-Doppler in septal defects-correlation with oximetry. *Rev Port Cardiol*. 1989;8(1):35-40.

21. Lang RM, Badano LP, Mor-Avi V, et al. Recommendations for cardiac chamber quantification by echocardiography in adults: an update from the American Society of Echocardiography and the European Association of Cardiovascular Imaging. *J Am Soc Echocardiogr*. 2015;28(1): 1–39.e14. [\[Crossref\]](#)
22. Tamborini G, Marsan NA, Gripari P, et al. Reference values for right ventricular volumes and ejection fraction with real-time three-dimensional echocardiography: evaluation in a large series of normal subjects. *J Am Soc Echocardiogr*. 2010;23(1):109–115. [\[Crossref\]](#)
23. Abbas AE, Fortuin FD, Schiller NB, Appleton CP, Moreno CA, Lester SJ. A simple method for noninvasive estimation of pulmonary vascular resistance. *J Am Coll Cardiol*. 2003;41(6):1021–1027. [\[Crossref\]](#)
24. Steele PM, Fuster V, Cohen M, Ritter DG, McGoon DC. Isolated atrial septal defect with pulmonary vascular obstructive disease—long-term follow-up and prediction of outcome after surgical correction. *Circulation*. 1987;76(5):1037–1042. [\[Crossref\]](#)
25. Vogel M, Berger F, Kramer A, Alexi-Meshkishvili V, Lange PE. Incidence of secondary pulmonary hypertension in adults with atrial septal or sinus venosus defects. *Heart*. 1999;82(1):30–33. [\[Crossref\]](#)
26. Masutani S, Senzaki H. Left ventricular function in adult patients with atrial septal defect: implication for development of heart failure after transcatheter closure. *J Card Fail*. 2011;17(11):957–963. [\[Crossref\]](#)
27. Cooke JC, Gelman JS, Harper RW. Echocardiologists' role in the deployment of the Amplatzer atrial septal occluder device in adults. *J Am Soc Echocardiogr*. 2001;14(6):588–594. [\[Crossref\]](#)
28. Franke A, Kühl HP, Rulands D, et al. Quantitative analysis of the morphology of secundum-type atrial septal defects and their dynamic change using transesophageal three-dimensional echocardiography. *Circulation*. 1997;96(9 Suppl):II–323–7.
29. Hajizainali A, Sadeghian H, Rezvannard M, Alidoosti M, Zoroufian A, Volman MA. A comparison between size of the occluder device and two-dimensional transesophageal echocardiographic sizing of the ostium secundum atrial septal defect. *Cardiovasc J Afr*. 2013;24(5):161–164. [\[Crossref\]](#)
30. Rana BS. Echocardiography guidance of atrial septal defect closure. *J Thorac Dis*. 2018;10(Suppl 24):S2899–S2908. [\[Crossref\]](#)
31. Faletra F, Scarpini S, Moreo A, et al. Color Doppler echocardiographic assessment of atrial septal defect size: correlation with surgical measurements. *J Am Soc Echocardiogr*. 1991;4(5):429–434. [\[Crossref\]](#)
32. Saric M, Perk G, Purgess JR, Kronzon I. Imaging atrial septal defects by real-time three-dimensional transesophageal echocardiography: step-by-step approach. *J Am Soc Echocardiogr*. 2010;23(11):1128–1135. [\[Crossref\]](#)
33. Rao PS. Role of Echocardiography in the Diagnosis and Interventional Management of Atrial Septal Defects. *Diagnostics (Basel)*. 2022;12(6):1494. [\[Crossref\]](#)
34. Mallula K, Amin Z. Recent changes in instructions for use for the Amplatzer atrial septal defect occluder: how to incorporate these changes while using transesophageal echocardiography or intracardiac echocardiography? *Pediatr Cardiol*. 2012;33(7):995–1000. [\[Crossref\]](#)
35. Ho M.-L, Bhalla S, Bierhals A, Gutierrez F. MDCT of partial anomalous pulmonary venous return (PAPVR) in adults. *J Thorac Imag*. 2009;24(2):89–95. [\[Crossref\]](#)
36. Katre R, Burns SK, Murillo H, Lane MJ, Restrepo CS. Anomalous pulmonary venous connections. *Semin Ultrasound CT MR*. 2012;33(6):485–499. [\[Crossref\]](#)
37. Puchalski MD, Lui GK, Miller-Hance WC, et al. Guidelines for Performing a Comprehensive Transesophageal Echocardiographic: Examination in Children and All Patients with Congenital Heart Disease: Recommendations from the American Society of Echocardiography. *J Am Soc Echocardiogr*. 2019;32(2):173–215. [\[Crossref\]](#)
38. Podnar T, Martanovic P, Gavora P, Masura J. Morphological variations of secundum-type atrial septal defects: feasibility for percutaneous closure using Amplatzer septal occluders. *Catheter Cardiovasc Interv*. 2001;53(3):386–391. [\[Crossref\]](#)
39. Harper RW, Mottram PM, McGaw DJ. Closure of secundum atrial septal defects with the Amplatzer septal occluder device: techniques and problems. *Catheter Cardiovasc Interv*. 2002;57(4):508–524. [\[Crossref\]](#)
40. Meadows AK, Ordovas K, Higgins CB, Reddy GP. Magnetic resonance imaging in the adult with congenital heart disease. *Semin Roentgenol*. 2008;43(3):246–258. [\[Crossref\]](#)
41. Piaw CS, Kiam OT, Rapae A, et al. Use of non-invasive phase contrast magnetic resonance imaging for estimation of atrial septal defect size and morphology: a comparison with transesophageal echo. *Cardiovasc Intervent Radiol*. 2006;29(2):230–234. [\[Crossref\]](#)
42. Shah TR, Beig JR, Choh NA, Rather FA, Yaqoob I, Jan VM. Phase contrast cardiac magnetic resonance imaging versus transoesophageal echocardiography for the evaluation of feasibility for transcatheter closure of atrial septal defects. *Egypt Heart J*. 2022;74(1):27. [\[Crossref\]](#)
43. Goo HW, Park IS, Ko JK, et al. CT of congenital heart disease: normal anatomy and typical pathologic conditions. *Radiographics*. 2003;23 Spec No:S147–65.S165 [\[Crossref\]](#)
44. Eom HJ, Yang DH, Kang JW, et al. Preoperative cardiac computed tomography for demonstration of congenital cardiac septal defect in adults. *Eur Radiol*. 2015;25(6):1614–1622. [\[Crossref\]](#)
45. Bartakian S, El-Said HG, Printz B, Moore JW. Prospective randomized trial of transthoracic echocardiography versus transesophageal echocardiography for assessment and guidance of transcatheter closure of atrial septal defects in children using the Amplatzer septal occluder. *JACC Cardiovasc Interv*. 2013;6(9):974–980. [\[Crossref\]](#)
46. Azhar AS. Safety and efficacy of transthoracic versus transesophageal echocardiography in transcatheter closure of atrial septal defects. Reporting a single center experience from Saudi Arabia. *Saudi Med J*. 2016;37(11):1196–1205. [\[Crossref\]](#)
47. Yamano M, Yamano T, Nakamura T, et al. Appropriate selection of echocardiographic guidance for transcatheter atrial septal defect closure. *Int J Cardiovasc Imaging*. 2020;36(5):855–863. [\[Crossref\]](#)
48. Sobrino A, Basmadjian AJ, Ducharme A, et al. Multiplanar transesophageal echocardiography for the evaluation and percutaneous management of ostium secundum atrial septal defects in the adult. *Arch Cardiol Mex*. 2012;82:37–47.
49. Knepp MD, Rocchini AP, Lloyd TR, Aiyagari RM. Long-term follow up of secundum atrial septal defect closure with the amplatzer septal occluder. *Congenit Heart Dis*. 2010;5(1):32–37. [\[Crossref\]](#)
50. Mainzer G, Braver Y, Khoury A, et al. Morphologic, mechanical, conductive, and hemodynamic changes following transcatheter closure of atrial septal defect. *Congenit Heart Dis*. 2010;5(1):25–31. [\[Crossref\]](#)
51. Kılıçaslan B, Ekinçi S, Kurşun M, et al. Association of cardiac adaptations with NT-proBNP levels after percutaneous closure of atrial septal defect. *Turk Kardiyol Dern Ars*. 2019;47(4):258–264.
52. Wunderlich NC, Dalvi B, Ho SY, Küx H, Siegel RJ. Rheumatic Mitral Valve Stenosis: Diagnosis and Treatment Options. *Curr Cardiol Rep*. 2019;21(3):14. [\[Crossref\]](#)
53. Harken DE, Ellis LB. The surgical treatment of mitral stenosis; valvuloplasty. *N Engl J Med*. 1948;239(22):801–809. [\[Crossref\]](#)
54. Inoue K, Owaki T, Nakamura T, et al. Clinical application of transvenous mitral commissurotomy by a new balloon catheter. *J Thorac Cardiovasc Surg*. 1984;87(3):394–402. [\[Crossref\]](#) [https://doi.org/10.1016/S0022-5223\(19\)37390-8](https://doi.org/10.1016/S0022-5223(19)37390-8)
55. Vahanian A, Palacios IF. Percutaneous approaches to valvular disease. *Circulation*. 2004;109(13):1572–1579. [\[Crossref\]](#)
56. Palacios IF, Sanchez PL, Harrell LC, Weyman AE, Block PC. Which patients benefit from percutaneous mitral balloon valvuloplasty? Prevalvuloplasty and post valvuloplasty variables that predict long-term outcome. *Circulation*. 2002;105(12):1465–1471. [\[Crossref\]](#)
57. Nobuyoshi M, Arita T, Shin-Ichi S, et al. Percutaneous balloon mitral valvuloplasty: a review. *Circulation*. 2009;119: e211–e219. [\[Crossref\]](#)
58. Ben Farhat M, Ayari M, Maatouk F, et al. Percutaneous balloon versus surgical closed and open mitral commissurotomy: seven-year follow-up results of a randomized trial. *Circulation*. 1998; 97(3):245–250.
59. Vahanian A, Alfieri O, Andreotti F, et al. Guidelines on the management of valvular heart disease (version 2012): The Joint Task Force on the Management of Valvular Heart Disease of the European Society of Cardiology (ESC) and the European Association for Cardio-Thoracic Surgery (EACTS). *Eur Heart J*. 2012;33(19):2451–2496. [\[Crossref\]](#)

60. Passeri JJ, Dal-Bianco JP. Percutaneous Balloon Mitral Valvuloplasty Echocardiographic Eligibility and Procedural Guidance. *Intervent Cardiol Clin*. 2018;7(3):405–413. [\[Crossref\]](#)
61. Perez de Isla L, Casanova C, Almeria C, et al. Which method should be the reference method to evaluate the severity of rheumatic mitral stenosis? Gorlin's method versus 3D-echo. *Eur J Echocardiogr*. 2007;8(6):470–473. [\[Crossref\]](#)
62. Holmin C, Messika-Zeitoun D, Mezalek AT, et al. Mitral leaflet separation index: a new method for the evaluation of the severity of mitral stenosis? Usefulness before and after percutaneous mitral commissurotomy. *J Am Soc Echocardiogr*. 2007;20(10):1119–1124 [\[Crossref\]](#)
63. Duggal B, Bajaj M, Prabhu S, Mathew T. The mitral leaflet separation index for assessment of mitral stenosis during percutaneous mitral commissurotomy: validation of the index in the immediate post-PMC period. *Echocardiography*. 2012;29(10):1143–1148. [\[Crossref\]](#)
64. Seow SC, Koh LP, Yeo TC. Hemodynamic significance of mitral stenosis: use of a simple, novel index by 2-dimensional echocardiography. *J Am Soc Echocardiogr*. 2006;19(1):102–106. [\[Crossref\]](#)
65. Kinsara AJ, Awadallah AM, AlZaki M, Goda H, Nanda NC. Mitral leaflet separation index for mitral valve assessment during balloon mitral valvuloplasty. *Echocardiography*. 2020;37(8):1159–1163. [\[Crossref\]](#)
66. Bigdelu L, Poorzand H, Azari A, et al. Mitral leaflet separation to evaluate the severity of mitral stenosis: validation of the index by transesophageal three-dimensional echocardiography. *Echocardiography*. 2018;35(3):361–436. [\[Crossref\]](#)
67. Alkhouly AA, Al-Amin AM, Mukarrab MI. Role of three-dimensional transesophageal echocardiography in predicting mitral regurgitation after percutaneous balloon mitral valvuloplasty. *Indian Heart J*. 2018;70(6):836–842. [\[Crossref\]](#)
68. Wilkins GT, Weyman AE, Abascal VM, et al. Percutaneous balloon dilatation of the mitral valve: an analysis of echocardiographic variables related to outcome and the mechanism of dilatation. *Br Heart J*. 1988;60(4):299–308. [\[Crossref\]](#)
69. Cannan CR, Nishimura RA, Reeder GS, et al. Echocardiographic assessment of commissural calcium: a simple predictor of outcome after percutaneous mitral balloon valvotomy. *J Am Coll Cardiol*. 1997;29(1):175–180. [\[Crossref\]](#)
70. Padiyal LR, Freitas N, Sagie A, et al. Echocardiography can predict which patients will develop severe mitral regurgitation after percutaneous mitral valvotomy. *J Am Coll Cardiol*. 1996; 27(5):1225–1231. [\[Crossref\]](#)
71. Nunes MC, Tan TC, Elmariah S, et al. The echo score revisited: impact of incorporating commissural morphology and leaflet displacement to the prediction of outcome for patients undergoing percutaneous mitral valvuloplasty. *Circulation*. 2014;129(8):886–895. [\[Crossref\]](#)
72. Anwar AM, Attia WM, Nosir YF, et al. Validation of a new score for the assessment of mitral stenosis using real-time three-dimensional echocardiography. *J Am Soc Echocardiogr*. 2010;23:13–22. [\[Crossref\]](#)
73. Sanati HR, Kiavar M, Salehi N, et al. Percutaneous mitral valvuloplasty—a new method for balloon sizing based on maximal commissural diameter to improve procedural results. *Am Heart Hosp J*. 2010;8(1):29–32.
74. Meneguz-Moreno RA, Costa R, Gomes NL. Very long term follow-up after percutaneous balloon mitral valvuloplasty. *J Am Coll Cardiol Intv*. 2018;11(19):1945–1952. [\[Crossref\]](#)
75. Thomas JD, Wilkins GT, Choong CY, et al. Inaccuracy of mitral pressure half-time immediately after percutaneous mitral valvotomy. Dependence on transmitral gradient and left atrial and ventricular compliance. *Circulation*. 1988;78(4):980–993. [\[Crossref\]](#)
76. Koren O, Israeli A, Rozner E, Darawshy N, Turgeman Y. Clinical and echocardiographic trends in percutaneous balloon mitral valvuloplasty. *J Cardiothorac Surg*. 2021;16(1):68. [\[Crossref\]](#)
77. Chen CR, Cheng TO. Percutaneous balloon mitral valvuloplasty by the Inoue technique: a multicenter study of 4832 patients in China. *Am Heart J*. 1995;129(6):1197–203. [\[Crossref\]](#)
78. Nunes MC, Levine RA, Braulio R, et al. Mitral regurgitation after percutaneous mitral valvuloplasty insights into mechanisms and impact on clinical outcomes. *J Am Coll Cardiol Img*. 2020;13(12):2513–2526. [\[Crossref\]](#)
79. Salemi A, Worku BM. Standard imaging techniques in transcatheter aortic valve replacement. *J Thorac Dis*. 2017;9(Suppl 4):S289–S298. [\[Crossref\]](#)
80. Perry TE, George SA, Lee B, et al. A guide for pre-procedural imaging for transcatheter aortic valve replacement patients. *Perioper Med (Lond)*. 2020;9(1):36. [\[Crossref\]](#)
81. Zamorano JL, Goncalves A, Lang R. Imaging to select and guide transcatheter aortic valve implantation. *Eur Heart J*. 2014;35(24):1578–1587. [\[Crossref\]](#)
82. Delgado V, CT Ng A, Shanks M, et al. Transcatheter aortic valve implantation: role of multimodality cardiac imaging. *Expert Rev Cardiovasc Ther*. 2010. 8(1): p. 113–23. [\[Crossref\]](#)
83. Duran, C., et al., Multidetector Computed Tomography (MDCT) Angiography in the pre-procedural assessment of patients undergoing transcatheter aortic valve replacement. *Eurasian J Med*. 2020; 52(1):86–93. [\[Crossref\]](#)
84. Guo R, Xie M, Yen Yim W, et al. Dose approach matter? A meta-analysis of outcomes following transfemoral versus transapical transcatheter aortic valve replacement. *BMC Cardiovasc Disord*. 2021.21(1):358. [\[Crossref\]](#)
85. Genevex P, Webb JG, Svensson LG, et al. Vascular complications after transcatheter aortic valve replacement: insights from the PARTNER (Placement of AoRTic TraNscatheteR Valve) trial. *J Am Coll Cardiol*. 2012;60(12):1043–1052. [\[Crossref\]](#)
86. Feuchtner G, Plank F, Bartel T, et al. Prediction of paravalvular regurgitation after transcatheter aortic valve implantation by computed tomography: value of aortic valve and annular calcification. *Ann Thorac Surg*. 2013;96(5):1574–1580. [\[Crossref\]](#)
87. Delgado V, CT Ng A, van de Veire NR, et al. Transcatheter aortic valve implantation: role of multi-detector row computed tomography to evaluate prosthesis positioning and deployment in relation to valve function. *Eur Heart J*. 2010;31(9):1114–1123 [\[Crossref\]](#).
88. Ribeiro HB, Nombela-Franco L, Urena M, et al. Coronary obstruction following transcatheter aortic valve implantation: a systematic review. *JACC Cardiovasc Interv*. 2013;6(5):452–461. [\[Crossref\]](#)
89. Rashid HN, Brown AJ, McCormick LM, et al. Subclinical leaflet thrombosis in transcatheter aortic valve replacement detected by multidetector computed tomography—a review of current evidence. *Circ J*. 2018;82(7):1735–1742. [\[Crossref\]](#)
90. Mehrotra P, Flynn AW, Jansen K, et al. Differential left ventricular outflow tract remodeling and dynamics in aortic stenosis. *J Am Soc Echocardiogr*. 2015;28(11):1259–1266. [\[Crossref\]](#)
91. LaBounty TM, Miyasaka R, Chetcuti S, et al. Annulus instead of LVOT diameter improves agreement between echocardiography effective orifice area and invasive aortic valve area. *JACC Cardiovasc Imaging*. 2014;7(10):1065–1066. [\[Crossref\]](#)
92. Binder RK, Webb JG, Willson AB, et al. The impact of integration of a multidetector computed tomography annulus area sizing algorithm on outcomes of transcatheter aortic valve replacement: a prospective, multicenter, controlled trial. *J Am Coll Cardiol*. 2013;62(5):431–438.
93. Jitaihiwi H, Kashif M, Fontana G, et al. Cross-sectional computed tomographic assessment improves accuracy of aortic annular sizing for transcatheter aortic valve replacement and reduces the incidence of paravalvular aortic regurgitation. *J Am Coll Cardiol*. 2012;59(14):1275–1286. [\[Crossref\]](#)
94. Stella S, Italia L, Geremi G, et al. Accuracy and reproducibility of aortic annular measurements obtained from echocardiographic 3D manual and semi-automated software analyses in patients referred for transcatheter aortic valve implantation: implication for prosthesis size selection. *Eur Heart J Cardiovasc Imaging*. 2019;20(1):45–55. [\[Crossref\]](#)
95. Hahn RT, Little SH, Monaghan MJ, et al. Recommendations for comprehensive intraprocedural echocardiographic imaging during TAVR. *JACC Cardiovasc Imaging*. 2015;8(3):261–287. [\[Crossref\]](#)

96. Otto CM, Kumbhani DJ, Alexander KP, et al. 2017 ACC Expert consensus decision pathway for transcatheter aortic valve replacement in the management of adults with aortic stenosis: a report of the American college of cardiology task force on clinical expert consensus documents. *J Am Coll Cardiol*. 2017;69(10):1313-1346. [\[Crossref\]](#)
97. Leon MB, Smith CR, Mack M, et al. Transcatheter aortic-valve implantation for aortic stenosis in patients who cannot undergo surgery. *N Engl J Med*. 2010; 363(17):1597-1607. [\[Crossref\]](#)
98. Shivaraju, A., et al., Tools and techniques - clinical: fluoroscopic balloon sizing of the aortic annulus before transcatheter aortic valve replacement (TAVR) - follow the "right cusp rule". *EuroIntervention*. 2015;11(7):840-842. [\[Crossref\]](#)
99. Hammermeister K, Sethi G K, Henderson W G, Grover F L, Oprian C, Rahimtoola S H. Outcomes 15 years after valve replacement with a mechanical versus a bioprosthetic valve: final report of the Veterans Affairs randomized trial. *J Am Coll Cardiol*. 2000;36(4):1152-1158. [\[Crossref\]](#)
100. Ionescu A, Fraser A G, Butchart E G. Prevalence and clinical significance of incidental paraprothestic valvar regurgitation: a prospective study using transoesophageal echocardiography. *Heart*. 2003;89(11):1316-1321. [\[Crossref\]](#)
101. Rallidis L S, Moysakis I E, Ikonomidis I, Nihoyannopoulos P. Natural history of early aortic paraprothestic regurgitation: a five- year follow- up. *Am Heart J*. 1999;138(2 Pt 1):351-357. [\[Crossref\]](#)
102. Davila-Roman VG, Waggoner AD, Kennard ED, Holubkov R, Eric Jamieson WR, Englberger L, Carrel T P, et al. Prevalence and severity of paravalvular regurgitation in the Artificial Valve Endocarditis Reduction Trial (AVERT) echocardiography study. *J Am Coll Cardiol*. 2004;44(7):1467-1472. [\[Crossref\]](#)
103. Van Belle E, Juthier F, Susen S, et al. Postprocedural aortic regurgitation in balloon- expandable and self- expandable transcatheter aortic valve replacement procedures: analysis of predictors and impact on long- term mortality: insights from the FRANCE2 registry. *Circulation*. 2014;129(13):1415-1427. [\[Crossref\]](#)
104. Athappan G, Patvardhan E, Tuzcu EM, et al. Incidence, predictors, and outcomes of aortic regurgitation after transcatheter aortic valve replacement: meta-analysis and systematic review of literature. *J Am Coll Cardiol*. 2013;61(15):1585-1595. [\[Crossref\]](#)
105. Pate GE, Al Zubaidi A, Chandavimol M, et al. Percutaneous closure of prosthetic paravalvular leaks: case series and review. *Catheter Cardiovasc Interv*. 2006;68(4):528-533. [\[Crossref\]](#)
106. Otto CM, Nishimura RA, Bonow O, et al. 2020 ACC/AHA guideline for the management of patients with valvular heart disease: executive summary: a report of the American college of cardiology/ American heart association joint committee on clinical practice guidelines. *Circulation*. 2021;143(5):e35-e71. [\[Crossref\]](#)
107. Lancellotti P, Pibarot P, Chambers J, et al. Recommendations for the imaging assessment of prosthetic heart valves: a report from the European Association of Cardiovascular Imaging endorsed by the Chinese Society of Echocardiography, the Inter-American Society of Echocardiography, and the Brazilian Department of Cardiovascular Imaging. *Eur Heart J Cardiovasc Imaging*. 2016;17(6):589-590. [\[Crossref\]](#)
108. Lázaro C, Hinojar R, Zamorano JL. Cardiac imaging in prosthetic paravalvular leaks. *Cardiovasc Diagn Ther*. 2014;4(4):307-313. [\[Crossref\]](#)
109. Pibarot P, Dumesnil JG. Prosthetic heart valves: selection of the optimal prosthesis and long-term management. *Circulation*. 2009;119(7):1034-1048. [\[Crossref\]](#)
110. De Cicco G, Russo C, Moreo A, et al. Mitral valve periprosthetic leakage: anatomical observations in 135 patients from a multicentre study. *Eur J Cardiothorac Surg*. 2006;30(6):887-891. [\[Crossref\]](#)
111. Bach DS. Transesophageal echocardiographic (TEE) evaluation of prosthetic valves. *Cardiol Clin*. 2000;18(4):751-771. [\[Crossref\]](#)
112. Zoghbi WA, Chambers JB, Dumesnil JG, et al. Recommendations for evaluation of prosthetic valves with echocardiography and doppler ultrasound: a report From the American Society of Echocardiography's Guidelines and Standards Committee and the Task Force on Prosthetic Valves, developed in conjunction with the American College of Cardiology Cardiovascular Imaging Committee, Cardiac Imaging Committee of the American Heart Association, the European Association of Echocardiography, a registered branch of the European Society of Cardiology, the Japanese Society of Echocardiography and the Canadian Society of Echocardiography, endorsed by the American College of Cardiology Foundation, American Heart Association, European Association of Echocardiography, a registered branch of the European Society of Cardiology, the Japanese Society of Echocardiography, and Canadian Society of Echocardiography. *J Am Soc Echocardiogr*. 2009;22(9):975-1014; quiz 1082-1084. [\[Crossref\]](#)
113. Zamorano JL, Badano LP, Bruce C, et al. EAE/ASE recommendations for the use of echocardiography in new transcatheter interventions for valvular heart disease. *Eur Heart J*. 2011;32(17):2189-2214. [\[Crossref\]](#)
114. Giblett JP, Rana BS, Shapiro LM, Calvert. PA. Percutaneous management of paravalvular leaks. *Nat Rev Cardiol*. 2019;16(5):275-285. [\[Crossref\]](#)
115. Franco E, Almería C, Alberto de Agustín J, et al. Three-dimensional color Doppler transesophageal echocardiography for mitral paravalvular leak quantification and evaluation of percutaneous closure success. *J Am Soc Echocardiogr*. 2014;27(11):1153-1163. [\[Crossref\]](#)
116. Gafoor S, Franke J, Bertog S, et al. A quick guide to paravalvular leak closure. *Interv Cardiol*. 2015;10(2):112-117. [\[Crossref\]](#)
117. Babur Güler G, Ertürk M. Aortik paravalvüler kaçaklarda görüntüleme. Kıрма C, editör. *Perkütan Paravalvüler Leak Kapatma*. 1. Baskı. Ankara: Türkiye Klinikleri; 2020. p.19-26.
118. Kronzon I, Sugeng L, Perk G, et al. Real-time 3-dimensional transesophageal echocardiography in the evaluation of post-operative mitral annuloplasty ring and prosthetic valve dehiscence. *J Am Coll Cardiol*. 2009;53(17):1543-7. [\[Crossref\]](#)
119. Krishnaswamy A, Kapadia SR, Tuzcu EM. Percutaneous paravalvular leak closure- imaging, techniques and outcomes. *Circ J*. 2013;77(1):19-27. [\[Crossref\]](#)
120. Dvir D, Barbash IM, Ben-Dor I, et al. Paravalvular regurgitation after transcatheter aortic valve replacement: diagnosis, clinical outcome, preventive and therapeutic strategies. *Cardiovasc Revasc Med*. 2013;14(3):174-181. [\[Crossref\]](#)
121. Pibarot P, Hahn RT, Weissman NJ, Monaghan MJ. Assessment of paravalvular regurgitation following TAVR: a proposal of unifying grading scheme. *JACC Cardiovasc Imaging*. 2015;8(3):340-360. [\[Crossref\]](#)
122. Pflaumer A, Schwaiger M, Hess J, Lange R, Smet H. Quantification of periprosthetic valve leakage with multiple regurgitation jets by magnetic resonance imaging. *Pediatr Cardiol*. 2005;26(5):593-594. [\[Crossref\]](#)
123. Jerez-Valero M, Urena M, Webb JG, et al. Clinical impact of the presence of aortic regurgitation following transcatheter aortic valve implantation: insights into the degree and acuteness of presentation. *J Am Coll Cardiol Interv*. 2014;7(9): 1022-1032. [\[Crossref\]](#)
124. Kumar R, Jelmin V, Kliger C, Ruiz CE. Percutaneous paravalvular leak closure. *Cardiol Clin*. 2013;31(3):431-440. [\[Crossref\]](#)
125. Hildick-Smith D, Behan MWH, De Giovanni J. Percutaneous closure of an aortic paravalvular leak via the transradial approach. *Catheter Cardiovasc Interv*. 2007;69(5):708-710. [\[Crossref\]](#)
126. Rihal CS, Sorajja P, Booker JD, Hagler DJ, Cabalka AK. Principles of percutaneous paravalvular leak closure. *JACC Cardiovasc Interv*. 2012;5(2):121-130. [\[Crossref\]](#)
127. Singh P, Manda J, Hsiung MC, et al. Live/real time three- dimensional transesophageal echocardiographic evaluation of mitral and aortic valve prosthetic paravalvular regurgitation. *Echocardiography*. 2009;26(8):980-987. [\[Crossref\]](#)
128. Arribas- Jimenez A, Rama-Merchan JC, Barreiro-Pérez M, et al. Utility of real-time 3-dimensional transesophageal echocardiography in the assessment of mitral paravalvular leak. *Circ J*. 2016;80(3):738-744. [\[Crossref\]](#)
129. Biner S, Rafique AM, Kar S, Siegel RJ. Live three-dimensional transesophageal echocardiography-guided transcatheter closure of a mitral paraprothestic leak by Amplatzer occluder. *J Am Soc Echocardiogr*. 2008;21(11):1282.e7-1282.e9. [\[Crossref\]](#)

130. Becerra JM, Almeria C, de Isla LP, Zamorano J. Usefulness of 3D transoesophageal echocardiography for guiding wires and closure devices in mitral perivalvular leaks. *Eur J Echocardiogr.* 2009;10(8):979-981. [\[Crossref\]](#)
131. Ruparelia N, Cao J, Newton JD, Wilson N, Daniels MJ, Ormerod OJ. Paravalvular leak closure under intracardiac echocardiographic guidance. *Catheter Cardiovasc Interv.* 2018;91(5):958-965. [\[Crossref\]](#)
132. Al'Aref SJ, Devereux RB, Cheung JW, Bergman G. Bioprosthetic mitral valve paravalvular leak closure using intracardiac echocardiography-guided three dimensional electroanatomic mapping. *Catheter Cardiovasc Interv.* 2018;92(2):E135-E138. [\[Crossref\]](#)
133. Kliger C, Eiros R, Isasti G, et al. Review of surgical prosthetic paravalvular leaks: diagnosis and catheter-based closure. *Eur Heart J.* 2013;34(9):638-649. [\[Crossref\]](#)
134. McElhinney DB. Will there ever be a food and drug administration-approved device for transcatheter paravalvular leak closure? *Circ Cardiovasc Interv.* 2014;7(1):2-5. [\[Crossref\]](#)
135. Gafoor S, Steinberg DH, Franke J, et al. Tools and techniques -- clinical: paravalvular leak closure. *EuroIntervention.* 2014;9(11):1359-1363. [\[Crossref\]](#)
136. Cruz-Gonzalez I, Rama-Merchan JC, Rodríguez-Collado J, et al. Transcatheter closure of paravalvular leaks: state of the art. *Neth Heart J.* 2017;25(2):116-124. [\[Crossref\]](#)
137. O'Rourke DJ, Palac RT, Malenka DJ, Marrin CA, Arbuckle BE, Plehn JF. Outcome of mild periprosthetic regurgitation detected by intraoperative transesophageal echocardiography. *J Am Coll Cardiol.* 2001;38(1):163-166. [\[Crossref\]](#)
138. Cho JJ, Moon J, Shim CY, et al. Different clinical outcome of paravalvular leakage after aortic or mitral valve replacement. *Am J Cardiol.* 2011;107(2):280-284. [\[Crossref\]](#)
139. Cho JJ, Hong GR, Lee S, Byung-Chul C, Jong-Won Ha, Chung N. Predictors of prognosis in patients with mild to moderate paravalvular leakage after mitral valve replacement. *J Card Surg.* 2014;29(2):149-154. [\[Crossref\]](#)
140. Alfieri O, Maisano F, De Bonis M, et al. The double-orifice technique in mitral valve repair: a simple solution for complex problems. *J Thorac Cardiovasc Surg.* 2001;122(4):674-681. [\[Crossref\]](#)
141. Stone GW, Lindenfeld J, Abraham WT, et al. Transcatheter mitral-valve repair in patients with heart failure. *N Engl J Med.* 2018;379(24):2307-2318. [\[Crossref\]](#)
142. Vahanian A, Beyersdorf F, Praz F, et al. 2021 ESC/EACTS Guidelines for the management of valvular heart disease. *Eur Heart J.* 2022;43(7):561-632. [\[Crossref\]](#)
143. Biner S, Perk G, Kar S, et al. Utility of combined two-dimensional and three-dimensional transesophageal imaging for catheter-based mitral valve clip repair of mitral regurgitation. *J Am Soc Echocardiogr.* 2011;24(6):611-617. [\[Crossref\]](#)
144. Silvestry FE, Rodriguez LL, Herrmann HC, et al. Echocardiographic guidance and assessment of percutaneous repair for mitral regurgitation with the Evalve MitraClip: lessons learned from EVEREST I. *J Am Soc Echocardiogr.* 2007;20(10):1131-1140. [\[Crossref\]](#)
145. Feldman T, Wasserman HS, Herrmann HC, et al. Percutaneous mitral valve repair using the edge-to-edge technique: six-month results of the EVEREST Phase I Clinical Trial. *J Am Coll Cardiol.* 2005;46(11):2134-2140. [\[Crossref\]](#)
146. Franzen O, Baldus S, Rudolph V, et al. Acute outcomes of MitraClip therapy for mitral regurgitation in high-surgical-risk patients: emphasis on adverse valve morphology and severe left ventricular dysfunction. *Eur Heart J.* 2010;31(11):1373-1381. [\[Crossref\]](#)
147. Biner S, Siegel RJ, Feldman T, et al. Acute effect of percutaneous MitraClip therapy in patients with haemodynamic decompensation. *Eur J Heart Fail.* 2012;14(8):939-945. [\[Crossref\]](#)
148. Katz WE, Conrad Smith AJ, Crock FW, Cavalcante JL. Echocardiographic evaluation and guidance for MitraClip procedure. *Cardiovasc Diagn Ther.* 2017;7(6):616-632. [\[Crossref\]](#)
149. Mantovani F, Clavel MA, Vatury O, et al. Left-like indentations in myxomatous mitral valves by three-dimensional echocardiographic imaging. *Heart.* 2015;101(14):1111-1117. [\[Crossref\]](#)
150. Estévez-Loureiro R, Franzen O, Winter R, et al. Echocardiographic and clinical outcomes of central versus noncentral percutaneous edge-to-edge repair of degenerative mitral regurgitation. *J Am Coll Cardiol.* 2013;62(25):2370-2377. [\[Crossref\]](#)
151. Tamburino C, Ussia GP, Maisano F, et al. Percutaneous mitral valve repair with the MitraClip system: acute results from a real world setting. *Eur Heart J.* 2010;31(11):1382-1389. [\[Crossref\]](#)
152. Aman E, Smith TW. Echocardiographic guidance for transcatheter mitral valve repair using edge-to-edge clip. *J Echocardiogr.* 2019;17(2):53-63. [\[Crossref\]](#)
153. Sherif MA, Paranskaya L, Yucel S, et al. MitraClip step by step; how to simplify the procedure. *Neth Heart J.* 2017;25(2):125-130. [\[Crossref\]](#)
154. Wunderlich NC, Siegel RJ. Peri-interventional echo assessment for the MitraClip procedure. *Eur Heart J Cardiovasc Imaging.* 2013;14(10):935-949. [\[Crossref\]](#)
155. Faletra FF, Pedrazzini G, Pasotti E, et al. Role of real-time three dimensional transoesophageal echocardiography as guidance imaging modality during catheter based edge-to-edge mitral valve repair. *Heart.* 2013;99(16):1204-1215. [\[Crossref\]](#)
156. Labrousse L, Dijos M, Leroux L, et al. Guidance of the MitraClip® procedure by 2D and 3D imaging. *Arch Cardiovasc Dis.* 2018;111(6-7):432-440. [\[Crossref\]](#)
157. Bhattacharya S, He Z. Mechanics of mitral valve edge-to-edge-repair and MitraClip procedure. *J Long Term Eff Med Implants.* 2015;25(1-2):135-145. [\[Crossref\]](#)
158. Quaipe RA, Salcedo EE, Carroll JD. Procedural guidance using advance imaging techniques for percutaneous edge-to-edge mitral valve repair. *Curr Cardiol Rep.* 2014;16(2):452. [\[Crossref\]](#)
159. Huerta SPC, de Agustín Loeches JA. Intraoperative echocardiographic assessment of mitral regurgitation after mitral clip implantation: literature review. *REC Interv Cardiol.* 2022;4:47-56. [\[Crossref\]](#)
160. Maisano F, Redaelli A, Pennati G, Fumero R, Torracca L, Alfieri O. The hemodynamic effects of double-orifice valve repair for mitral regurgitation: a 3D computational model. *Eur J Cardiothorac Surg.* 1999;15(4):419-425. [\[Crossref\]](#)
161. Topilsky Y, Maltais S, Medina Inojosa J, et al. Burden of tricuspid regurgitation in patients diagnosed in the community setting. *JACC Cardiovasc Imaging.* 2019;12(3):433-442. [\[Crossref\]](#)
162. Chorin E, Rozenbaum Z, Topilsky Y, et al. Tricuspid regurgitation and long-term clinical outcomes. *Eur Heart J Cardiovasc Imaging.* 2020;21(2):157-165. doi [\[Crossref\]](#)
163. Topilsky Y, Nkomo VT, Vatury O, et al. Clinical outcome of isolated tricuspid regurgitation. *JACC Cardiovasc Imaging.* 2014;7(12):1185-1194. [\[Crossref\]](#)
164. Nath J, Foster E, Heidenreich PA. Impact of tricuspid regurgitation on longterm survival. *J Am Coll Cardiol.* 2004;43(3):405-409. [\[Crossref\]](#)
165. Hahn RT, Zamorano JL. The need for a new tricuspid regurgitation grading scheme. *Eur Heart J Cardiovasc Imaging.* 2017;18(12):1342-1343. [\[Crossref\]](#)
166. Hahn RT, Meduri CU, Davidson CJ, et al. Early feasibility study of a transcatheter tricuspid valve annuloplasty: SCOUT trial 30-day results. *J Am Coll Cardiol.* 2017;69(14):1795-1806. [\[Crossref\]](#)
167. Dreyfus GD, Corbi PJ, Chan KM, Bahrami T. Secondary tricuspid regurgitation or dilatation: which should be the criteria for surgical repair?. *Ann Thorac Surg.* 2005;79(1):127-132. [\[Crossref\]](#)
168. Ling LF, Obuchowski NA, Rodriguez L, Popovic Z, Kwon D, Marwick TH. Accuracy and interobserver concordance of echocardiographic assessment of right ventricular size and systolic function: a quality control exercise. *J Am Soc Echocardiogr.* 2012;25(7):709-713. [\[Crossref\]](#)
169. Rudski LG, Lai WW, Afilalo J, et al. Guidelines for the echocardiographic assessment of the right heart in adults: a report from the American Society of Echocardiography endorsed by the European Association of Echocardiography, a registered branch of the European Society of Cardiology, and the Canadian Society of Echocardiography. *J Am Soc Echocardiogr.* 2010;23(7):685-788. [\[Crossref\]](#)
170. Antoniou T, Koletsis EN, Prokakis C, et al. Hemodynamic effects of combination therapy with inhaled nitric oxide and iloprost in patients with pulmonary hypertension and right ventricular dysfunction after high-risk cardiac surgery. *J Cardiothorac Vasc Anesth.* 2013;27(3):459-466. [\[Crossref\]](#)

171. McLaughlin VV, Archer SL, Badesch DB, et al. ACCF/AHA 2009 expert consensus document on pulmonary hypertension: a report of the American College of Cardiology Foundation Task Force on Expert Consensus Documents and the American Heart Association developed in collaboration with the American College of Chest Physicians; American Thoracic Society, Inc.; and the Pulmonary Hypertension Association. *J Am Coll Cardiol*. 2009;53(17):1573-1619. [\[Crossref\]](#)
172. Wang J, Han J, Li Y, et al. Impact of surgical ablation of atrial fibrillation on the progression of tricuspid regurgitation and right-sided heart remodeling after mitral-valve surgery: a propensity-score matching analysis. *J Am Heart Assoc*. 2016;5(12):e004213. Published 2016 Dec 5. [\[Crossref\]](#)
173. Stulak JM, Schaff HV, Dearani JA, Orszulak TA, Daly RC, Sundt TM 3rd. Restoration of sinus rhythm by the Maze procedure halts progression of tricuspid regurgitation after mitral surgery. *Ann Thorac Surg*. 2008;86(1):40-45. [\[Crossref\]](#)
174. Kadri AN, Menon V, Sammour YM, et al. Outcomes of patients with severe tricuspid regurgitation and congestive heart failure. *Heart*. 2019;105(23):1813-1817. [\[Crossref\]](#)
175. Van de Veire NR, Braun J, Delgado V, et al. Tricuspid annuloplasty prevents right ventricular dilatation and progression of tricuspid regurgitation in patients with tricuspid annular dilatation undergoing mitral valve repair. *J Thorac Cardiovasc Surg*. 2011;141(6):1431-1439. [\[Crossref\]](#)
176. Chikwe J, Itagaki S, Anyanwu A, Adams DH. Impact of concomitant tricuspid annuloplasty on tricuspid regurgitation, right ventricular function, and pulmonary artery hypertension after repair of mitral valve prolapse. *J Am Coll Cardiol*. 2015;65(18):1931-1938. [\[Crossref\]](#)
177. McCarthy PM, Bhudia SK, Rajeswaran J, et al. Tricuspid valve repair: durability and risk factors for failure. *J Thorac Cardiovasc Surg*. 2004;127(3):674-685. [\[Crossref\]](#)
178. Zack CJ, Fender EA, Chandrashekar P, et al. National trends and outcomes in isolated tricuspid valve surgery. *J Am Coll Cardiol*. 2017;70(24):2953-2960. [\[Crossref\]](#)
179. De Meester P, Van De Bruaene A, Voigt JU, Herijgers P, Budts W. Outcome and determinants of prognosis in patients undergoing isolated tricuspid valve surgery: retrospective single center analysis. *Int J Cardiol*. 2014;175(2):333-339. [\[Crossref\]](#)
180. Dreyfus J, Ghalem N, Garbarz E, et al. Timing of referral of patients with severe isolated tricuspid valve regurgitation to surgeons (from a French nationwide database). *Am J Cardiol*. 2018;122(2):323-326. [\[Crossref\]](#)
181. Dreyfus J, Flagiello M, Bazire B, et al. Isolated tricuspid valve surgery: impact of aetiology and clinical presentation on outcomes. *Eur Heart J*. 2020;41(45):4304-4317. [\[Crossref\]](#)
182. Dreyfus J, Audureau E, Bohbot Y, et al. TRI-SCORE: a new risk score for in-hospital mortality prediction after isolated tricuspid valve surgery. *Eur Heart J*. 2022;43(7):654-662. [\[Crossref\]](#)
183. Mehr M, Taramasso M, Besler C, et al. 1-year outcomes after edge-to-edge valve repair for symptomatic tricuspid regurgitation: results from the trivalve registry. *JACC Cardiovasc Interv*. 2019;12(15):1451-1461. [\[Crossref\]](#)
184. Orban M, Rommel KP, Ho EC, et al. Transcatheter edge-to-edge tricuspid repair for severe tricuspid regurgitation reduces hospitalizations for heart failure. *JACC Heart Fail*. 2020;8(4):265-276. [\[Crossref\]](#)
185. Besler C, Orban M, Rommel KP, et al. Predictors of procedural and clinical outcomes in patients with symptomatic tricuspid regurgitation undergoing transcatheter edge-to-edge repair. *JACC Cardiovasc Interv*. 2018;11(12):1119-1128. [\[Crossref\]](#)
186. Lurz P, Stephan von Bardeleben R, Weber M, et al. Transcatheter edge-to-edge repair for treatment of tricuspid regurgitation. *J Am Coll Cardiol*. 2021;77(3):229-239. [\[Crossref\]](#)
187. Nickenig G, Weber M, Lurz P, et al. Transcatheter edge-to-edge repair for reduction of tricuspid regurgitation: 6-month outcomes of the TRILUMINATE single-arm study [published correction appears in *Lancet*. 2020 Mar 14;395(10227):870]. *Lancet*. 2019;394(10213):2002-2011. [\[Crossref\]](#)
188. Rdzanek A, Szymański P, Gackowski A, et al. Percutaneous tricuspid edge-to-edge repair - patient selection, imaging considerations, and the procedural technique. Expert opinion of the Working Group on Echocardiography and Association of Cardiovascular Interventions of the Polish Cardiac Society. *Kardiol Pol*. 2021;79(10):1178-1191. [\[Crossref\]](#)
189. Karam N, Mehr M, Taramasso M, et al. Value of echocardiographic right ventricular and pulmonary pressure assessment in predicting transcatheter tricuspid repair outcome. *JACC Cardiovasc Interv*. 2020;13(10):1251-1261. [\[Crossref\]](#)
190. Hahn RT. State-of-the-art review of echocardiographic imaging in the evaluation and treatment of functional tricuspid regurgitation. *Circ Cardiovasc Imaging*. 2016;9(12):e005332. [\[Crossref\]](#)
191. Martinez RM, O'Leary PW, Anderson RH. Anatomy and echocardiography of the normal and abnormal tricuspid valve. *Cardiol Young*. 2006;16(Suppl 3):4-11. [\[Crossref\]](#)
192. Xanthos T, Dalivigkas I, Ekmektzoglou KA. Anatomic variations of the cardiac valves and papillary muscles of the right heart. *Ital J Anat Embryol*. 2011;116(2):111-26.
193. Dahou A, Levin D, Reisman M, Hahn RT. Anatomy and physiology of the tricuspid valve. *JACC Cardiovasc Imaging*. 2019;12(3):458-468. [\[Crossref\]](#)
194. Silver MD, Lam JHC, Ranganathan N, Wigle ED. Morphology of the human tricuspid valve. *Circulation*. 1971;43(3):333-48. [\[Crossref\]](#)
195. Fukuda S, Saracino G, Matsumura Y, et al. Three-dimensional geometry of the tricuspid annulus in healthy subjects and in patients with functional tricuspid regurgitation: a real-time, 3-dimensional echocardiographic study. *Circulation*. 2006;114(1 suppl):I492-I498. [\[Crossref\]](#)
196. Fawzy H, Fukamachi K, Mazer CD, et al. Complete mapping of the tricuspid valve apparatus using three-dimensional sonomicrometry. *J Thorac Cardiovasc Surg*. 2011;141(4):1037-43. [\[Crossref\]](#)
197. Mahmood F, Kim H, Chaudary B, et al. Tricuspid annular geometry: a three-dimensional transesophageal echocardiographic study. *J Cardiothorac Vasc Anesth*. 2013;27(4):639-46. [\[Crossref\]](#)
198. Rodés-Cabau J, Hahn RT, Latib A, et al. Transcatheter therapies for treating tricuspid regurgitation. *J Am Coll Cardiol*. 2016;67(15):1829-45. [\[Crossref\]](#)
199. Ancona F, Stella S, Taramasso M, et al. Multimodality imaging of the tricuspid valve with implication for percutaneous repair approaches. *Heart*. 2017;103(14):1073-1081. [\[Crossref\]](#)
200. Chan KL, Veinot JP. *Anatomic Basis of Echocardiographic Diagnosis*. London: Springer; 2011. [\[Crossref\]](#)
201. Badano LP, Agricola E, Perez de Isla L, Gianfagna P, Zamorano JL. Evaluation of the tricuspid valve morphology and function by trans-thoracic real-time three-dimensional echocardiography. *Eur J Echocardiogr*. 2009;10(4):477-484. [\[Crossref\]](#)
202. Muraru D, Hahn RT, Soliman OI, Faletta FF, Basso C, Badano LP. 3-dimensional echocardiography in imaging the tricuspid valve. *JACC Cardiovasc Imaging*. 2019;12(3):500-515. [\[Crossref\]](#)
203. Ro R, Tang GHL, Seetharam K, et al. Echocardiographic imaging for transcatheter tricuspid edge-to-edge repair. *J Am Heart Assoc*. 2020;9(5):e015682. [\[Crossref\]](#)
204. Hahn RT, Nabauer M, Zuber M, et al. Intraprocedural imaging of transcatheter tricuspid valve interventions. *JACC Cardiovasc Imaging*. 2019;12(3):532-553. [\[Crossref\]](#)
205. Go AS, Hylek EM, Phillips KA, et al. Prevalence of diagnosed atrial fibrillation in adults: national implications for rhythm management and stroke prevention: the AnTicoagulation and Risk Factors in Atrial Fibrillation (ATRIA) Study. *JAMA*. 2001;285(18):2370-2375. [\[Crossref\]](#)
206. Camm AJ, Lip GY, De Caterina R, et al. 2012 focused update of the ESC Guidelines for the management of atrial fibrillation: An update of the 2010 ESC Guidelines for the management of atrial fibrillation. Developed with the special contribution of the European Heart Rhythm Association. *Eur Heart J*. 2012;33(21):2719-2747. [Published correction appears in *Eur Heart J*. 2013 Mar;34(10):790] [Published correction appears in *Eur Heart J*. 2013;34(36):2850-1]. [\[Crossref\]](#)
207. Reddy VY, Sievert H, Halperin J, et al. Percutaneous left atrial appendage closure vs warfarin for atrial fibrillation: a randomized clinical trial. *JAMA*. 2014;312(19):1988-1998. [Published correction appears in *JAMA*. 2015 Mar 10;313(10):1061] [\[Crossref\]](#)

208. Al-Saady NM, Obel OA, Camm AJ. Left atrial appendage: structure, function, and role in thromboembolism. *Heart*. 1999;82(5):547-554. [Crossref]
209. Vainrib AF, Harb SC, Jaber W, et al. Left atrial appendage occlusion/exclusion: Procedural image guidance with transesophageal echocardiography. *J Am Soc Echocardiogr*. 2018;31(4):454-474. [Crossref]
210. Wunderlich NC, Beigel R, Swaans MJ, Ho SY, Siegel RJ. Percutaneous interventions for left atrial appendage exclusion: Options, assessment, and imaging using 2D and 3D echocardiography. *JACC Cardiovasc Imaging*. 2015;8(4):472-488. [Crossref]
211. Di Biase L, Santangeli P, Anselmino M, et al. Does the left atrial appendage morphology correlate with the risk of stroke in patients with atrial fibrillation? Results from a multicenter study. *J Am Coll Cardiol*. 2012;60(6):531-538. [Crossref]
212. Dudzinski DM, Schwartzberg S, Upadhyay GA, Hung J. Role of transesophageal echocardiography in left atrial appendage device closure. *Interv Cardiol Clin*. 2014;3(2):255-280. [Crossref]
213. Saw J, Kar S, Price MJ. Left atrial appendage closure: Mechanical approaches to stroke prevention in atrial fibrillation, 1st edition, Humana Press, 2016. [Crossref]
214. Iriart X, Ciobotaru V, Martin C, et al. Role of cardiac imaging and three-dimensional printing in percutaneous appendage closure. *Arch Cardiovasc Dis*. 2018;111(6-7):411-420. [Crossref]
215. Chan SK, Kannam JP, Douglas PS, Manning WJ. Multiplane transesophageal echocardiographic assessment of left atrial appendage anatomy and function. *Am J Cardiol*. 1995;76(7):528-530. [Crossref]
216. Chen S, Chun KRJ, Bordignon S, et al. Left atrial appendage occlusion using LAmbre Amulet and Watchman in atrial fibrillation. *J Cardiol*. 2019;73(4):299-306. [Crossref]
217. Zhou Q, Song H, Zhang L, et al. Roles of real-time three-dimensional transesophageal echocardiography in peri-operation of transcatheter left atrial appendage closure. *Medicine (Baltimore)*. 2017;96(4):e5637. [Crossref]
218. Meier B, Blaauw Y, Khattab AA, et al. EHRA/EAPCI expert consensus statement on catheter-based left atrial appendage occlusion. *EuroIntervention*. 2015;10(9):1109-1125. [Crossref]
219. Ali M, Rigopoulos AG, Mammadov M, et al. Systematic review on left atrial appendage closure with the LAmbre device in patients with non-valvular atrial fibrillation. *BMC Cardiovasc Disord*. 2020;20(1):78. [Crossref]
220. Athanassopoulos GD. 3D printing for left atrial appendage (LAA) modeling based on transesophageal echocardiography: A step forward in closure with LAA devices. *Cardiology*. 2016;135(4):249-254. [Crossref]
221. Viles-Gonzalez JF, Kar S, Douglas P, et al. The clinical impact of incomplete left atrial appendage closure with the Watchman Device in patients with atrial fibrillation: A percutaneous closure of the left atrial appendage versus warfarin therapy for prevention of stroke in patients with atrial fibrillation (PROTECT AF) substudy. *J Am Coll Cardiol*. 2012;59(10):923-929. [Crossref]
222. Elliott PM, Anastakis A, Borger MA, et al. 2014 ESC guidelines on diagnosis and management of hypertrophic cardiomyopathy: The task force for the diagnosis and management of hypertrophic cardiomyopathy of the European Society of Cardiology (ESC). *Eur Heart J*. 2014;35(39): 2733-2779 [Crossref]
223. Ommen SR, Mital S, Burke MA, et al. 2020 AHA/ACC Guideline for the diagnosis and treatment of patients with hypertrophic cardiomyopathy: Executive summary: A report of the American College of Cardiology/American Heart Association Joint Committee on Clinical Practice Guidelines. *Circulation*. 2020;142:e558-e631. [Crossref]
224. Ommen SR, Maron BJ, Olivetto I, et al. Long-term effects of surgical septal myectomy on survival in patients with obstructive hypertrophic cardiomyopathy. *J Am Coll Cardiol*. 2005;46(3):470-476. [Crossref]
225. Sitges M, Qin JX, Lever HM, et al. Evaluation of left ventricular outflow tract area after septal reduction in obstructive hypertrophic cardiomyopathy: a real-time 3-dimensional echocardiographic study. *Am Heart J*. 2005;150(4):852-858. [Crossref]
226. vanDokum WG, Beek AM, ten Cate FJ, et al. Early onset and progression of left ventricular remodeling after alcohol septal ablation in hypertrophic obstructive cardiomyopathy. *Circulation*. 2005;111(19):2503-2508. [Crossref]
227. Mazur W, Nagueh SF, Lakkis NM, et al. Regression of left ventricular hypertrophy after nonsurgical septal reduction therapy for hypertrophic obstructive cardiomyopathy. *Circulation*. 2001;103(11):1492-1496. [Crossref]
228. Meliga E, Steendijk P, Valgimigli M, Ten Cate FJ, Serruys PW. Effects of percutaneous transluminal septal myocardial ablation for obstructive hypertrophic cardiomyopathy on systolic and diastolic left ventricular function assessed by pressure-volume loops. *Am J Cardiol*. 2008;101(8):1179-1184. [Crossref]
229. Nishihara K, Mikami T, Takatsuji H, et al. Usefulness of early diastolic flow propagation velocity measured by color M-mode Doppler technique for the assessment of left ventricular diastolic function in patients with hypertrophic cardiomyopathy. *J Am Soc Echocardiogr*. 2000;13(9):801-808. [Crossref]
230. Jassal DS, Neilan TG, Fifer MA, et al. Sustained improvement in left ventricular diastolic function after alcohol septal ablation for hypertrophic obstructive cardiomyopathy. *Eur Heart J*. 2006;27(15):1805-1810. [Crossref]
231. Come PC, Riley MF. Hypertrophic cardiomyopathy. Disappearance of auscultatory, carotid pulse, and echocardiographic manifestations of obstruction following myocardial infarction. *Chest*. 1982;82(4):451-454. [Crossref]
232. Kuhn H, Gietzen F, Leuner C, Gerenkamp T. Induction of subaortic septal ischaemia to reduce obstruction in hypertrophic obstructive cardiomyopathy. Studies to develop a new catheter-based concept of treatment. *Eur Heart J*. 1997;18(5):846-851. [Crossref]
233. Sigwart U. Non-surgical myocardial reduction for hypertrophic obstructive cardiomyopathy. *Lancet*. 1995;346(8969):211-214. [Crossref]
234. Goodwin JF, Oakley CM, Sigwart U. Non-surgical myocardial reduction for hypertrophic obstructive cardiomyopathy. *Lancet*. 1995;346(8990):1624. [Crossref]
235. Maron BJ. Controversies in cardiovascular medicine. Surgical myectomy remains the primary treatment option for severely symptomatic patients with obstructive hypertrophic cardiomyopathy. *Circulation*. 2007;116(2):196-206. [Crossref]
236. Braunwald E. A new treatment for hypertrophic cardiomyopathy? *Eur Heart J*. 1997;18:709-710. [Crossref]
237. Faber L, Seggewiss H, Gleichmann U. Percutaneous transluminal septal myocardial ablation in hypertrophic obstructive cardiomyopathy: Results with respect to intraprocedural myocardial contrast echocardiography. *Circulation*. 1998;98(22):2415-2421. [Crossref]
238. Veselka J, Faber L, Liebrechts M, et al. Short- and long-term outcomes of alcohol septal ablation for hypertrophic obstructive cardiomyopathy in patients with mild left ventricular hypertrophy: A propensity score matching analysis. *Eur Heart J*. 2019;40(21):1681-1687. [Crossref]
239. Veselka J, Jensen M, Liebrechts M, et al. Alcohol septal ablation in patients with severe hypertrophy. *Heart*. 2020;106(6):462-466. [Crossref]
240. Veselka J. Ten tips and tricks for performing alcohol septal ablation in patients with hypertrophic obstructive cardiomyopathy. *Int J Angiol*. 2020;29(3):180-182. [Crossref]
241. Cuoco F, Gold MR. Newer applications of cardiac pacemakers and extracardiac stimulation. In: Zipes DP, Jalife J, Stevenson WG, eds. *Cardiac Electrophysiology From Cell to Bedside*. Philadelphia, PA Elsevier; 2018:1167-1172. [Crossref]
242. Leal S, Galeote G, Jiménez-Valero S, et al. Percutaneous alcohol septal ablation for hypertrophic obstructive cardiomyopathy: Technical review and long-term clinical and echocardiographic outcomes. *Rev Port Cardiol*. 2012;31(5):363-371. [Crossref]
243. Contrast Agents Introduction to contrast, escardio.org. July 6, 2020. Available at: <https://www.escardio.org/Education/Practice-Tools/EACVI-toolboxes/Contrast-Echo/Lectures/Contrast-Agents>. Accessed April 12, 2022.

244. Faber L, Seggewiss H, Welge D, et al. Echo-guided percutaneous septal ablation for symptomatic hypertrophic obstructive cardiomyopathy: 7 years of experience. *Eur J Echocardiogr.* 2004;5(5):347-355. [\[Crossref\]](#)
245. Arias EA, Peña-Duque MA, Martínez Ríos MA. Bubble contrast echocardiography for alcohol septal ablation. *Rev esp cardiol.* 2019;72(5):416-416. [\[Crossref\]](#)
246. Seggewiss H, Batzner A. Alcohol septal ablation in obstructive hypertrophic cardiomyopathy is a safe procedure in experienced hands. *Rev Port Cardiol.* 2020;39(6):305-307. [\[Crossref\]](#)
247. Nagueh SF, Bierig SM, Budoff MJ, et al. American Society of Echocardiography clinical recommendations for multimodality cardiovascular imaging of patients with hypertrophic cardiomyopathy. *J Am Soc Echocardiogr.* 2011;24(5):473-498. [\[Crossref\]](#)
248. La Canna G, Scarfò I, Arendar I, et al. Targeting alcohol septal ablation in patients with obstructive hypertrophic cardiomyopathy candidates for surgical myectomy: Added value of three-dimensional intracoronary myocardial contrast echocardiography. *J ClinMed.* 2021;10(10):2166. [\[Crossref\]](#)
249. Faber L, Ziemssen P, Seggewiss H. Targeting percutaneous transluminal septal ablation for hypertrophic obstructive cardiomyopathy by intraprocedural echocardiographic monitoring. *J Am Soc Echocardiogr.* 2000;13(12):1074-1079. [\[Crossref\]](#)
250. Kashtanov MG, Rzhannikova AD, Chernyshev SD, et al. Outcomes of hypertrophic obstructive cardiomyopathy patients undergoing alcohol septal ablation with a standard 3 mL dose of ethanol: Focus on long-term safety. *Catheter Cardiovasc Interv.* 2020;95(6):1212-1218. [\[Crossref\]](#)
251. Yoerger DM, Picard MH, Palacios IF, Vlahakes GJ, Lowry PA, Fifer MA. Time course of pressure gradient response after first alcohol septal ablation for obstructive hypertrophic cardiomyopathy. *Am J Cardiol.* 2006;97(10):1511-1514. [\[Crossref\]](#)
252. El Masry H, Breall JA. Alcohol septal ablation for hypertrophic obstructive cardiomyopathy. *Current Cardiology Reviews.* 2008;4(3):193-197. [\[Crossref\]](#)
253. Kashtanov M, Rzhannikova A, Chernyshev S, Kardapoltsev L, Idov E, Berdnikov S. Results of ten-year follow-up of alcohol septal ablation in patients with obstructive hypertrophic cardiomyopathy. *Int J Angiol.* 2018;27(4):202-207. [\[Crossref\]](#)
254. Okay T. Hipertrofik obstrüktif kardiyomiyopati septal arter ablasyonu. In: Enar R, ed. *Pratik invaziv kardiyoloji, klinik ve teknik ipuçları.* İstanbul: Nobel Matbaacılık;2014:537-545.
255. Delgado V, Sitges M, Andrea R, et al. Clinical and echocardiographic follow-up of patients with hypertrophic obstructive cardiomyopathy treated by percutaneous septal ablation. *Rev Esp Cardiol.* 2006;59(11):1123-1130. [\[Crossref\]](#)
256. Reeves ST, Finley AC, Skubas NJ, et al. Basic perioperative transesophageal echocardiography examination: A consensus statement of the American Society of Echocardiography and the Society of Cardiovascular Anesthesiologists. *J Am Soc Echocardiogr.* 2013;26(5):443-56. [\[Crossref\]](#)
257. Reeves ST, Glas KE, Eltzschig H, et al. Guidelines for performing a comprehensive epicardial echocardiography examination: recommendations of the American Society of Echocardiography and the Society of Cardiovascular Anesthesiologists. *J Am Soc Echocardiogr.* 2007;20(4):427-37. [\[Crossref\]](#)
258. Hilberath JN, Oakes DA, Shernan SK, Bulwer BE, D'Ambra MN, Eltzschig HK. Safety of transesophageal echocardiography. *J Am Soc Echocardiogr.* 2010;23(11):1115-27. [\[Crossref\]](#)
259. Freitas-Ferraz AB, Rodés-Cabau J, Junquera Vega L, et al. Transesophageal echocardiography complications associated with interventional cardiology procedures. *Am Heart J.* 2020;221:19-28. [\[Crossref\]](#)
260. Han S, Park J, Hong SH, Park CS, Choi J, Chae MS. Cardiovascular manifestation of end-stage liver disease and perioperative echocardiography for liver transplantation: anesthesiologist's view. *Anesth Pain Med.* 2022;17(2):132-144. [\[Crossref\]](#)
261. Thaden JJ, Malouf JF, Rehfeldt KH, et al. Adult intraoperative echocardiography: A comprehensive review of current practice. *J Am Soc Echocardiogr.* 2020;33(6):735-55. [\[Crossref\]](#)
262. Bartunek J, Sys SU, Rodrigues AC, van Schuerbeeck E, Mortier L, de Bruyne B. Abnormal systolic intraventricular flow velocities after valve replacement for aortic stenosis: Mechanisms, predictive factors, and prognostic significance. *Circulation.* 1996;93(4):712-9. [\[Crossref\]](#)
263. Lau WC, Carroll JR, Deeb GM, Tait AR, Bach DS. Intraoperative transesophageal echocardiographic assessment of the effect of protamine on paraprothestic aortic insufficiency immediately after stentless tissue aortic valve replacement. *J Am Soc Echocardiogr.* 2002;15(10 pt 2):1175-80. [\[Crossref\]](#)
264. le Polain de Waroux JB, Pouleur AC, Robert A, et al. Mechanisms of recurrent aortic regurgitation after aortic valve repair: Predictive value of intraoperative transesophageal echocardiography. *JACC Cardiovasc Imaging.* 2009;2(8):931-9. [\[Crossref\]](#)
265. Tufekcioglu O, Firincioglu CL, Arda K, Fansa I, Saritas A, Karahan M. Echocardiography findings in 16 cases of cardiac echinococcosis: Proposal for a new classification system. *J Am Soc Echocardiogr.* 2007;20(7):895-904. [\[Crossref\]](#)